NAVAL POSTGRADUATE SCHOOL
Monterey, California

THESIS

A CASE STUDY OF
THE MONTEREY BAY SEA BREEZE
ON 25 AUGUST 1997

by

Steven M. Taylor

September 1998

Thesis Advisor: Wendell A. Nuss
Co-Advisor: Douglas K. Miller

Approved for public release; distribution is unlimited.

REPORT DOCUMENTATION PAGE

Form Approved
OMB No. 0704-0188

1. AGENCY USE ONLY *(Leave blank)*	2. REPORT DATE	3. REPORT TYPE AND DATES COVERED
	September 1998	Master's Thesis

4. TITLE AND SUBTITLE
A Case Study of the Monterey Bay Sea Breeze on 25 August 1997

5. FUNDING NUMBERS

6. AUTHOR(S)
Taylor, Steven M.

7. PERFORMING ORGANIZATION NAME(S) AND ADDRESS(ES)
Naval Postgraduate School
Monterey, CA 93943-5000

8. PERFORMING ORGANIZATION REPORT NUMBER

9. SPONSORING / MONITORING AGENCY NAME(S) AND ADDRESS(ES)

10. SPONSORING / MONITORING AGENCY REPORT NUMBER

11. SUPPLEMENTARY NOTES
The views expressed in this thesis are those of the author and do not reflect the official policy or position of the Department of Defense or the U.S. Government.

12a. DISTRIBUTION / AVAILABILITY STATEMENT
Approved for public release; distribution is unlimited.

12b. DISTRIBUTION CODE

13. ABSTRACT *(maximum 200 words)*

On 25 August a controlled burn on the former Fort Ord property raged out of control. The sea breeze was responsible for transporting the acrid smoke into the Salinas Valley. The PSU/NCAR mesoscale model, MM5, was run at 4 km grid resolution twice using two different PBL schemes (MRF and Burk-Thompson) and then verified by observations from several local mesoscale networks, including wind profiler data. The MM5 simulation was able to depict the 3-D structure of the sea breeze and differentiate between the local mountain-valley forcing and the large-scale sea breeze forcing. These two individual forcing mechanisms were responsible for an observed double surge in the time series of winds at Fort Ord. Further investigation is needed into the surface parameterization/land use tables to improve the surface forcing.

14. SUBJECT TERMS	15. NUMBER OF PAGES
Sea Breeze, Mesoscale Modeling, MM5 Simulations, Monterey Bay, Salinas Valley, Land Breeze	132
	16. PRICE CODE

17. SECURITY CLASSIFICATION OF REPORT	18. SECURITY CLASSIFICATION OF THIS PAGE	19. SECURITY CLASSIFI- CATION OF ABSTRACT	20. LIMITATION OF ABSTRACT
Unclassified	Unclassified	Unclassified	UL

Approved for public release; distribution is unlimited

A CASE STUDY OF THE MONTEREY BAY SEA BREEZE ON 25 AUGUST 1997

Steven M. Taylor
B.S., Pennsylvania State University, 1992

Submitted in partial fulfillment of the
requirements for the degree of

MASTER OF SCIENCE IN METEOROLOGY

from the

NAVAL POSTGRADUATE SCHOOL
September 1998

ABSTRACT

On 25 August a controlled burn on the former Fort Ord property raged out of control. The sea breeze was responsible for transporting the acrid smoke into the Salinas Valley. The PSU/NCAR mesoscale model, MM5, was run at 4 km grid resolution twice using two different PBL schemes (MRF and Burk-Thompson) and then verified by observations from several local mesoscale networks, including wind profiler data. The MM5 simulation was able to depict the 3-D structure of the sea breeze and differentiate between the local mountain-valley forcing and the large-scale sea breeze forcing. These two individual forcing mechanisms were responsible for an observed double surge in the time series of winds at Fort Ord. Further investigation is needed into the surface parameterization/land use tables to improve the surface forcing.

TABLE OF CONTENTS

ACKNOWLEDGMENT

This thesis could not have been completed without the help of my fellow staff and faculty. I would especially like to thank Professor Wendell Nuss for his guidance and patience through this process. I would also like to thank Professor Doug Miller for running the model, guidance, and patience. My thanks go out to Bob Creasey and Mary Jordan for their help in the data manipulation realm. Extended thanks goes to Silicon Graphics Incorporated of Minnesota for allow us to run our model on their computer system and to Chad Daniel, Iowa State University, for some of the GEMPAK data used in this thesis.

Most of all, I would like to thank Sylvia, my wife, for her patience and support. Two theses at once can be quiet trying, but quite the accomplishment.

I would like to dedicate this thesis to our future child, who was on the way during the writing of this thesis.

I. INTRODUCTION

The sea breeze circulation has been studied for well over half a century and its effects have been known for centuries, making it one of the more extensively studied weather phenomenon. Although the sea breeze occurs along both coasts of the United States, its evolution varies considerably from location to location. This basic circulation can be simple and straightforward such as along the Gulf Coast or quite complicated such as along the West Coast where the coastline has complex terrain. The more complex terrain of the West Coast can create channeling through the passes and valleys as well as complicate the thermal forcing of the sea breeze. In contrast, the relatively flat coastal terrain of the East Coast with a gradual slope results in more uniform thermal forcing and a more clearly defined sea breeze front with a strong shear zone. In addition, the presence of the North Pacific Ocean sea-level high pressure center and intense daytime heating of the inland areas results in a persistent gradient wind flow from the north along the coast. This results in upwelling, which cools the waters immediately along the coast (Johnson and O'Brien 1973), to produce water that is considerably cooler than the warm waters of the Gulf of Mexico. Consequently, the strong thermal gradient along the West Coast of the United States can cause a very strong sea

breeze circulation. Although the strong thermal gradient along the West Coast is present throughout the summer, the day to day variations in the local sea breeze can be quite large, which poses a significant forecast problem.

For example, the unanticipated evolution of the sea breeze during a controlled burn, set on the former Fort Ord property near Monterey, CA, resulted in a fire that raged out of control in the afternoon hours filling the Salinas Valley with acrid smoke (Figure 1). Mesoscale model forecasts are becoming more routinely available and have been shown to capture the evolution of the sea breeze in other areas. The primary objective of this research is to determine whether or not the Pennsylvania State University/National Center for Atmospheric Research (PSU/NCAR) MM5 model can accurately simulate the sea breeze horizontal and vertical structure and evolution that occurred during this fire. The implications and requirements to use higher resolution grids, such as 4 km, to capture the detailed thermal forcing in complex terrain will be examined. This research has implications for the use of mesoscale modeling in complex terrain in forest fire suppression and prescribed burns, air pollution or air quality control, and the prediction of mesoscale flows in a complex coastal environment. If MM5 can accurately forecast the coastal weather, it could be used to initialize wildfire

behavior models such as the Los Alamos National Laboratory's (LANL) FIRETEC (Bossert et al. 1998).

Chapter II examines previous research on thermally driven sea breezes and highlights research relevant to this thesis. Chapter III describes the synoptic conditions, type of sea breeze and its evolution on the particular day of the fire, as well as the data and model used. Chapter IV compares the model forecast to available observations and examines the mesoscale model performed to determine forcing on different scales. Chapter V presents conclusions and recommendations for further research.

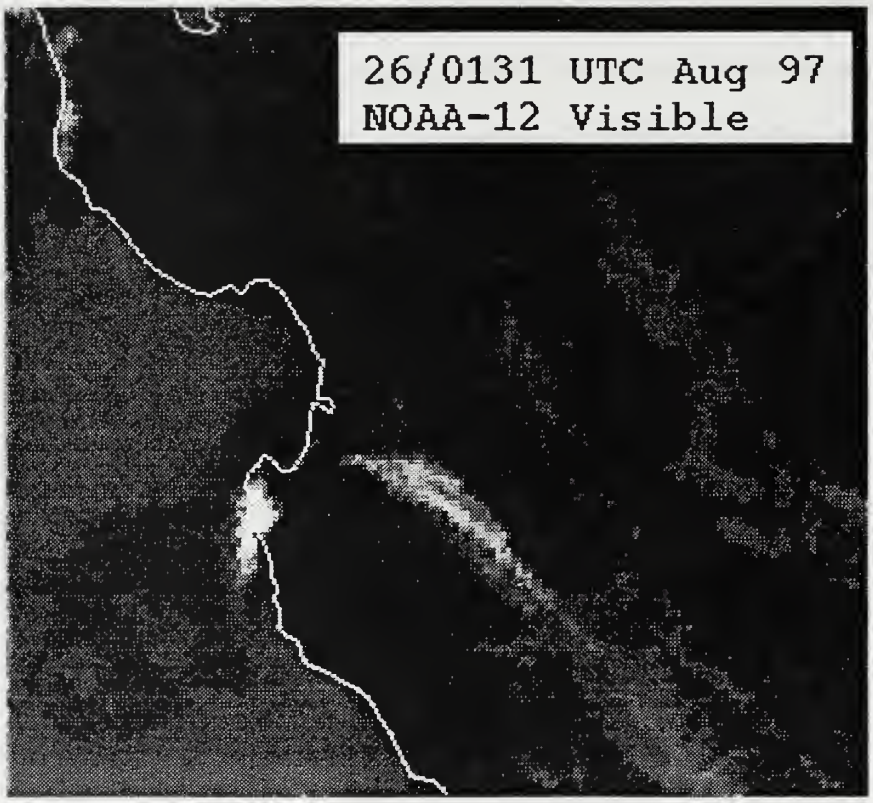

Figure 1. A NOAA-12 visible satellite image of the smoke plume from the Fort Ord fire advected through the Salinas Valley at 01:31 UTC 26 August 1997.

II. BACKGROUND

As described in many previous studies, the driving force of the basic sea breeze circulation is the differential heating that occurs between the land and the ocean. The land heats up considerably quicker than the water creating low relative pressure over the land and high pressure over the water, resulting in a cross-coast acceleration of the wind. The temperature gradient that is initially set up along the coast as a result of the differential heating starts to push the coastal front inland as the winds increase. The wind ushers in the cooler marine air behind the front as it surges inland. This characteristic evolution is best described by Pielke (1984):

1. A flat pressure surface across the coast occurs in the early morning hours so no winds occur. (0800 LST)
2. During late morning, mass is mixed upward over the land by turbulence in the unstable boundary layer, creating an offshore pressure gradient at some distance above the ground. Little heating occurs over the ocean surface. (1100 LST)
3. The offshore flow aloft creates a low pressure region at the ground over the land and an onshore wind begins (sea breeze). (1300 LST)

4. This onshore flow transports cooler marine air over the land thereby advecting the horizontal temperature gradient and sea breeze inland. The heating over the land dictates the extent of the inland penetration of the sea breeze as it determines the magnitude of the cross-coast pressure gradient and the acceleration of the flow.(1600 LST)
5. As the sun sets, longwave radiational cooling becomes dominant over solar heating as the land begins to cool, while the local wind field removes the horizontal temperature gradient. The pressure surfaces return to horizontal again.(1600 LST)
6. The air near the ground becomes more dense and sinks with more cooling. This results in an onshore wind a short distance above the ground as the pressure gradient is reversed. (2200 LST)
7. The loss of mass above the water results in a pressure minimum at the surface immediately off the coast. An offshore wind results across the coast due to this pressure fall offshore. (land breeze) (0100 LST)
8. Cooling over the land governs the extent of the offshore penetration of the land breeze. The land breeze is a shallower and weaker circulation due to the stably stratified boundary layer.

This characteristic evolution can be strongly modified by a variety of factors, which dictate the sea breeze evolution on a given day.

One key modifying influence is the coastline itself, which has a determining effect on the sea breeze by producing horizontal convergence and divergence not seen in simple two-dimensional models. Generally speaking, in the absence of coastal topography, peninsulas or points tend to produce winds that converge as they move inland. If the peninsula is large enough, individual sea breeze fronts will converge. The opposite will happen in bays, where the winds are divergent as they propagate inland. The strength of the divergence depends on the speed of the winds as well as the shape of the bay and the roughness of the coastline. The importance of these geometric factors in determining the sea breeze evolution when topography is present is largely unknown.

Previous studies performed on the sea breeze have classified the sea breeze based on its development characteristics. Wexler (1946) discusses two types of sea breezes, gradual growth; on days with calm or light gradient winds, and frontal; on days with an offshore gradient wind. Wexler described boundary layer stability over the landmass as the key to the onset of the sea breeze. The weaker the boundary layer stability, the greater the vertical mixing due to heating, which results in a stronger sea breeze and

the greater the stability of the air mass over land, the less likely it is for the sea breeze to make it to the shore. He also states that the Coriolis force acts on the sea breeze and may be the cause for the flow to not be perpendicular to the coast. The different characteristic patterns of sea breeze development depend upon a variety of factors that influence the sea breeze forcing.

For the Monterey Bay region, Round (1993) classified the sea breeze development from time series at Fort Ord. Round's categories are as follows:

1. Gradual development - Similar to Wexler (1946), where the gradient onshore flow is enhanced by the sea breeze.
2. Clear onset - Very similar to the gradual development type except for a more definitive onset signal. This category includes all days with either a definite wind shift without a speed increase, or onshore wind conditions prior to sea breeze onset with the onset being distinguished by a pronounced increase in onshore wind speed.
3. Frontal - Similar to Wexler (1946) where the sea breeze resembles the passage of a cold front. The sea breeze onset is characterized by a wind shift, temperature decrease, moisture increase, and wind speed increase.

4. Double Surge - This includes all days in which two separate and distinct onshore events occurred.
5. Unclassifiable days.
6. No Sea Breeze.

Foster (1996) expanded on Round's sea breeze categories by making them more site specific for points along the California coast. For this study the main focus is on the Monterey Bay and the Fort Ord profiler since it was relatively close to the controlled burn. Foster's categories for the Fort Ord site were as follows:

1. Frontal Sea Breeze (frontal westerly for Fort Ord) - Similar to Round (1993) but with an eighty-two degree wind shift threshold imposed.
2. Gradual (Gradual-Westerly for Fort Ord) - Again similar to Round (1993), with westerly winds persistent through midnight.
3. Rapid Onset - Similar to the frontal sea breeze. Main difference is the sharp increase in the wind speed at onset and little change in wind directions.
4. Unclassified - These were days that were either missing data, synoptic scale transition days, such as a frontal passage, or weak sea breeze days.

Foster found that of the all the summer days of 1993, 1994, and 1995, 92% of the days were classified as sea breeze

category days. Of these days, 44% were gradual-westerly, 33% were frontal-westerly, and 15% rapid onset.

Schroeder et al. (1967) give a general description of the sea breeze and the effects of the monsoon flow from the North Pacific Ocean high and how this interacts with the mountains. They summarized the monsoon as a feature of the general circulation that undergoes modification on the coast and interacts with the sea breeze and synoptic-scale systems in a very shallow layer. Because of this monsoon flow, the sea breeze along the North Pacific coast, unlike those found elsewhere, has no significant moisture contrast across its front.

Fosberg and Schroeder (1966) explored the evolution of the sea breeze in complex coastal terrain in their studies north of the San Francisco bay area. This study determined the structure of the sea breeze front and the effect of the terrain on the flow. Fosberg and Schroeder characterized the sea breeze front as a shear line separating the marine flow from the light, variable background circulation. They found that on warm sea breeze days, defined by the temperature at Sacramento > 38°C, channeling by the terrain is more noticeable than on cooler days, defined by the Sacramento temperature < 32°C. This may be partly due to the shallower marine layer during warm days, and a thicker marine layer an cool days, which would allow the flow to spill over the coastal mountains. Warm and cool days are

related to the synoptic patterns under which the sea breeze develops. When an upper level trough was present in the Fosberg and Schroeder (1966) study, the day was cool and the sea breeze was weak. When the North Pacific Ocean high was present, the day was warm and the sea breeze was strong.

Knapp (1994) looked into the large-scale patterns along the West Coast and defined three characteristic synoptic-scale patterns: a Ridge (Figure 2) regime, occurring 13% of the time, a Trough (Figure 3) regime, occurring 52% of the time, a Gradient (Figure 4) regime, occurring 27% of the time, and a miscellaneous category for those that did not fit the 3 primary regimes, occurring 8% of the time. These were based on the synoptic scale sea level pressure patterns from 01 May 1993 to 30 September 1993. Knapp, using the sea breeze categories for the Monterey Bay area of Round (1993), found that the type of sea breeze evolution was directly related to these synoptic regimes. These results are in general agreement with Estogue (1961), discussed later.

The Land/Sea Breeze Experiment (LASBEX) was performed in the Monterey Bay region, from 15 to 30 September 1987 and gives insight into the vertical structure and Mesoscale variation of the land/sea breeze in complex terrain (Inrieri et al. 1990). Fagan (1988) used the data from LASBEX to study the structure of the sea breeze circulation over Monterey Bay and found that the sea breeze circulation fit typical values of vertical velocities of 0.2 to 1.0 m/s

upwards at the sea breeze front, and that the off-shore flow was two times deeper than the on-shore flow. The average on-shore flow height was 659 meters.

Yetter (1990) examined the propagation of the sea breeze front using linear geometry and found speeds along the Monterey Bay varying from 1 m/s to 3 m/s with a mean direction of 125 degrees $\pm$ 26 degrees. These results from the LASBEX data set were in good agreement with previous observations of Kondo and Gambo (1979) and Atkinson (1981). Frosberg and Shroeder (1966) found initial propagation speeds of 2 to 4 m/s, but when the sea breeze interacted with an up-valley circulation in the San Francisco Bay area, the speed increased to 5 to 7 m/s.

Banta (1995), using the LASBEX data set, found that there were two possible sea breeze forcings in the Monterey Bay area. The local heating of the coastal hills and valleys drove a shallow sea breeze below 300 meters. A larger scale forcing from the California Central Valley drove an upper level sea breeze between 300 meters and 1000 meters, the deep sea breeze. As the deep sea breeze developed, it absorbed the shallow sea breeze. Banta (1995) also noted that the shallow sea breeze was quicker to react to radiational cooling, generating a shallow land breeze layer. Wexler (1946) noted a similar situation regarding two different forcings of the sea breeze in Boston. His explanation was that there was a forcing resulting from the

interaction of the atmosphere with the local bay and a larger scale forcing due to the interaction of the coast and the open ocean.

Stec (1996) re-examined the various features of the sea breeze circulation observed during LASBEX and other studies in the Monterey Bay region. Stec used 915 MHz wind profiler and RASS systems to enable verification of these earlier studies. Monthly composites of the sea breeze were derived for each profiler site including the Fort Ord site, which is a critical site for this experiment both due to the data and the proximity to the controlled burn. Stec (1996) used monthly-averaged wind and temperature data for 1994 to describe the sea breeze over the Fort Ord site. The range of the profiler extended from 60 meters up to 1500 meters with 60-meter resolution (Figure 5). For the month of August, the onset time was 1000 PST with the maximum surface winds of 15 kts between 1200 and 1400 PST. Strong winds aloft with speeds greater than 15 kts were seen at 100 m beyond 1800 PST while surface winds decreased. Aloft the northwesterly flow backed to westerly in response to the large-scale continental sea breeze. Return flow over the site was not evident. Further comparisons to this data will be in the Case Study Section of this thesis.

Estoque (1961), using a primitive equation model, studied the interaction of the synoptic scale flow with the sea breeze over homogeneous terrain and a long straight

coast. Arritt (1993), using a two-dimensional nonlinear model, also examined the effects of the ambient wind on the development of typical features of the sea breeze. Both of these studies found that when the onshore synoptic flow was in the same direction as the sea breeze, there was a weak temperature perturbation and a weak sea breeze. When there was calm or moderate opposing synoptic flow, the sea breeze is the strongest due to the strong positive thermal perturbation in a region of negative to near-neutral static stability. When synoptic flow is strong to very strong opposing, the sea breeze is weak to non-existent, respectively. There is very strong static stability suppressing any vertical motion over the land. Both these studies noted that onshore flow of only a few meters per second was enough to suppress the sea breeze, but when the offshore flow was 11 m/s, the sea breeze was still apparent. These studies suggest the very important role of the larger-scale circulation on the sea breeze development.

Johnson and O'Brien (1973) in a descriptive study of the sea breeze along the Oregon coast, found that the low level onshore flow of the sea breeze was limited to being within the marine layer. The marine layer deepened at the sea breeze onset, and there were surges in the return flow aloft that corresponded to surges in the onshore flow at the surface. These results differ from those of Banta (1995) where, in his study, the onshore flow resides both within

and above the marine layer and the return flow is rather weak. This suggests that the local geography/topography may dictate the sea breeze evolution.

As computers become more powerful and more affordable, mesoscale models are now widely used and many universities run them in real time to produce local forecasts. Recent studies of the sea breeze using these models demonstrate their applicability to diagnosing the complex forcing of the sea breeze circulation. For example, Zhong and Takle (1993) used the Lawrence Livermore National Laboratory (LLNL) boundary layer model to run three-dimensional numerical experiments in order to examine the effects of the large scale flow on the evolution of the sea breeze circulation over the Kennedy Space Center/Cape Canaveral area. They also found that onshore background flow weakened the sea breeze while offshore background flow resulted in an intensification of the sea breeze and the thermal structure. In addition, the onset of the sea breeze was found to be inversely proportional to the onshore component of the wind and that inland bodies of water can interact with the sea breeze resulting in small perturbations in the flow. Buckley and Kurzeja (1996) used the Colorado State University Regional Atmospheric Modeling System (RAMS) to look at characteristics of the inland sea breeze over southwestern South Carolina. They found the model to be in rather good agreement with regard to the general features,

but showed some lack of detail mainly due to the lack of horizontal grid spacing (10 km) along the coast. Similar types of sea breeze modeling have been conducted along the Florida panhandle. Gould et al. (1996) and Herbster and Ruscher (1996) both studied the sea breeze over the Tallahassee area using the Tallahassee Area Sea Breeze Experiment (TASBEX) data set and the Penn State/NCAR MM5 model. Both studies identified that MM5 was able to produce the general characteristics of the inland-advancing sea breeze front based on the model winds and mixing ratio, as well as the winds, divergence, and precipitation fields. These results are highly encouraging about the ability of these mesoscale models to simulate the sea breeze over flat terrain.

Meososcale modeling is also being used for direct wildfire forecasting and initialization of wildfire behavior models. Herbster et al. (1998) studied in detail the MM5 16 km gridded domain forecasts over the Florida peninsula. They found the model verified very well for this case, but different cases were needed to conduct further verification. Ferguson (1998) also used MM5 but ran the model on the West Coast, mainly in the Puget Sound area. This model was initialized without observational data, with a nested grid resolution of 4 km and the lowest level in the model was 40 meters. Ferguson stated that MM5 forecasts have enhanced the numerical weather forecasts for the area since it can

simulate the complex flow through Puget Sound. The output is now being used as input for air pollution models and fire behavior models, that can reach resolutions of 30 meters.

However, the ability to simulate the detailed sea breeze in a region of complex coastal mountains and offshore coastal upwelling has not been examined. The circulation becomes more complicated due to upslope and downslope winds in the topography which feeds back on the thermal forcing. The complex evolution of the sea breeze in the Monterey Bay area will be examined in this study to demonstrate the potential application of mesoscale model forecasts to controlled burn forecasts or fire weather conditions.

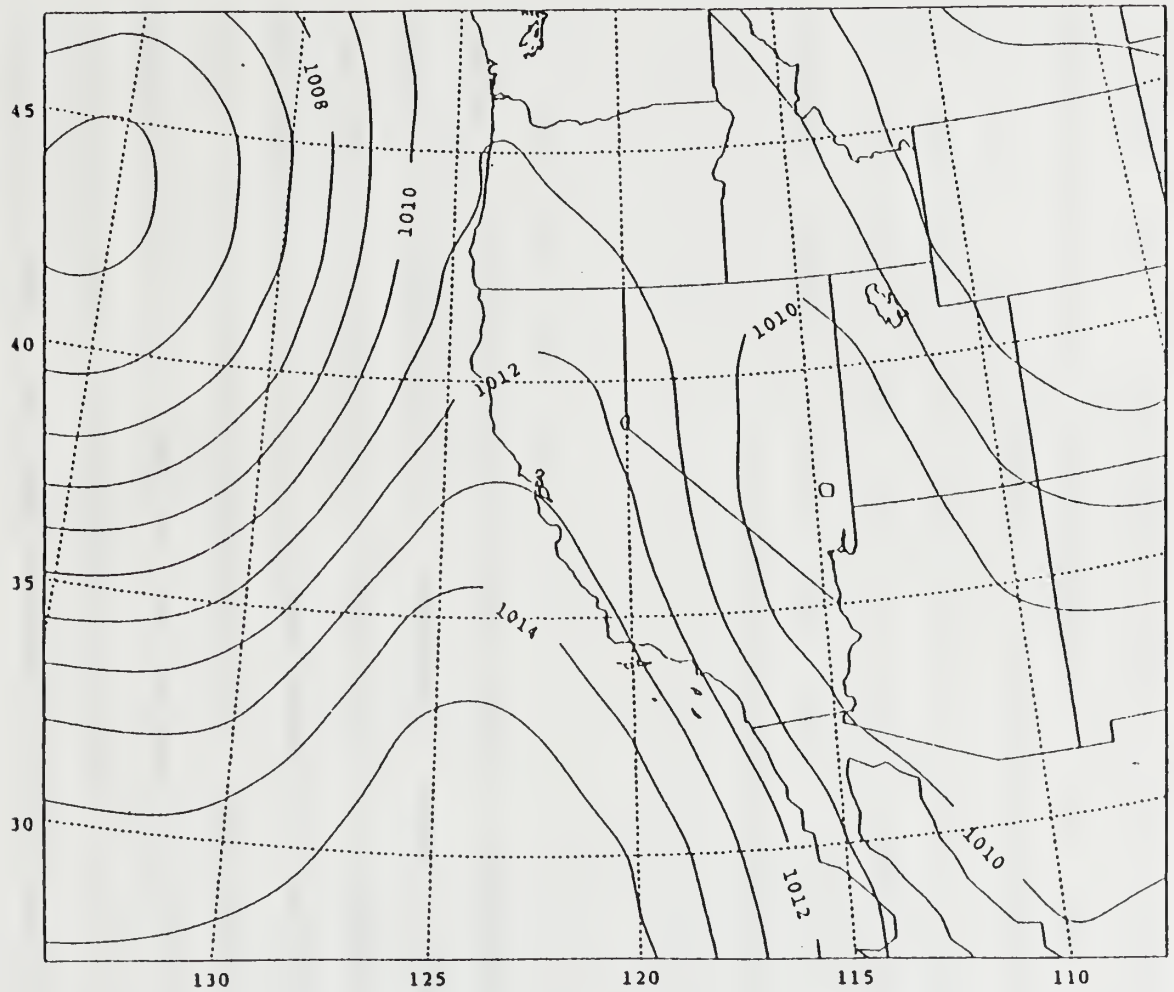

Figure 2. Mean Ridge regime pressure distribution for May - Sep 1993. Knapp (1994)

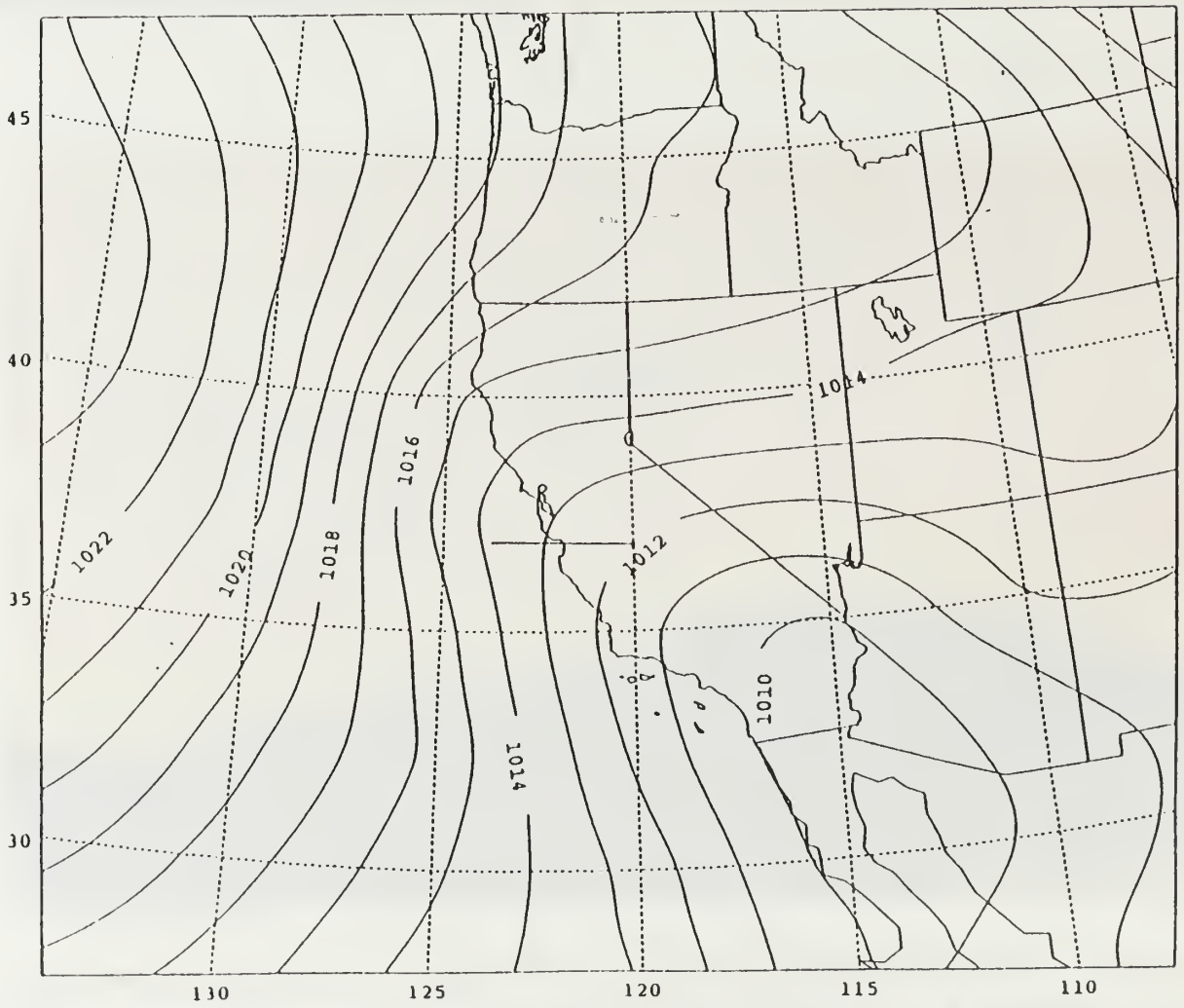

Figure 3. Mean Trough regime pressure distribution for May - Sep 1993. Knapp (1994)

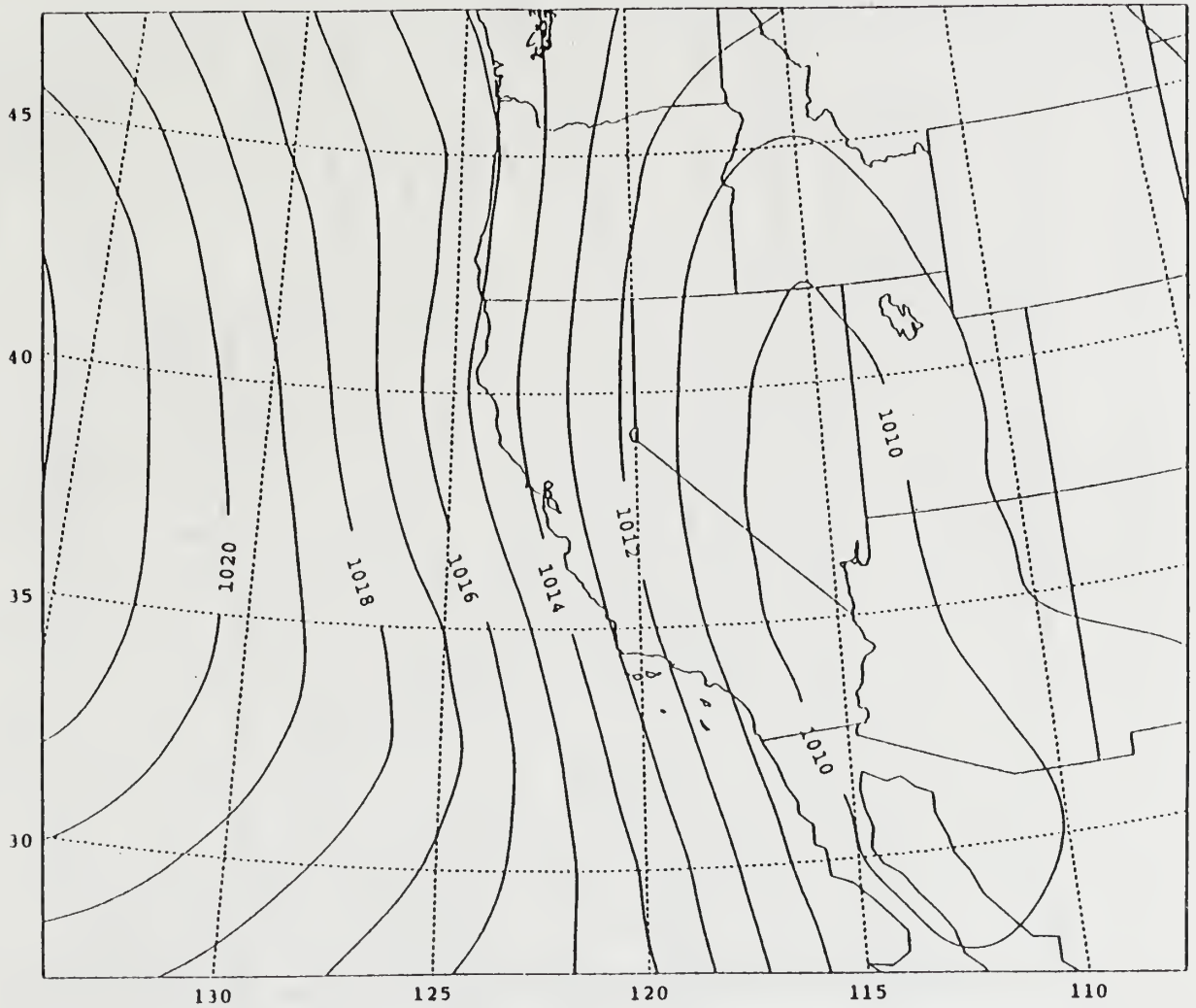

Figure 4. Mean Gradient regime pressure distribution for May - Sep 1993. Knapp (1994)

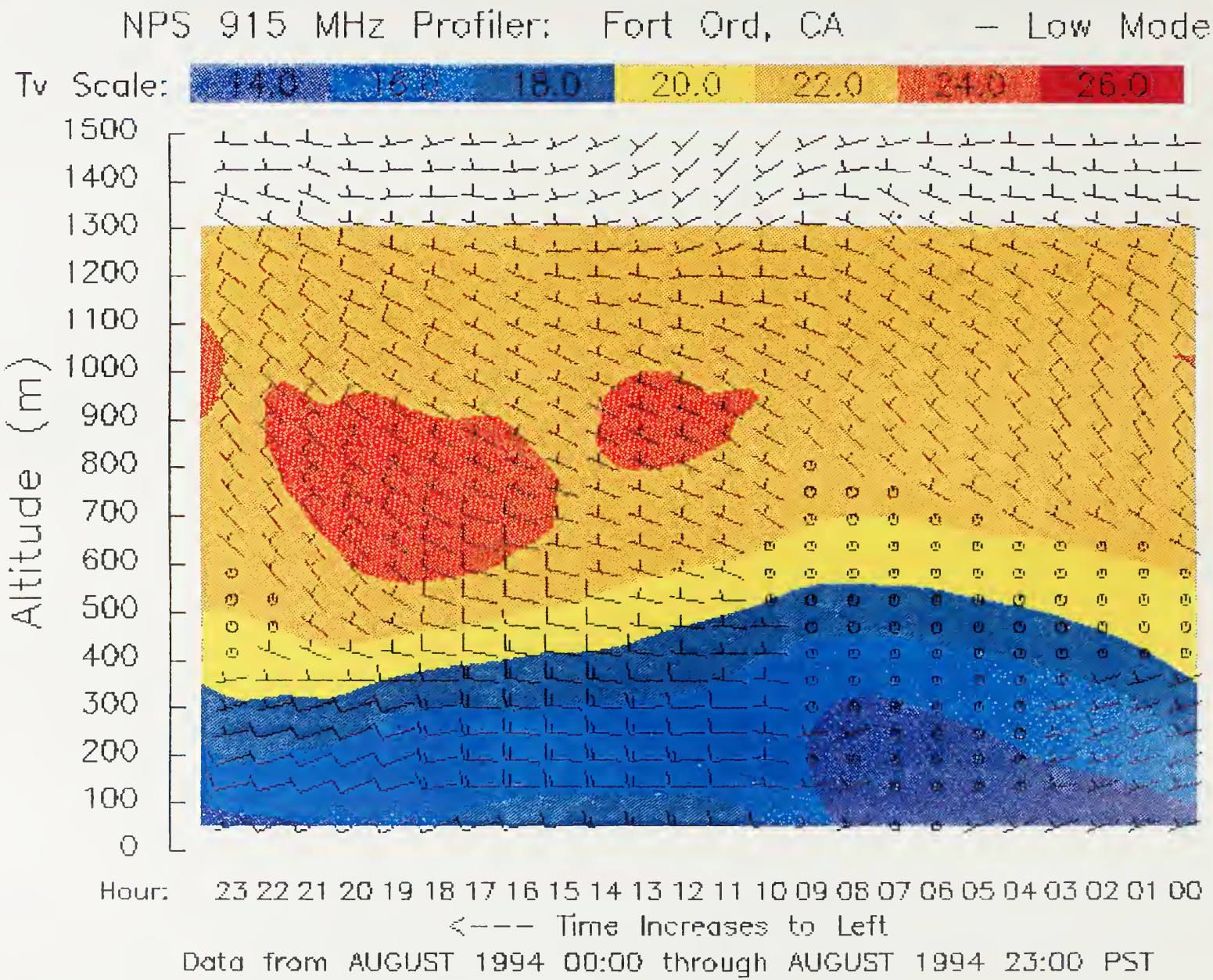

Figure 5. 915-MHz wind profiler averages for 1-31 August 1994 at Fort Ord, CA. The data returns have 60 m resolution. Stec (1996)

III. THE CASE STUDY

Prescribed burns are becoming important tools in forest management. It reduces the risk for extreme forest fires that can destroy housing and devastate the ecosystem. On 25 August 1997, a controlled burn was ignited on the former Fort Ord Army base in order to clear brush to allow environmental clean up teams to search and remove ordinance. This fire was intended to burn 400 acres, but instead ended up raging out of control caused by an alleged military flare that was launched across control lines into an unburned area. The unanticipated sea breeze literally pushed the flames eastward towards a housing development located on the Salinas River bluffs on the backside of the fort. Flames began to subside as the sea breeze began to subside, but not before consuming 700 acres while burning near the housing development and filling the Salinas Valley with acrid smoke (Figure 1). The air quality/pollution control board received numerous complaints resulting in an investigation.

The following sections are a detailed look at the sea breeze evolution as it occurred across the Monterey Bay region, as observed by the Naval Postgraduate School's Doppler wind profiler and surface observation site, and the preceding synoptic conditions.

A. THE SEA BREEZE EVOLUTION

The sea breeze evolution over the former Fort Ord will be described using the Fort Ord profiler site given its previous application in research and its proximity to the fire (less than 5 miles away). On this particular day, the sea breeze was not a classic sea breeze. Figure 6a,b shows the time series of Fort Ord surface observations indicating that there were two separate speed jumps in the wind. The first is a gradual increase in the wind speed at 1600 UTC and the second is a more pronounced speed jump at 2000 UTC. This sea breeze is a double surge sea breeze (Round 1993). The only variability in the wind direction occurred when the speed decreased to light and variable in the morning hours from 1200 UTC to 1500 UTC. This is most likely the offshore flow or land breeze weakened by the large-scale flow. After the initial onset of the sea breeze, the wind speed increases and the direction shifts to continuous westerlies thereafter. There is no jump in dewpoint temperature, as might be expected in a classic sea breeze but a slight drop and leveling off. The wind speed shows a very gradual increase in speed to 10 kts through 2000 UTC. This is hypothesized to be in response to the local heating of the Salinas Valley, the local sea breeze. The pronounced second surge in the wind speed from 10 to 20 kts between 2000 UTC and 2100 UTC (Figure 6a) is hypothesized as a deep or large-

scale sea breeze similar to that described by Banta (1995) and Wexler (1946). The sea breeze remains strong until 0100 UTC when the wind slowly drops to calm by 0800 UTC (Figure 6b).

The vertical structure of the observed sea breeze can be determined from the Ft. Ord profiler (Figure 7a,b). The profiler also shows calm winds initially from 1200 UTC to 1600 UTC in the lowest 600 meters to 800 meters later in the morning. The initial sea breeze is confined to the lower levels, 300 m to 400 m and below from 1600 UTC until the second surge at 2100 UTC associated with the large-scale sea breeze. The stronger, deeper winds of the large-scale sea breeze climb from approximately 400 m at 2100 UTC to 800 m by 2300 UTC. This level corresponds to the average height of the onshore flow of the sea breeze based on the monthly average composite for August 1994 (Figure 5). This deep flow continues until 0300 UTC 26 August at which time the height of the sea breeze circulation drops sharply to 500 m and then weakens or reverses to a land breeze by 0700 UTC. A similar scenario is seen in Stec's (1996) average composite. A weak inversion formed at about 600 m during this sea breeze evolution starting at 2000 UTC 25 August, with the onset of the large-scale sea breeze and the invasion of marine air. The inversion weakens after 0600 UTC 26 August and burns off after 1800 UTC 26 August. This contrasts sharply with the average structure shown in Figure

5, which shows a strong inversion of 8°C and a marine layer depth of 450 meters. Key differences between the day of the fire and the monthly average are that the maximum heating occurred at the surface the day of the fire versus aloft in the monthly average. The temperatures at 800 meters are 6°C warmer on an average day resulting in a stronger inversion. At the surface, the average temperatures are 5°C cooler than those recorded on the day of the fire. This strengthens the argument that the temperature gradient remained along the coast until the large-scale sea breeze propagated inland. The local forcing in the Salinas Valley is not the main driving factor for the sea breeze front (the temperature gradient) to propagate inland, but rather, the larger scale sea breeze front propagating into California's Central Valley is responsible for the push of the marine air inland over the Monterey Bay area.

Horizontal plots of the observations over the region demonstrate the complexity of the forcing of the sea breeze. In the early morning (Figure 8), the wind speed at 1800 UTC increases from less than 5 kts to 10 kts at Salinas and elsewhere and turns up valley (northerly) before the large-scale sea breeze has begun at the coast. The winds along the Monterey Bay coastline are less than 5 kts. Due to the northwest/southeast orientation of the Salinas Valley to the Monterey Bay, the wind increase could be confused as the start to the large-scale sea breeze except that the winds at

the coast are weaker than those in the Salinas Valley. Potentially, the heating of the eastern face of the coastal mountains bordering the Salinas Valley to the west in the early morning hours results in rising motion along the mountains, thereby initiating a mountain-valley circulation. The temperature rises as dew point and relative humidity drop at the profiler site at 1800 UTC (Figure 6a), not typical of the classic sea breeze. This initial surge of winds is therefore believed to be a local thermally driven circulation in the Salinas Valley. There is no indication of this local sea breeze in the mountain passes to the north and east of the Monterey Bay (top right hand corner of Figure 8) during this time confirming that this is specific to the Salinas Valley. Figure 9 shows the model terrain to emphasize the mountain passes. This will be further examined with the model data and hopefully prove true the hypothesis of the heating of the east aspect causing the local Salinas Valley sea breeze.

As the day progresses, temperatures keep rising across the region, a large-scale temperature gradient builds along the coast. The large-scale sea breeze starts propagating up the valley at 2100 UTC (1400 PDT) when there is a strong thermal gradient along the coast resulting in the wind speed increasing to 15 kts. This speed maximum is seen in the time series (Figure 6a) as the sea breeze winds increase abruptly at the observation sites up the Salinas Valley. By

0000 UTC 26 August (Figure 10) the sea breeze has propagated up the Salinas Valley to well past King City, evident by the 15 kts winds. By this time it has passed through the southern tip of the Santa Clara valley where it then merges with the sea breeze from the north and pushes through the Pacheco Pass and into California's Central Valley. According to the observations, there is a strong response to the air mass temperatures differences seen in Pacheco Pass, which is most likely, enhanced by terrain. Wind speeds start out at 10 knots in the morning hours, but increase to 15 - 20 knots once the sea breeze reaches the pass and remains strong through 1200 UTC 26 August, the end of the case study. This terrain-induced flow will be examined more closely with the model simulation.

B. THE SYNOPTIC CONDITIONS

The synoptic pattern changed very little over the Monterey Bay during the fire. The upper-level flow is characterized by southwesterly flow downstream from a broad upper-level through over the Eastern Pacific Ocean (Figure 11a,b). At 1200 UTC 25 Aug, the 300 mb ETA analysis (Figure 11a) shows a jet streak of 90 knots situated over northern California extending through southwestern Oregon. This jet streak intensifies somewhat during the next 12 hours and becomes more southwesterly. At 500 mb, (Figure 11b), the decaying trough off the Pacific Northwest coast begins to

amplify after 1200 UTC 25 August as two weak short waves move through the trough. Even so, there is little change in the 500 mb height pattern over the Monterey Bay area. At the surface (Figure 11d), a weak surface ridge extends Northeastward across Northern California from a high center near 30°N 130°W. A broad area of low pressure remains off the Pacific Northwest coast below the upper trough through 26 August. During the next 12 hours, the thermal low starts to deepen over the northern Gulf of California and the Desert Southwest in response to the desert heating and the short wave rotating through the 500 mb trough. By 0000 UTC 26 August (not shown) the thermal low broadens covering the Intermountain West while centered in the vicinity of the 4 corners region. In response to this and the 500 mb short waves rotating through the trough, the surface ridge retreats resulting in an increased synoptic pressure gradient across central California. The surface ridge axis across northern California at 1200 UTC 25 August starts to slide down the coast as the upper trough amplifies where it establishes itself in the San Francisco Bay area by 0000 UTC 26 August. The 850 mb pattern, shown in Figure 11c, looks very similar to the surface with a ridge centered around 30°N, 130°W with the heights remaining rather flat over the Central Coast. The evolution of the 850 mb height pattern during the next 12 hrs results in the 850 mb ridge axis becoming more pronounced just off the Central California

coast and into northern California. This is consistent with the intensification of the trough aloft.

Based on the synoptic description above, which is shown in Figure (11d), this synoptic pattern best fits the Ridge pattern described by Knapp (1994), Figure 2. This pattern is generally described as having a weakly stratified atmosphere and allows the potential for coupling of the sea breeze winds with the background flow. If the stratification is strong, then the sea breeze and the background flow are decoupled by the inversion, which is not observed in this case study.

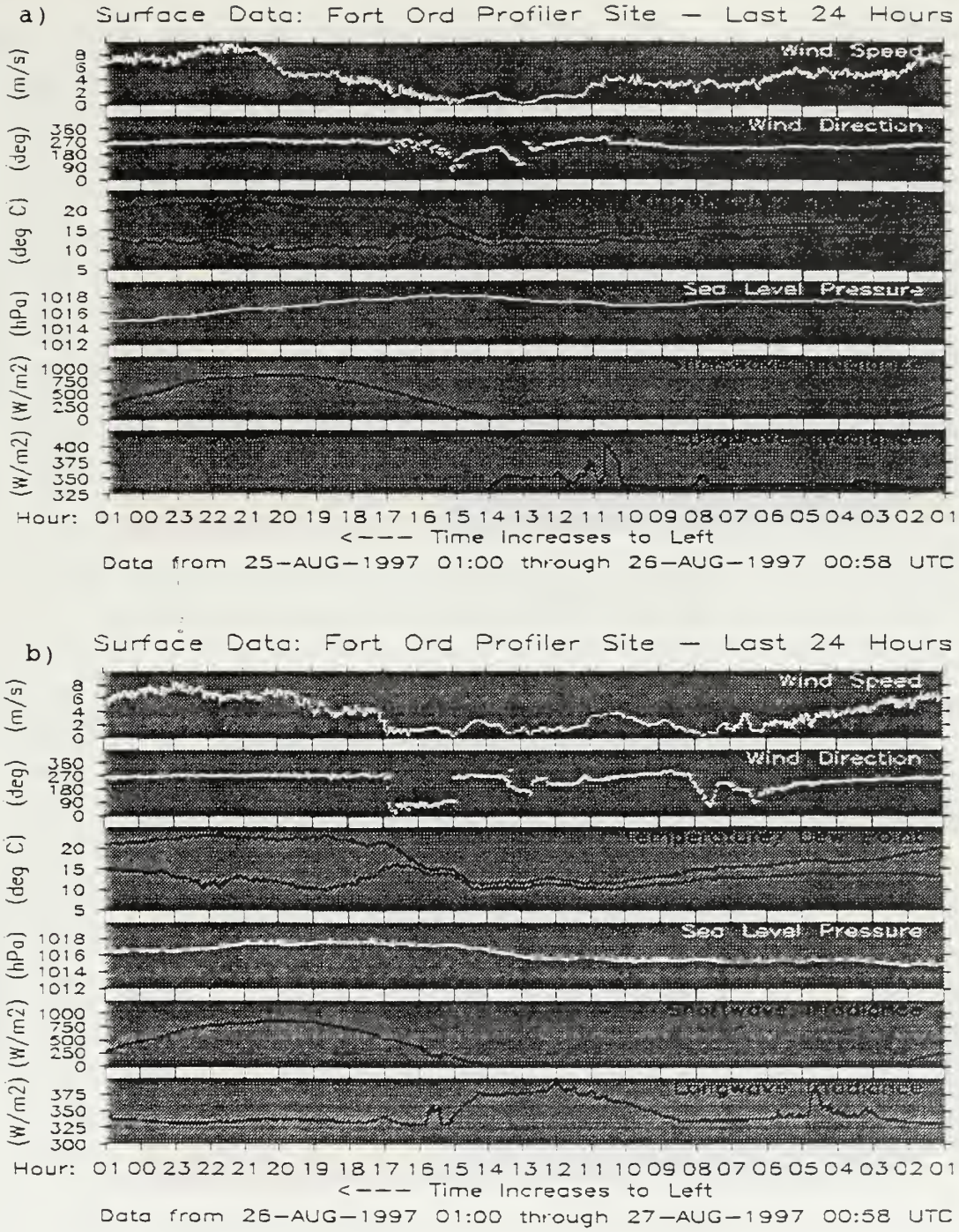

Figures 6a,b. Surface observations from the Fort Ord profiler site on (a) 25-26 August UTC and (b) 26-27 August UTC.

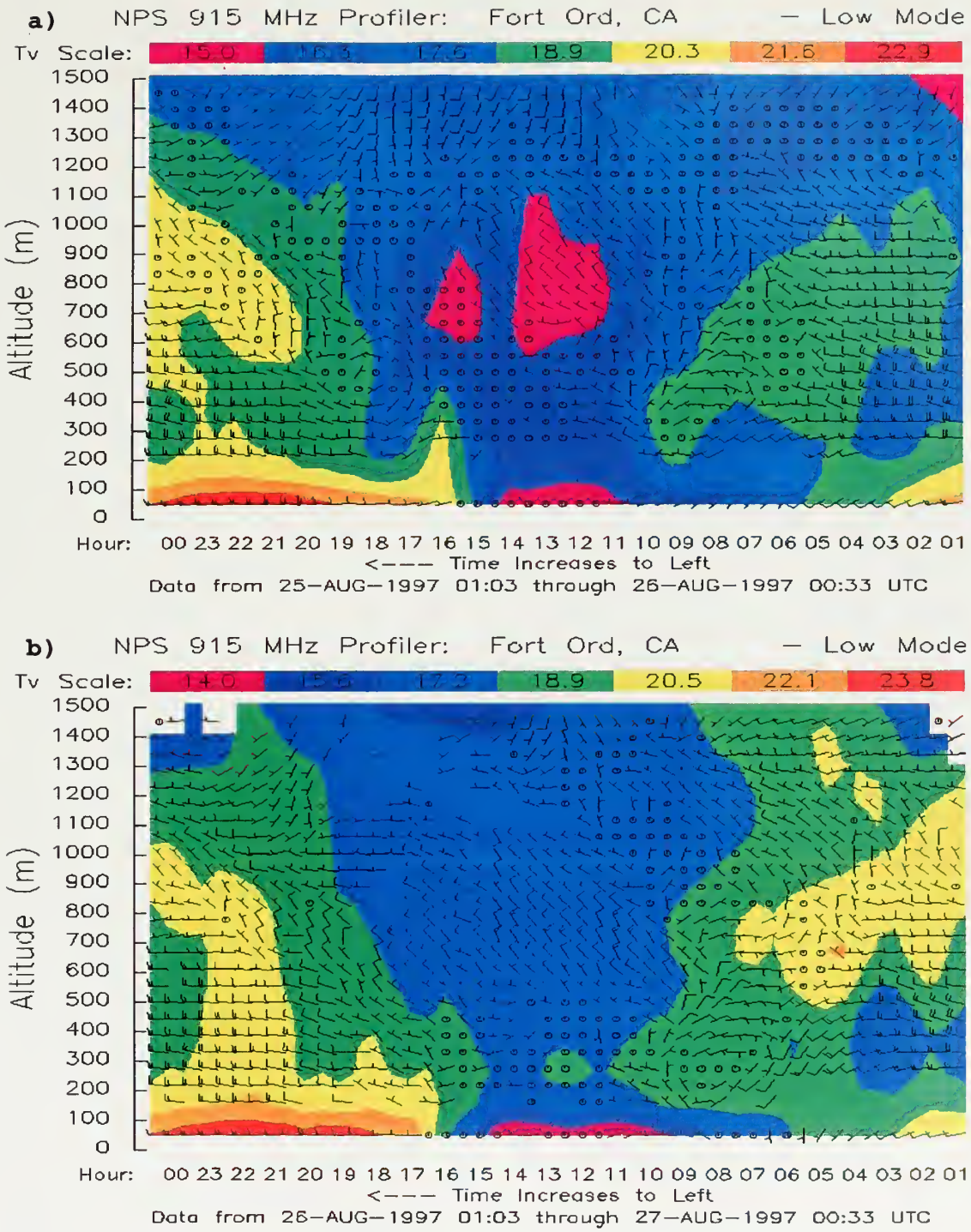

Figures 7a,b. 915 MHz profiler wind and virtual temperature profiles for (a) 25 August UTC and (b) 26 August UTC at the Fort Ord proflier site.

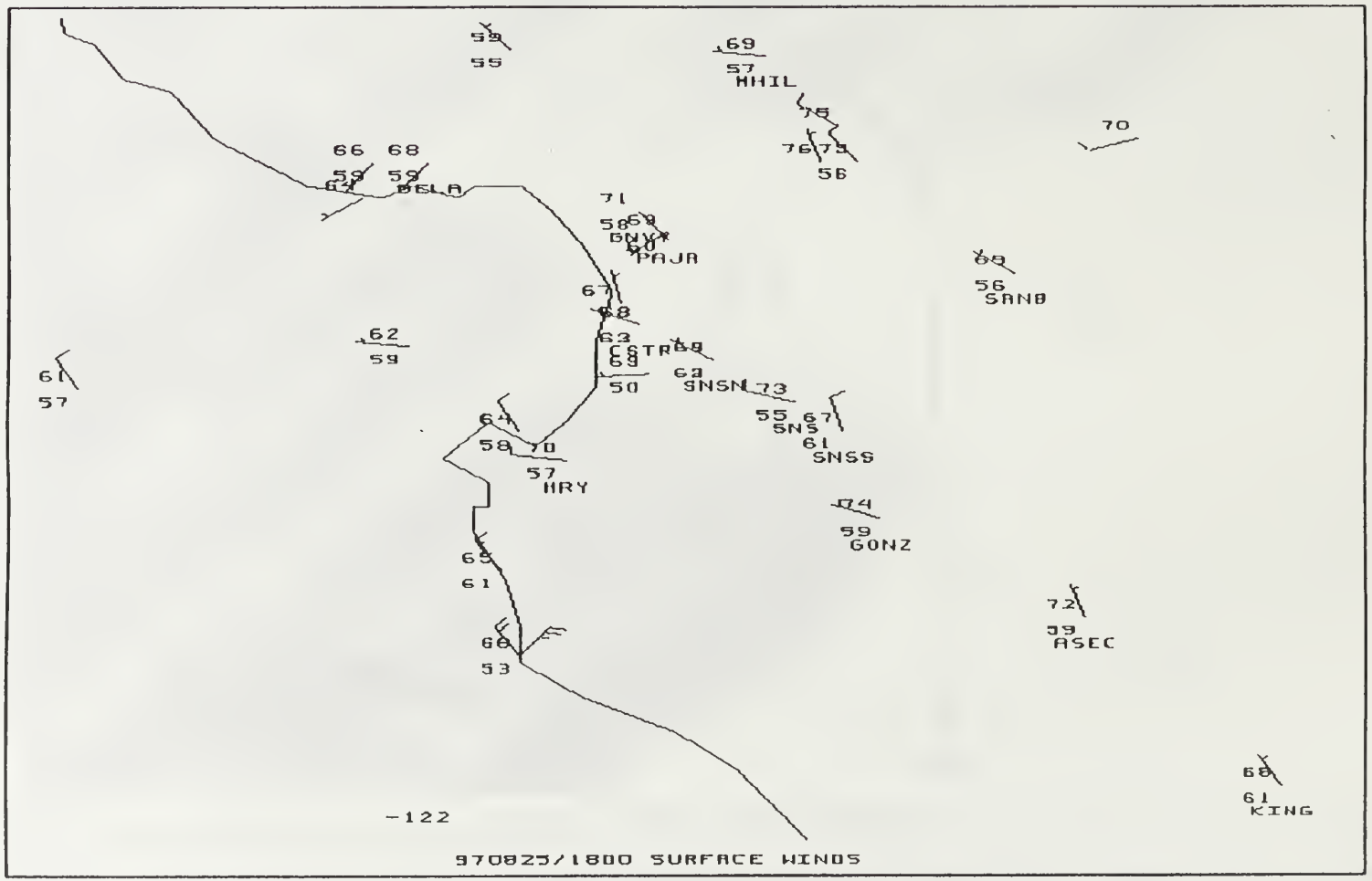

Figure 8. The 1800 UTC surface reports for the Monterey Bay/Salinas Valley region. These data include the METAR, REINAS and CIMIS sites.

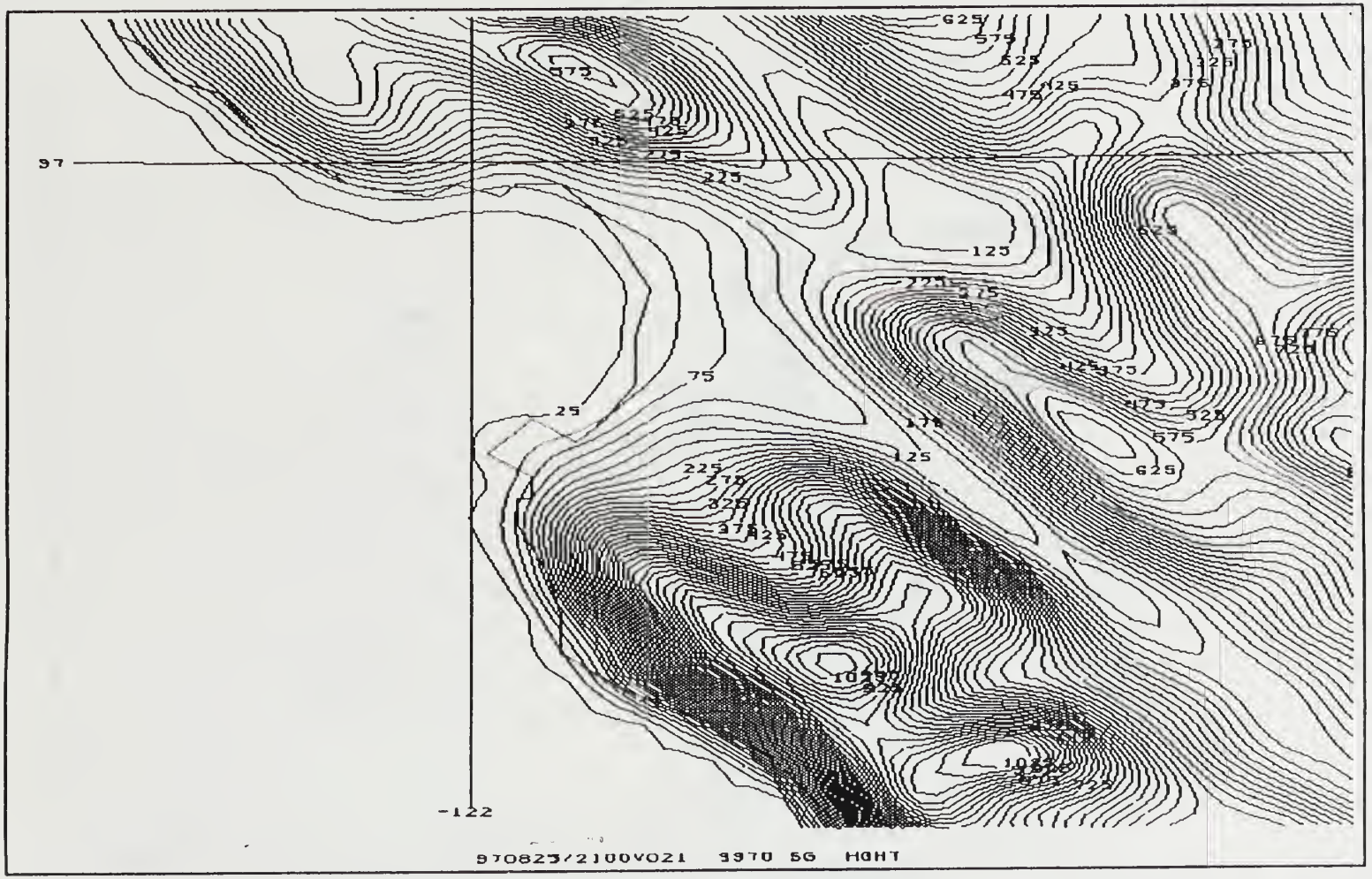

Figure 9. MM5 model terrain at 4 km resolution and contoured at every 25 m, starting at 25 m.

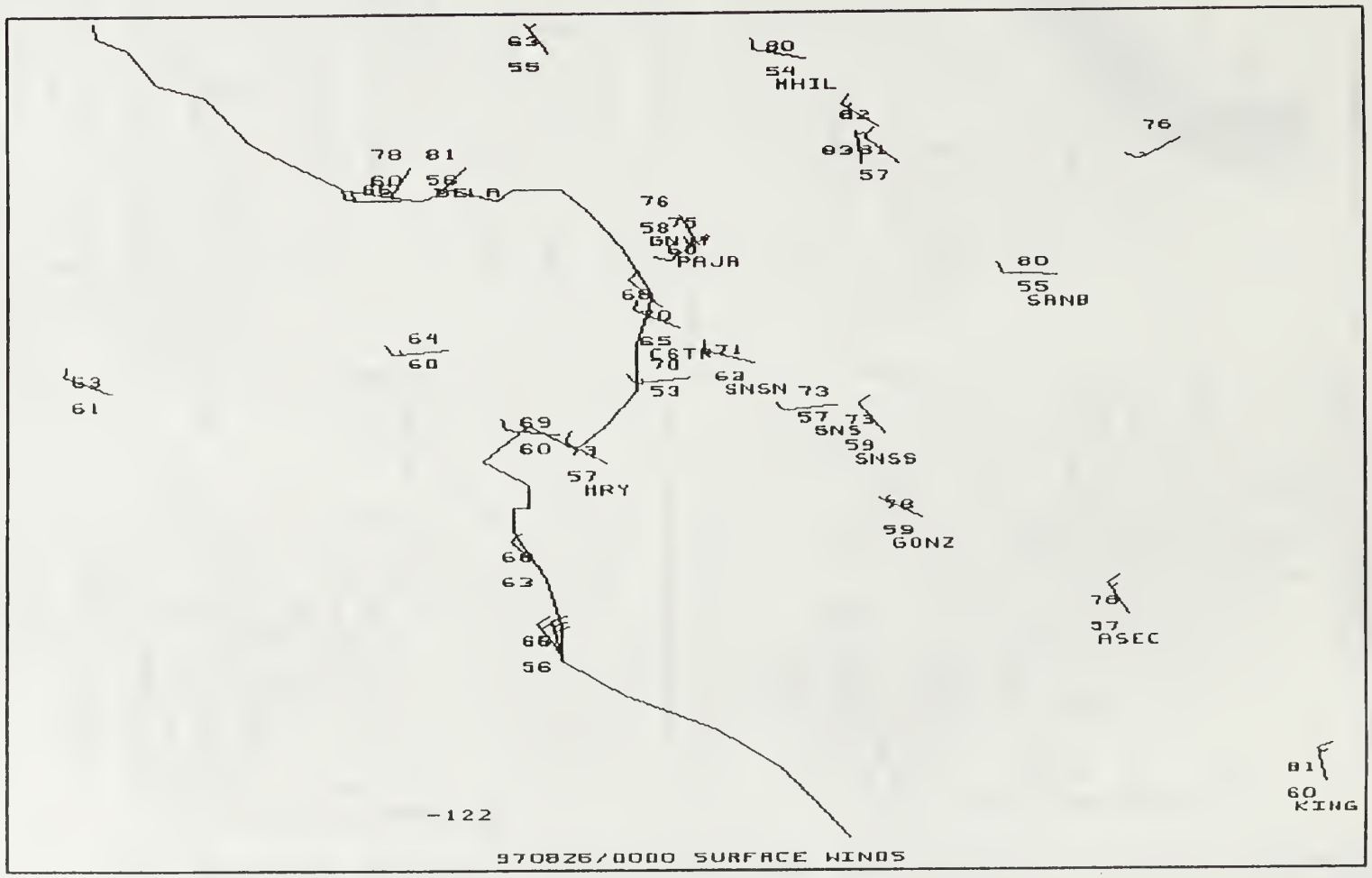

Figure 10. Same as Figure 8, except at 0000 UTC 26 August.

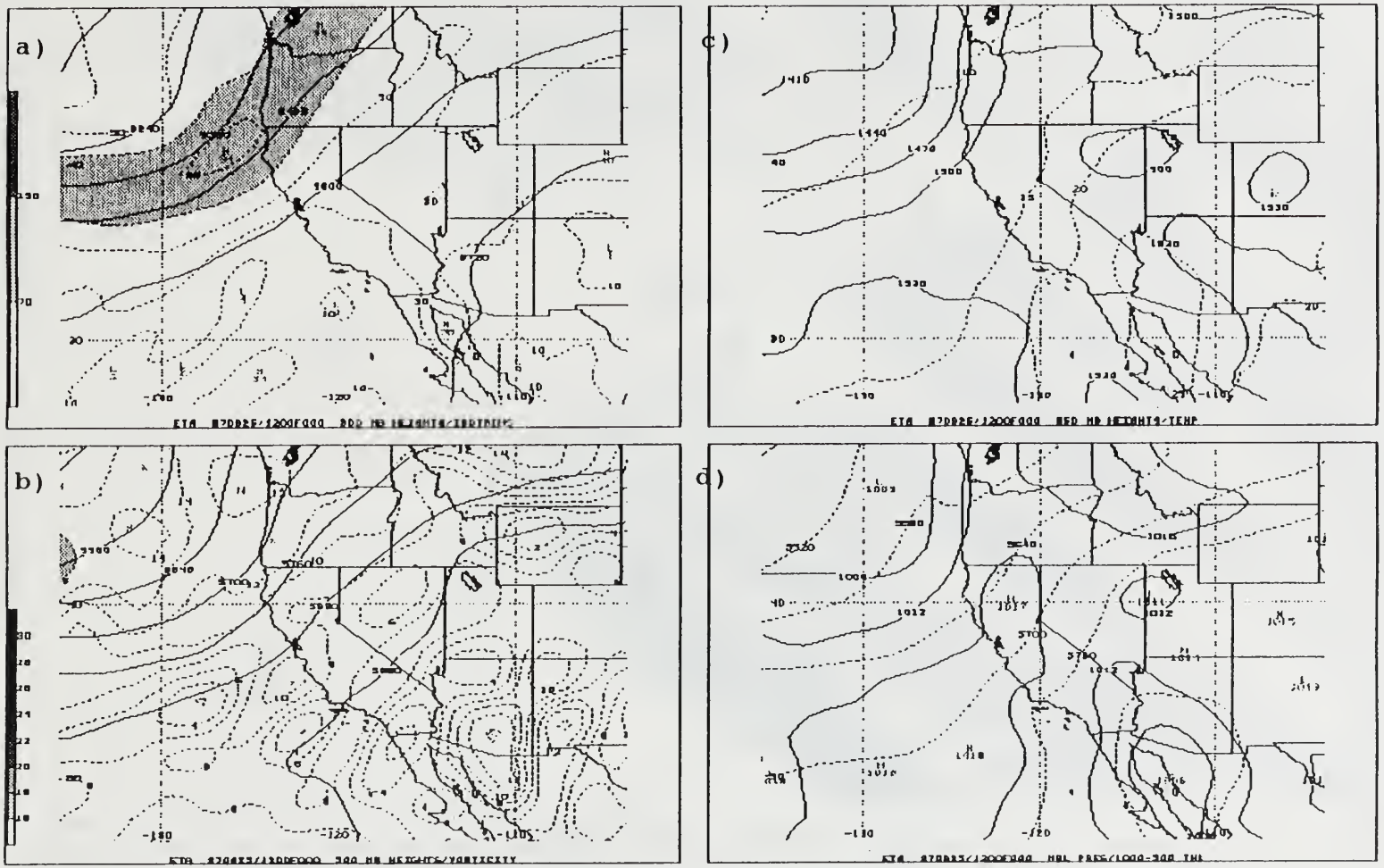

Figure 11a,b,c,d. The 970825 1200 UTC ETA analysis at (a) 300 mb heights and isotaches, (b) 500 mb heights and vorticity, (c) 850 mb heights and temperature, (d) mean sea level pressure and 1000-500 mb thicknesses.

IV. THE MODEL AND DATA

A. THE MODEL

The fifth generation PSU/NCAR mesoscale model (MM5) version 2 (Grell et al. 1995) was used to simulate the sea breeze and mesoscale structure over the Monterey Bay area for this case. There were four MM5 domains used for this case which are depicted in Figure 12. The outer domain had a grid resolution of 108km grid, the inner domains were 36km, 12km and finally 4km. The model had 30 vertical levels with 12 below 850 mb.

Unique to the Naval Postgraduate School (NPS), this model was initialized with a two-dimensional Multiquadric Interpolation scheme (Nuss and Titley 1994) using available GEMPAK format observations and the Navy's NOGAPS (Bayler and Lewitt 1992) data instead of the more common four-dimensional data assimilation system via nudging and the NCAR database. This scheme is a univariate multiquatric interpolation such that each variable is analyzed independently of others. Two-dimensional interpolation implies data is interpolated at a given level independent of influences from other levels, which can be a disadvantage in some cases. Each grid was initialized separately to retain the finest structure for a given domain. In other words, this allows each domain down to the four-kilometer grid to

initialize independently with the two and a half-degree NOGAPS analysis for the boundary and initial first guess conditions in the outer domain every 12 hours out to 36 hours. The initialization included observations from the GEMPAK data and the Real-time Environmental Information Network and Analysis System (REINAS) mesoscale network. The larger domains would have the tendency to smooth out the REINAS data due to the grid spacing, therefore the initial first guess was used in all four domains. MM5 was started from a cold start, which means that there were no cloud or rain fields in the model initially and the mass and wind field was not balanced in the model. This adjustment process as well as the lack of vertical structure in the NPS NOGAPS GEMPAK files, which only has 11 standard pressure levels plus one at the surface, requires a minimum of six hours for the model to achieve dynamic balance and develop realistic vertical structure, particularly within the boundary layer. The model was initialized at 0000 UTC 25 August to allow the model to spin up prior to the development of the sea breeze on August 25.

To assess the impact of the PBL evolution on the sea breeze, MM5 was run twice using different planetary boundary layer parameterizations, the Medium Range Forecast (MRF) scheme (Hong and Pan 1996) and the second run used Burk-Thompson (Burk and Thompson 1989). The MRF scheme has a 6-layer soil model and the Burk-Thompson scheme treats the

surface as a slab. Although no more detail of the PBL schemes will be given since it beyond the scope of this thesis, the difference between the simulations were examined to determine the impact of the PBL scheme on the results. The Burk-Thompson scheme was considered the default model run. The Sea Surface Temperature (SST) field used as MM5 input was a one-degree NOGAPS SST analysis. Kain-Fritsch cumulus parameterization (Kain and Fritsch 1990) was chosen along with Dudhia's simple cloud and ice microphysics (Dudhia 1989)(these choices should have minimal impact on the model run since the skies were clear during the event). The temporal resolution of the model output is hourly out to 36 hours. Each run had the 15 lower levels interpolated to isobaric levels into GEMPAK format files to allow for visualization and savings of computer space and time.

B. THE OBSERVATIONAL DATA

The data used in this experiment were from a wide variety of sources. The most reliable data was the Fort Ord Profiler site data, including both the surface observations and the profiler data from a 915 MHz boundary layer wind profiler and a Radio Acoustic Sounding System (RASS). METAR and upper air reports were used from the Unidata Internet feed.

In an attempt to improve the forecast of the Mesoscale model, METAR and upper air GEMPAK files, along with the

REINAS mesoscale observations were used in the initialization. REINAS is a joint venture between the University of Santa Cruz and NPS in which a Mesoscale network of observations can be stored and retrieved in real time. The goal of this project is to provide an environmental database to advance both real-time and retrospective regional scale environmental sciences (Stec 1996). Since its inception, additional data has been added to REINAS. These include The California Department of Forest and Fire Protection weather stations, California Irrigation Management Information System (CIMIS) data, National Weather Service/FAA ASOS data, besides the REINAS mesonet stations. Unfortunately the CIMIS data was not available for inclusion in the model runs, but was made available later in the research to be included with the above mentioned data sets for model verification.

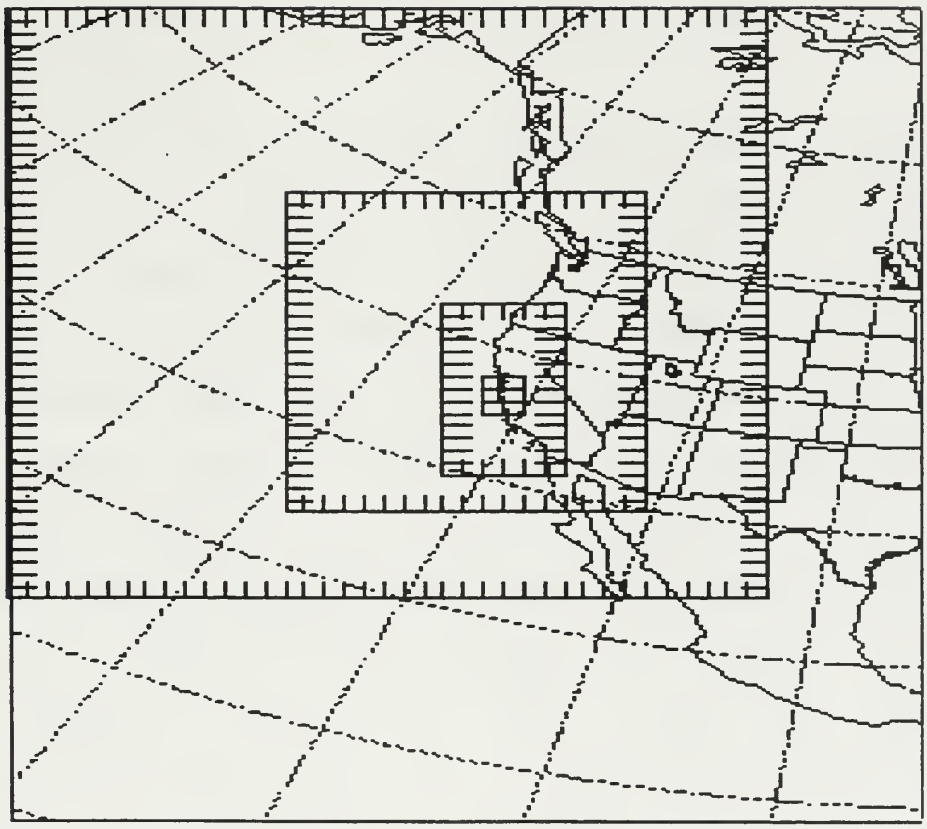

Figure 12. MM5 nested domains shaded, 108 km, 36 km, 12 km, 4 km.

V. THE MM5 MODEL SIMULATION

A. SURFACE EVOLUTION AND COMPARISON TO OBSERVATIONS

To gain confidence in the model simulation, the available data were used to verify horizontal and vertical sea breeze signatures over the time period of the fire. Model verification started at 1200 UTC 25 August and ends at 1200 UTC 26 August.

The sea breeze evolution simulated over the Monterey Bay area is very similar to that of the actual sea breeze recorded by observations. Figure 13 shows the 12 hour forecast and observed winds are light and variable at 1200 UTC 25 August over much of the Monterey Bay and Salinas Valley region. Figure 14 shows the Model terrain along with the cross section as a point of reference. A 12 hour forecast cross section from over the Monterey Bay and through the Salinas Valley (Figure 15) shows that light winds extend up through 870 mb. This flow persisted throughout most of the morning hours with some offshore (easterly) flow through the Pacheco Pass and through the Route 101 corridor located to the northeast of the Monterey Bay. At 1800 UTC (Figure 16) a distinct sea breeze develops at the Monterey Bay coastline as indicated by the cross coast winds in the model (18 hour forecast), which agree well with observations along the coast. Within the Salinas

Valley, northwesterly winds also develop in the model in agreement with the observations in that region. This northwesterly flow in the model is distinctly separated from the coastal sea breeze by a zone of northeasterly flow between the coast and the city of Salinas. The observed winds in the Salinas Valley show a light northwest wind at 1800 UTC, while the 18 hour forecast near surface winds show the flow lifing up the valley slopes. These surface observations compare better to the 890 mb 18 hour forecast winds (Figure 33) since the valley floor is close to this pressure level. This suggests that the coastal and Salinas Valley circulations are forced by different mechanisms. This is also evident in a cross section of the Salinas Valley extending out into the Monterey Bay (bottom left hand corner of Figure 17), which shows a very shallow sea breeze at the coast and deeper Northwesterly flow in the Salinas Valley. At 2100 UTC (Figure 18) when the second surge in sea breeze winds in the Fort Ord time series occurs (Figure 6a), the cross coast flow has propagated inland reaching such places as Salinas (SNS) and Castroville (CSTR), with no distinct Salinas Valley circulation. The cross section at 2100 UTC (Figure 19) shows the local forcing through the middle of the valley, where the winds are 10 kts. The stronger surface winds of 15 kts are still behind the temperature gradient, which is just moving onshore (the bottom left hand corner of Figure 19). The modeled and

observed surface winds in Figure 18 agree very well everywhere except at Pacheco Pass (PACH) and out in the middle of Monterey Bay at buoy M1.

By 0000 UTC (Figure 20), the winds have increased in both the model and observations to 10 knots from the north/northwest at King City (KING) in the south part of the Salinas Valley. The stronger winds in the model lag the observed onset of the sea breeze by approximately 1 hour at stations in the Salinas Valley. The near surface winds in both the model and observations peak at 15 knots in the middle of the Salinas Valley. The 0000 UTC 26 August cross section (Figure 21) shows a strong temperature gradient throughout the Salinas Valley. The vertical extent of the sea breeze seems to be higher over the Salinas Valley reaching up to 890 mb, while out over the Monterey Bay the height of the sea breeze is only 965 mb. An offshore flow occurs above the sea breeze located over the bay, which may be influenced by the easterly flow of Pacheco Pass. In addition to the wind increase in the Salinas Valley, the observed wind in Figure 20 also increases from the west/southwest through the 101 and Pacheco passes. The model depicts this except in the Pacheco Pass region, where the flow is considerably weaker than the observations and the wind direction is opposite to what is observed through the majority of the day. This will be discussed in more detail later.

After the sun sets, around 0300 UTC, the winds begin to die down and become light and variable in both the model and observations in the Monterey Bay area and the strong winds in the Salinas Valley subside with time to become light and variable by 1200 UTC 26 August. Offshore flow develops in the model on the northeast side of the Monterey Bay, similar to that found at 1200 UTC 25 August and in close agreement with the observations in that region.

To gain insight into how well the model simulation depicted the thermal forcing of the low-level flow, the model surface temperature fields were compared to surface observations. This comparison showed that the temperatures during the burn day were reasonable during the daylight hours, but during the nighttime hours the model showed a significant warm bias. This warm bias is most obvious in the Salinas Valley where temperature differences at 1200 UTC 25 August (Figure 22) are greater than 10°F. This bias vanishes with the diurnal heating and by 2100 UTC the model forecasts temperatures within 1-3°F of observations across most of the region. Even in the tight gradient along the bay, the temperatures are within 3°F of the observations. There is some hint of larger model errors in California's Central Valley where the model temperatures are 3-5°F cooler than the observed temperatures (upper right corner of Figure 23). This error would have adverse effects on the thermal forcing through Pacheco Pass and will be discussed later.

There is reasonable agreement in the vertical structure when comparing the Fort Ord boundary layer wind profiler/RASS winds and temperatures (Figure 7a,b) to the model time/height series at the same latitude and longitude as the profiler (Figure 24). The vertical structure of the model winds (Figure 24) is similar to the profiler observations. The sea breeze at the surface starts by 1800 UTC and then deepens to a height of 930 mb or approximately 700 meters by 0000 UTC similar to the profiler observations (Figure 7a,b). Both show very weak winds above the sea breeze through the period of the sea breeze evolution (1800 - 0000 UTC). After 0000 UTC, the model forecasts strong northeasterly flow, which was not evident in the profiler. The profiler shows winds increasing aloft, but not as strong as the model and from the northwest instead of the northeast as in the model. The thermal structure aloft at the initiation of the sea breeze is rather similar, although the profiler shows more detail. The temperature gradient in Figure 18 that rises to 850 mb at 1800 UTC is symbolic of the whole column of air warming. The major problem in the model, apparent in both the vertical and horizontal plots, is the warm bias during nocturnal cooling after 0600 UTC on 26 August. This error can be as much as 5°C.

Time series plots of temperature and winds show that the model described the general trend of the sea breeze evolution both over land and out over the bay. The sites at

buoy M1 (Figure 25a,b) Salinas (Figure 26a,b), King City (Figure 27a,b), Pacheco Pass (Figure 28a,b), are chosen as a fair representation of the sea breeze flow in the Monterey Bay and Salinas Valley region. The general onset of the simulated sea breeze was within one hour of the observed and the time of maximum temperatures were also with one to two hours of the observed at all four sites. The largest discrepancies occurred after the sea breeze cycle during the night when the model had a significant warm bias except over the water. During this same time, after 0600 UTC, the wind speeds are also higher than the observed at all the sites. The wind direction was also generally correct at these three sites although at M1 and Salinas, the model winds tend to be too northerly and westerly, respectively. The site with the most noticeable difference is Pacheco Pass shown in Figure 28a,b. It was mentioned earlier that the model did not forecast the correct speed or direction throughout most of the sea breeze evolution. This time series shows that the winds were 180° from the observed through the entire 24-hour period. It also shows that the model sea breeze does not make it through the pass and into the Central Valley at the surface. This is most likely caused by incorrect thermal forcing at the surface between the coastal valleys and the Central Valley of California, which will be examined in the impacts of PBL parameterization section (Section C) of this Chapter.

Local mountain-valley forcing was simulated in the Salinas Valley in the early morning hours, 1200 UTC to 2000 UTC 25 August before the large-scale sea breeze develops. Northerly wind at Salinas (Figure 26a) through 2000 UTC suggests forcing from the mountain passes near Prunedale and from the southern extent of the Santa Clara Valley. The wind shifts with a slight westerly direction as the local forcing changes to sea breeze forcing after 2000 UTC. This site loses that westerly component by 0400 UTC 26 August after the sea breeze dissipates; and a north wind lasts through the end of the model simulation, 1200 UTC 26 August. The simulated winds keep an onshore (westerly) component through the entire 24-hour period. This localized increase in the northerly flow between 1500 UTC and 2000 UTC 25 August is in response to the heating of the eastern-facing mountainsides adjacent to the Salinas Valley. This increase in northerly flow is seen all along the Salinas Valley at 1800 UTC 25 August (Figure 29). The east and south aspects are heated first in the morning hours, evident by the near surface winds and the potential temperature at 1800 UTC. The potential temperature rises 4°K from 1200 UTC 25 August to 1800 UTC (Figure 30). The near surface wind follows the terrain up these particular slopes representing an acceleration forced by the thermal gradient. The winds respond to this by changing direction along the slope and increasing in speed to 10 kts in the Salinas Valley. By

2100 UTC (Figure 30) the heating shifts to the west aspects in the Salinas Valley, evident by the 4°K increase on the west aspects while the east aspects only rise 2°K in three hours. After 2100 UTC the sea breeze starts propagating southeastward through the Salinas Valley. By 0000 UTC 26 August (Figure 31), the sea breeze has propagated all the way to the southern end of the Salinas Valley and has deepened, filling the entire valley with onshore flow, which dominates any residual local forcing. A similar scenario takes place in the southern Santa Cruz Mountains. The potential temperature increases 3-4°K over the southern slopes of the mountains between 1200 UTC and 1800 UTC (Figure 29). By 1800 UTC the near surface winds turn and indicate rising up the slopes. The warming continues through 2100 UTC (Figure 30) over the mountains as the west aspects are being heated and the winds respond with a cross-coast component.

B. 3-D SEA BREEZE EVOLUTION

The three dimensional evolution of the sea breeze over the Monterey Bay region was determined by examining the flow at various levels above the surface. The 980 mb level winds and temperature show a similar evolution as the surface (in some areas, the 980 mb level is at the same elevation as the 9970 sigma level), which was mentioned above, but the signature is much stronger. There are light and variable

winds in the Salinas valley through 1400 UTC (Figure 32), but a persistent offshore flow that develops after 1400 UTC through the Pacheco Pass and the 101 corridor and out across the Monterey Bay. This flow intensifies by 1600 UTC, after which it remains steady until 1800 UTC. The winds and temperatures at 1800 UTC (Figure 33) demonstrate that the initial sea breeze at the surface is very shallow. Offshore flow is evident across the Monterey Bay at 980 mb where the surface winds are westerly. This offshore flow gradually weakens as the thermal gradient increases.

At 2100 UTC (Figure 34), the offshore flow has switched to weak onshore flow across the thermal gradient. By 2200 UTC, the winds have increased at Salinas and are increasing as far inland as Aroyo Seco. The sea breeze front (Strong thermal Gradient) propagates up the Salinas Valley with a speed of 20 km/hr or 10 kts, reaching King City by 0000 UTC 26 August (Figure 35). The same pattern of the stronger winds lagging behind the front are seen with 15 to 20 knot winds roughly one hour behind the sea breeze front. These strong winds remain throughout most of the valley from Soledad to King City and southward. The flow at this level shows little penetration into the Central Valley, although westerly flow increases at San Juan Batista by 2300 UTC. The offshore flow seen at 1200 UTC is reestablished over the Monterey Bay by 0900 UTC, but does not occur in the Salinas Valley.

The temperature pattern at 980 mb in the previous figure shows the thermal gradient advects along as a sea breeze front. However, most striking is the warming that occurs over the Monterey Bay at 2100 UTC (Figure 33), which is probably caused by the subsidence from the return flow above this level. There is a significant difference between the temperatures at 1010 mb (near the surface) and 980 mb. The 1010 mb temperatures are with in 1-2°F of the observations from the buoys in (Figure 36). The temperatures at 980 mb are up to 10°F warmer than those at 1010 mb and those reported by the buoys, which results in establishing a relatively strong near surface inversion. This 980 mb heating develops after the start of the cross shore winds of the sea breeze and slowly cools after the sea breeze dissipates, which suggests it is produced by the sea breeze circulation.

The sea breeze in the time series and profiler extends up to 965 mb or approximately 470 meters. A similar evolution occurs at this level as it does at 980 mb. The temperature gradient is much weaker along the coast, but starts propagating inland at 2100 UTC (Figure 37) even with offshore flow all along the bay. The onset of the sea breeze at this level is delayed by one hour when compared to the onset at the surface, matching the delay seen at the same level at the Fort Ord profiler site (Figure 7a). The offshore flow turns into the Salinas Valley before the winds

along the coast develops an onshore component. This is most likely because local mountain-valley forcing acting prior to the large scale sea breeze forcing. The winds are strong down the Salinas Valley with a speed maximum of 20 knots. The region of stronger winds propagates up the valley, reaching King City by 0000 UCT 26 September (Figure 38). The sea breeze moving through the northern passes is not as obvious, but is distinguishable since there is a wind reversal of 180 degrees. The sea breeze is not as strong as it is down at the surface mainly due to the weaker temperature gradient at this level and due to the fact that mass may be getting advected into this level from the surface. The land breeze returns by 0500 UCT 25 August, but strengthens to 20 kts by the end of the model run.

The large scale flow at 910 mb or 960 meters at 1200 UTC 25 August (Figure 39) favors weak offshore winds since there is a very weak east-west temperature gradient of 4°F and a weak cyclonic circulation offshore. The temperature gradient changes from east-west to a more north-south orientation at 1800 UTC 25 August (Figure 40). Within this north-south temperature gradient there are perturbations over the land caused by the local mountains and valleys. The winds respond to this north-south temperature gradient by turning more northerly. There is one exception to this turning located northeast of the Monterey Bay, where the winds remain from the northeast. This flow is most likely

caused by local mountain-valley forcing. This northeast flow remains over this region through 2100 UTC 25 August. The winds increase from light winds, 5 kts or less at 1800 UTC, to 5-10 kts at 2100 UTC 25 August (Figure 41) as the local temperature gradient increases to 4°F between Monterey Bay and San Juan Batista (SANB), the same magnitude as the east-west gradient that covered the entire region at 1200 UTC. This reversal in the local temperature is most likely in response to the sea breeze forcing. Out over the water, The winds continue northerly with a north-south temperature gradient.

There is some return flow from the sea breeze to the northeast of the bay, but the response is very weak and short lived. There is a wind shift from northerly to northwesterly in the Salinas Valley, but the wind speeds are very weak and only increase to 10 knots well after the sea breeze at the surface has subsided. The easterly winds of the sea breeze return flow start to propagate through the101 corridor and into Pacheco Pass starting at 2100 UTC (Figure 41) and lasts through the end of the simulation.

At 870 mb the flow is influenced by the synoptic scale forcing. At 1200 UTC 25 August (Figure 42) the west to southwest winds show cyclonic turning over the Monterey Bay and north, while the winds turn anticyclonic (southwest to west) south of the Monterey Bay, a pattern which matches the synoptic scale geostrophic flow at 850 mb in Figure 10c.

The 870 mb level will be used to compare the mesoscale simulation with the NCEP ETA model analyses. At 1800 UTC 25 August (Figure 43), the flow over the entire region has turned more west/northwest. The effects of the synoptic scale are evident with the winds opposite the south-north temperature gradient across the Monterey Bay and Salinas Valley region. By 2100 UTC 25 August (Figure 44) the winds are more anticycloninc as they turn from southwest over the ocean to northwest over land. The temperature gradient has also changed to a more northwest-southeast pattern helping to turn the winds at 2100 UTC. This change in the winds at this level is in agreement with the changes that occur synoptically at 850 mb by 0000 UTC 26 August (not shown). The 850 mb ridge strengthens and builds over the Monterey Bay region while the trough retreats north. At 2100 UTC, the 870 mb analysis shows an area of light winds to the east and north of the Monterey Bay. This suggests that the synoptic (background) flow is being acted upon by the return flow of the sea breeze. Since there is no evident reversal of the temperature gradient, the winds, though weak, remain onshore since the return flow is not able to overtake the larger scale thermal forcing from the heating of California's Central Valley. If the background flow, interpolated from the local grid points from the 36 km MM5 domain, (Figure 45) of 5 kts from the west was removed, the perturbed flow would show as east/northeast. At levels

above 870 mb, the flow appears to be primarily driven by the synoptic scale.

During this sea breeze evolution, a pattern was noticed along the boundaries of the 4km domain. The wind flow consistently flowed from the southern extent of the Salinas Valley and into the Central Valley, with return flow, out of the Central Valley and through the Pacheco Pass. This flow pattern was the result of some interesting large-scale circulations in the 12-km MM5 simulation located in the Central Valley. At 1800 UTC (Figure 46), there is a strong cyclonic circulation east of the Monterey Bay and a weak anticyclonic circulation at the south end of the San Joaquin Valley at 890 mb. These circulations may result from interaction with the mountains and valleys, where the major valleys are the inlets and outlets for the flow. This determines the location of these circulations. Further investigation showed that these circulations are probably the result of the changing synoptic scale features. The anticyclonic flow at the southern San Joaquin Valley is in response to the increased ridging over the region, while this same ridging weakens the cyclonic turning east of the Monterey Bay. There is a connection to the evolution of the sea breeze over the diurnal cycle. The sea breeze weakened the cyclonic circulation to the east of the Monterey Bay in Figure 47 while at the same time it enhances the anticyclonic flow in the southern San Joaquin Valley.

Further investigation is needed to both confirm and determine the cause of these circulations and their impact on the sea breeze and vice versa.

C. IMPACT OF PBL PARAMETERIZATION

To examine the impact that PBL parameterization would have on the circulation and to possibly improve the simulation, two MM5 simulations with different PBL schemes, as mentioned in the model description, were compared. Even though both the MRF and Burk-Thompson PBL schemes show a rather strong warm nocturnal bias, it is this author's opinion that the MRF PBL scheme is more successful forecating on the surface temperatures than the Burk-Thompson PBL scheme when compared to observations, as described below.

Incorrect thermal forcing is believed to be the main reason for the poor wind simulation in the Pacheco Pass. The model winds are the opposite of the observed winds in the pass for most of the simulation in both schemes since they underestimate maximum surface temperatures in California's Central Valley. The 12 km domain was used to look at the temperatures in the Central Valley. Figures 48 & 49, and Figure 28ab show that the Burk-Thompson scheme compares better to the surface observations in the coastal valley to the east of the Pacheco Pass with the difference being 1-2°F during the sea breeze cycle. Figures 50 & 51,

and (Figure 28ac) show the MRF scheme as a comparison. In Figures 48, 49, 50, 51 there are some obviuos incorrect observed temperatures in the Cetnral Valley. These observations are located near WEST (76, 77) and to the east of WEST, in the middle of the valley, (76,78 and 70,69). These could result from irrigating the fields, lush vegitaion or probably senor error. The MRF simulated temperatures in the coastal valleys are 4°F higher than the observations. The most significant difference in the thermal forcing was in the Central Valley. The Burk-Thompson scheme had simulated temperatures in the Central Valley at 2100 UTC 25 August (Figure 48) that were 3-4°F cooler than the observed temperatures to the east of Pacheco Pass. This resulted in the incorrect thermal forcing for this area keeping the winds offshore through most of the simulation. The MRF scheme, having a bias, shows a bias in both the coastal valley and in the Central Valley 4-6°F at 2100 UTC 25 August (Figure 50). Even with this warm bias, the MRF scheme simulated a warmer air mass in the Central Valley in the afternoon and may explain why there is a stronger response to the winds turning on-shore in the late afternoon/early evening in the pass and pushing into the Central Valley in Figure 28c.

This lack of thermal forcing across the Pacheco Pass may also be causing the directional discrepancies in the winds over the Monterey bay at buoys M1 Figure (25a,b,c) and

M2 (not shown). A more intense thermal forcing (stronger westerlies) across Pacheco Pass would tend to turn the wind more to the east and north in the Monterey Bay. Again since the MRF scheme forecasts the thermal forcing better and a significant sea breeze that propagates through the pass between 0000 UTC and 0700 UTC 26 August (Figure 28c), the simulated winds show more turning than the Burk-Thompson scheme (Figure 25b,c). The model winds at buoy M1 (Figure 25b) do not back as much as the observed (Figure 25a). There is some hint of the wind backing during the simulated sea breeze, 1800 UTC 25 August through 0300 UTC 26 August as the winds change approximately 20° in (Figure 25b), but the observed winds change as much as 50° at M1 (Figure 25a).

A vertical comparison of the MRF PBL scheme Figure (52) and the Burk-Thompson scheme Figure (53) reveal the general similarities of the two model runs. Based on the model verification, the Burk-Thompson scheme shows strong similarities to the observed sea breeze over the Fort Ord profiler site. Both schemes simulate the warming of the column from 18°C to 21°C between 1500 UTC and 1800 UTC, through both miss the small spike in temperature in the observed data, Figure(7a), around 1600 UTC. The thermal structures during the simulated sea breeze are rather similar. Both show an inversion with the onshore advection of the marine air. The heating aloft is as much as 2°C warmer than the observed data between 2100 UTC and 0300

UTC26 August in the Burk-Thompson model run Figure(53), while in the MRF scheme, Figure (52), temperatures above the inversion are 3°C warmer during the same period than in the observed. Both model schemes are within 1°C of the maximum temperature for the day, but the model runs have the maximum occurring three to four hours earlier than the observed maximum, which occurred around 2200 UTC.

Even with these minor discrepancies, both model runs have enough of the thermal structure correct to simulate the winds and sea breeze with good accuracy. The onset of the local mountain-valley forcing is simulated to within two hours of the observed onset Figure(6a). The winds increase with the large scale sea breeze between 2000 UTC and 2100 UTC. As the sea breeze weakens, 0100 UTC 26 August in the Burk-Thompson scheme Figure (54) and 0200 UTC 26 August in the MRF scheme Figure(55), the winds back to the southwest along the coastline of the Monterey Bay. This is believed to be in response to the eddy that develops out over the north Monterey Bay and propagates south before dissipating. This circulation may shut off the sea breeze up the Salinas Valley, hence ending the sea breeze evolution. After the eddy dissipates, the offshore flow resumes over the profiler site. Both model simulations show stronger winds than were observed during the time period from 0700 to 1200 UTC 26 August. The MRF scheme Figure (52) had a more realistic flow since the wind speeds are 10 kts or less, while the

Burk-Thompson scheme Figure (53) has winds that increase to 20 kts while the observed data Figure (7a) shows the winds weakening during this time period. This further emphasizes that a 36 hour simulation might be too long for the model to accurately depict aspects of the thermal cycle at this grid.

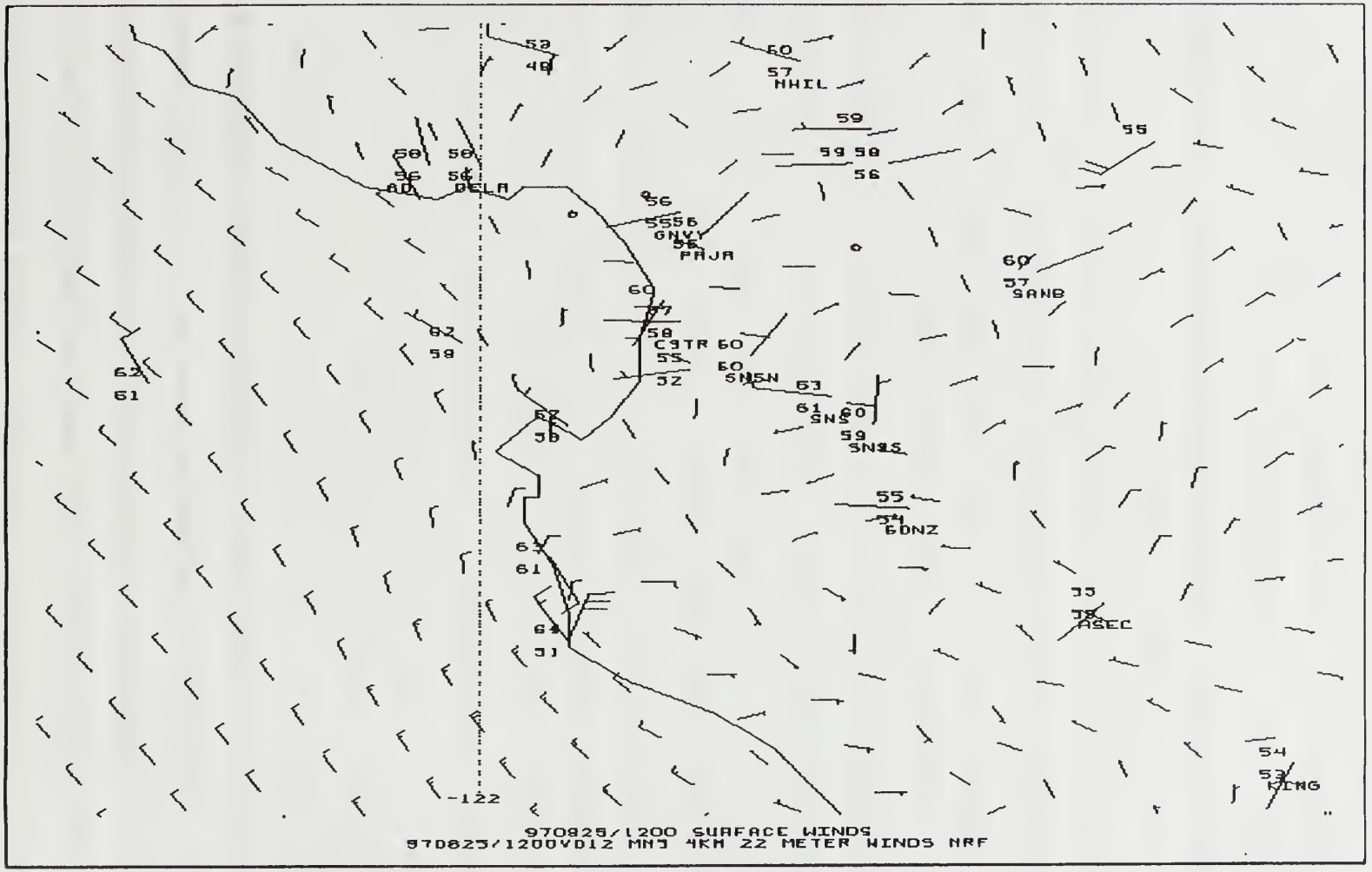

Figure 13. The near surface 12 hour forecast model winds and the corresponding surface observations for 1200 UTC 25 August.

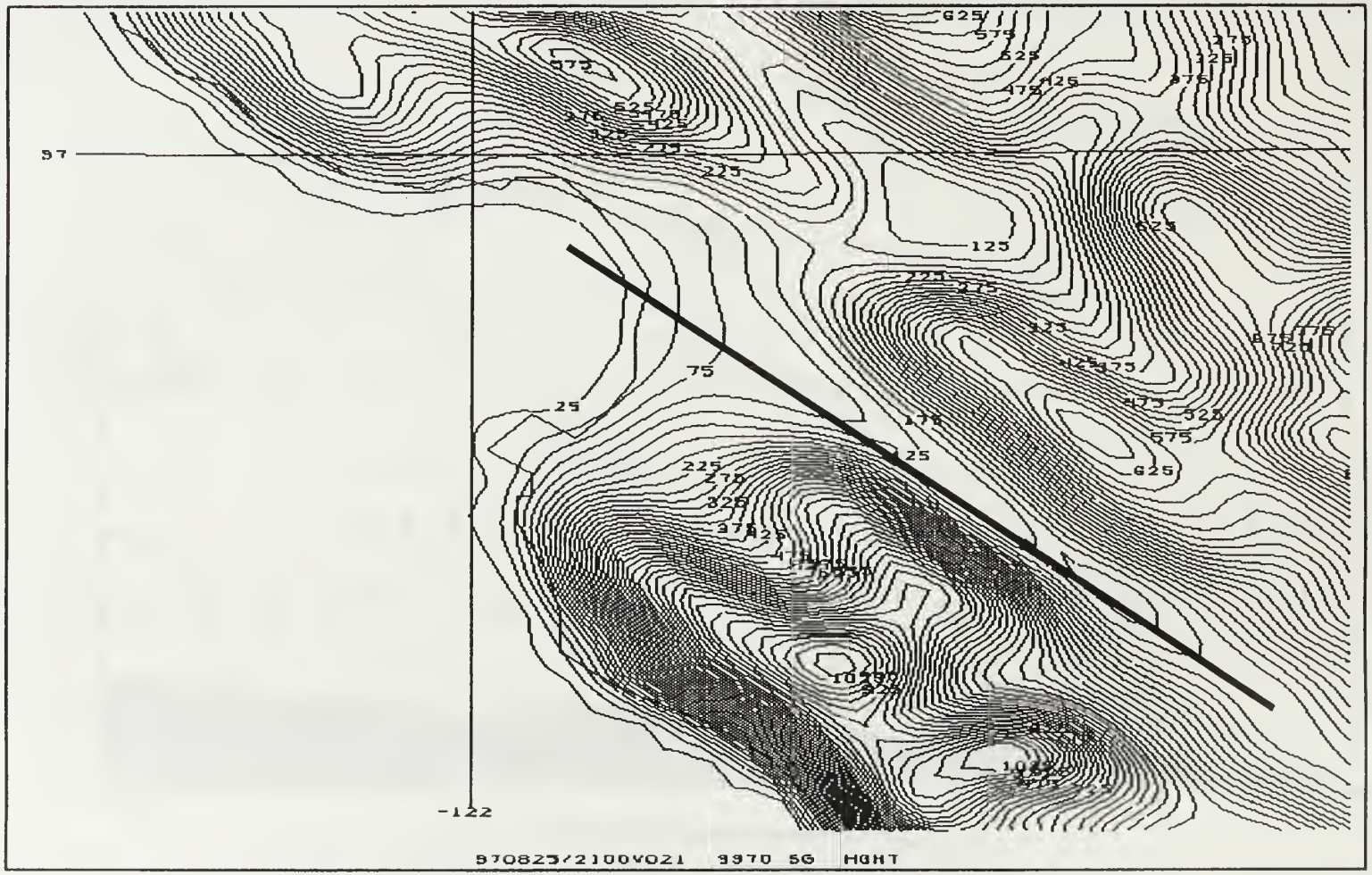

Figure 14. MM5 model terrain at 4 km resolution and contoured at every 25 m, starting at 25 m and the cross section (end points: 36.90,121.92; 36.15,121.0).

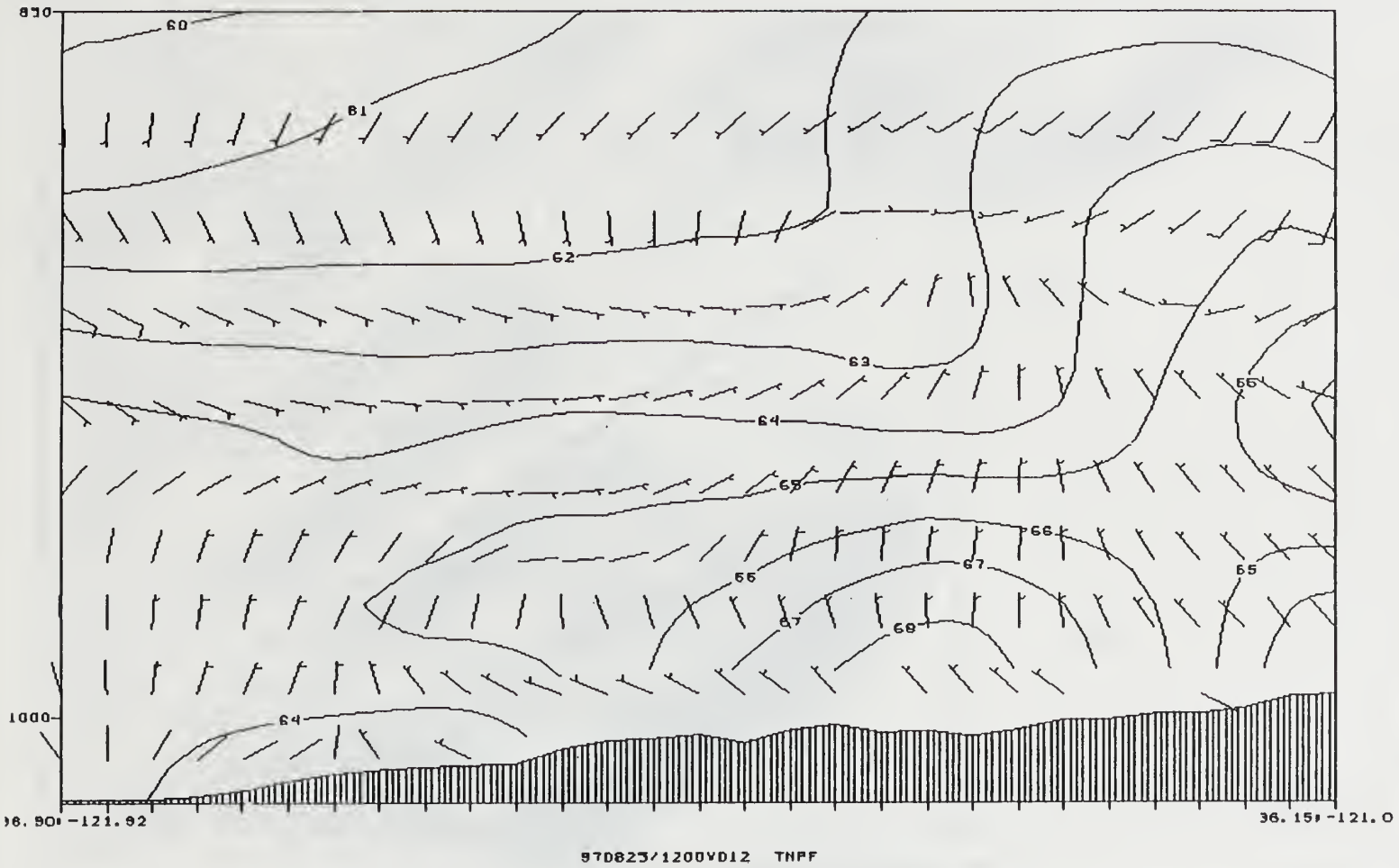

Figure 15. A model cross section of winds and temperature along the Salinas Valley for the 12 hour forecast valid 1200 UTC 25 August.

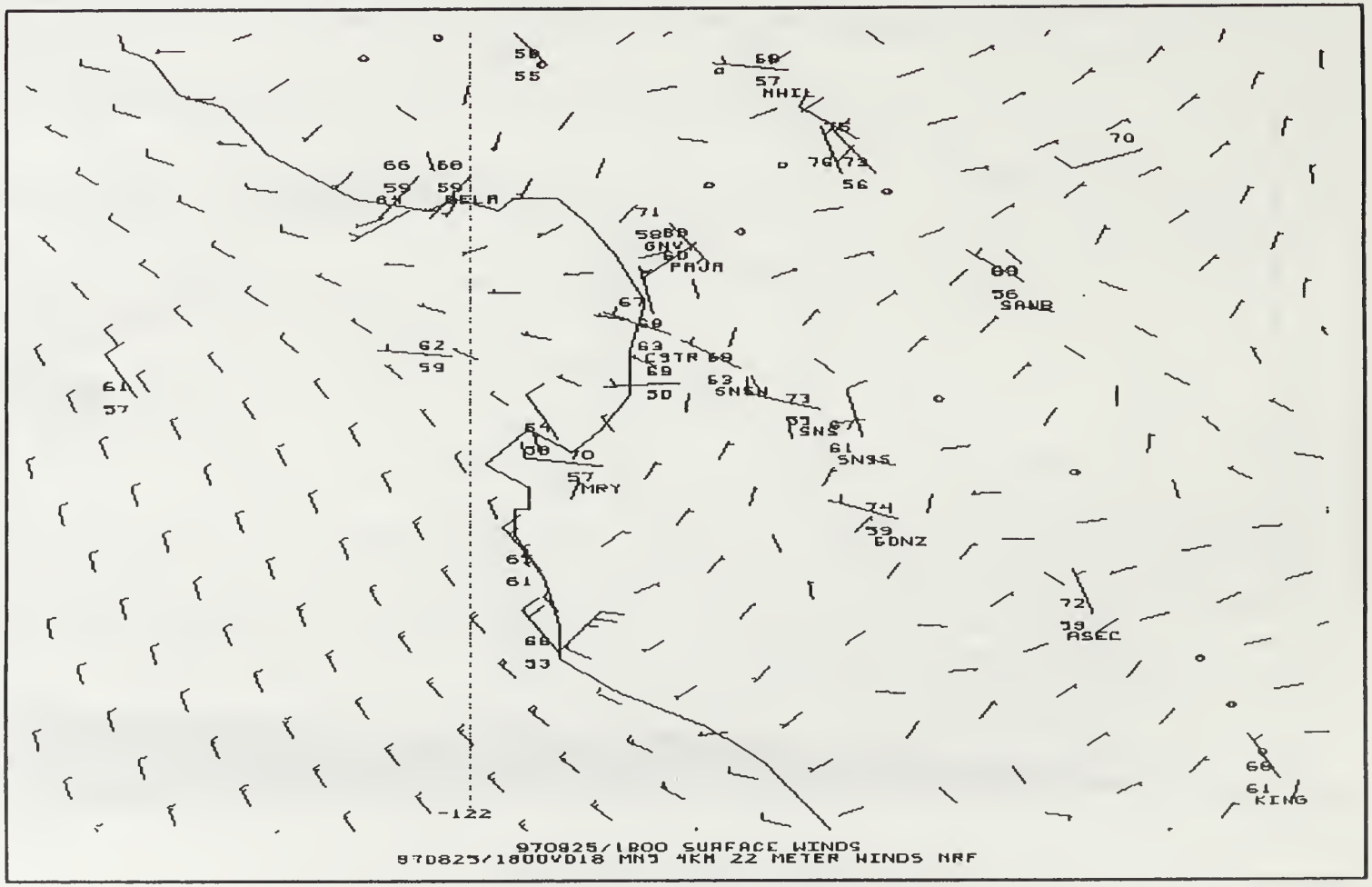

Figure 16. The near surface 18 hour forecast model winds and the corresponding surface observations for 1800 UTC 25 August.

Figure 17. A model cross section of winds and temperature along the Salinas Valley for the 18 hour forecast valid at 1800 UTC 25 August.

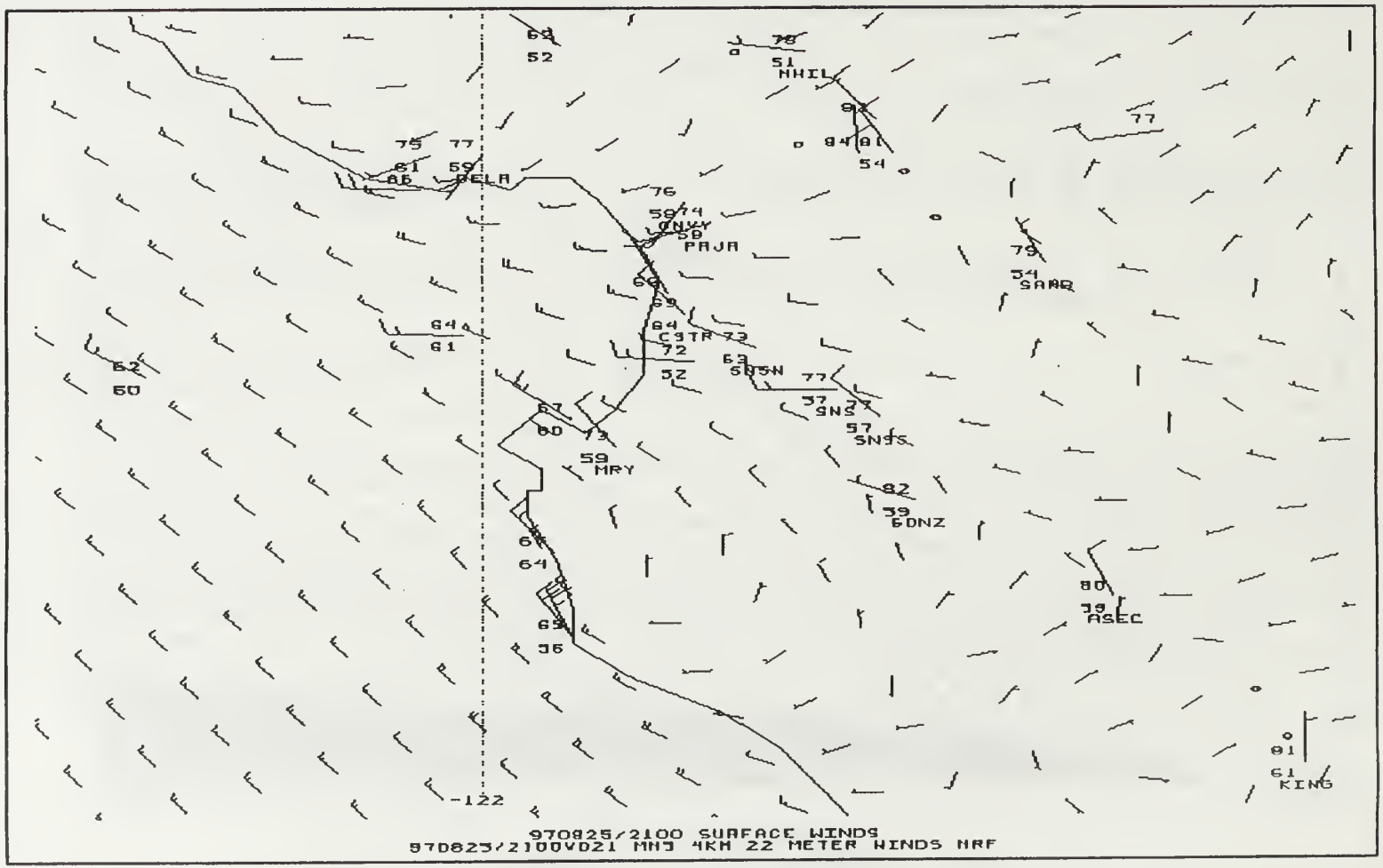

Figure 18. The near surface 21 hour forecast model winds and the corresponding surface observations for 2100 UTC 25 August.

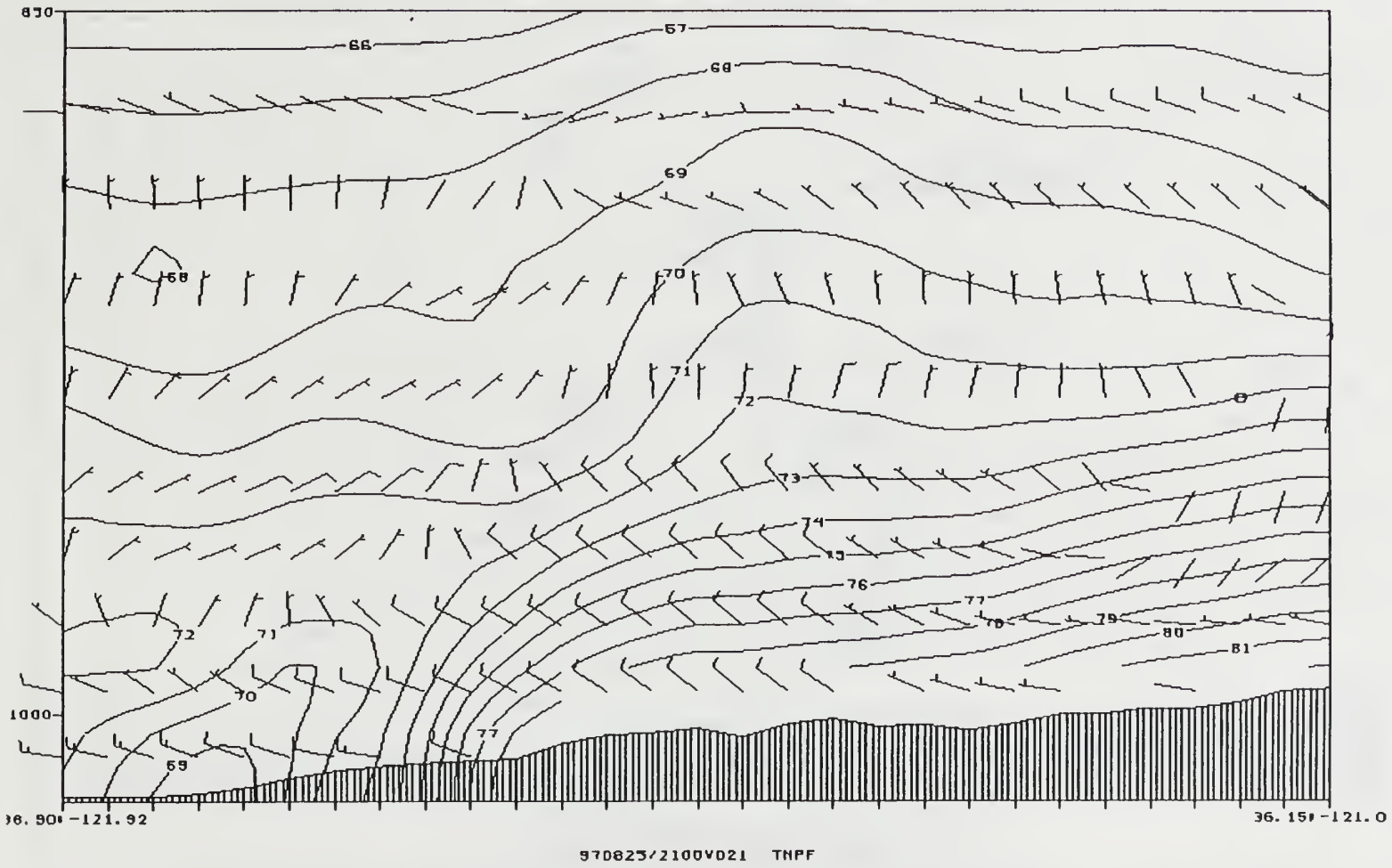

Figure 19. A model cross section of winds and temperature along the Salinas Valley for the 21 hour forecast valid 2100 UTC 25 August.

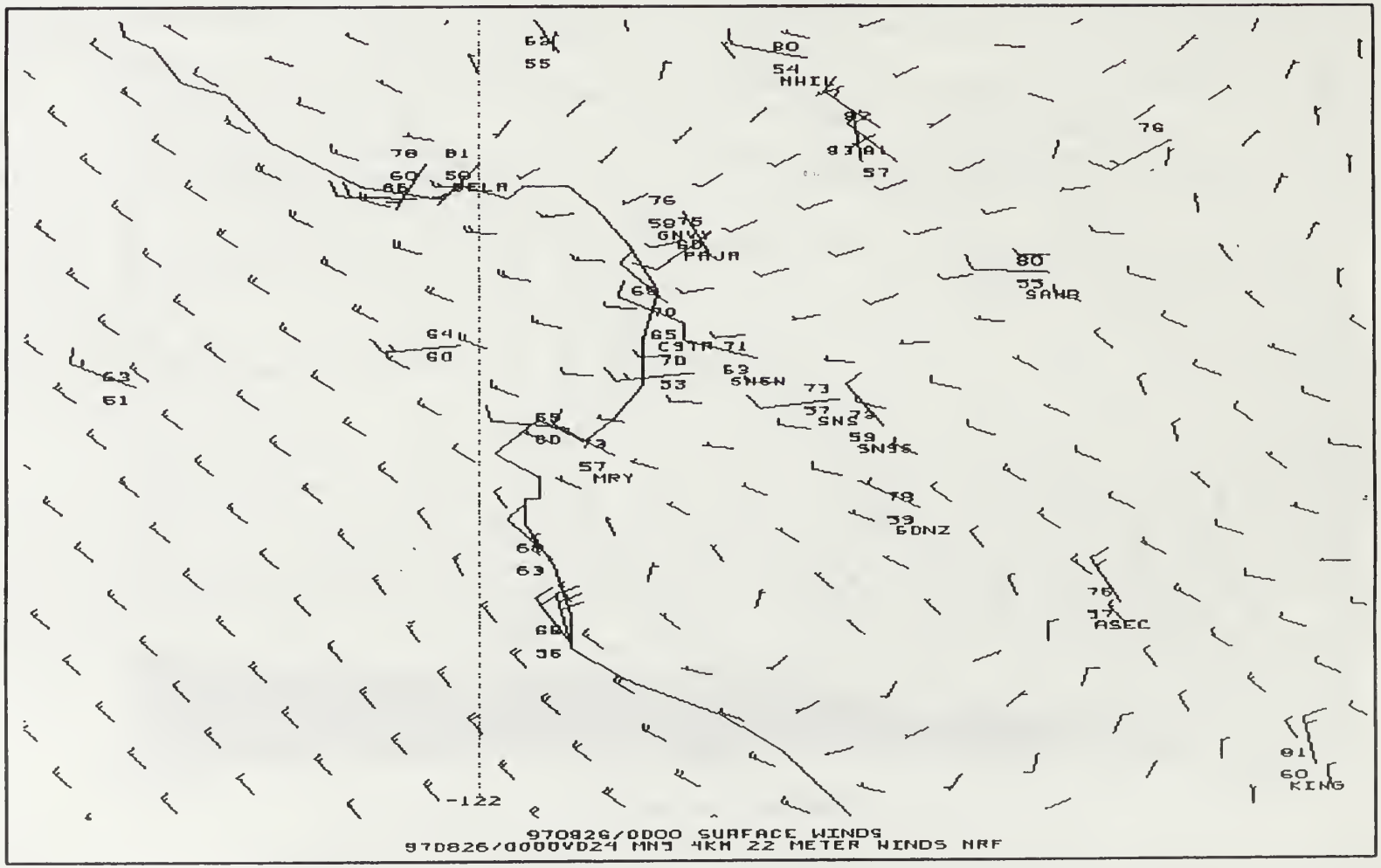

Figure 20. The 24 hour forecast near surface model winds and the corresponding surface observations for 0000 UTC 26 August.

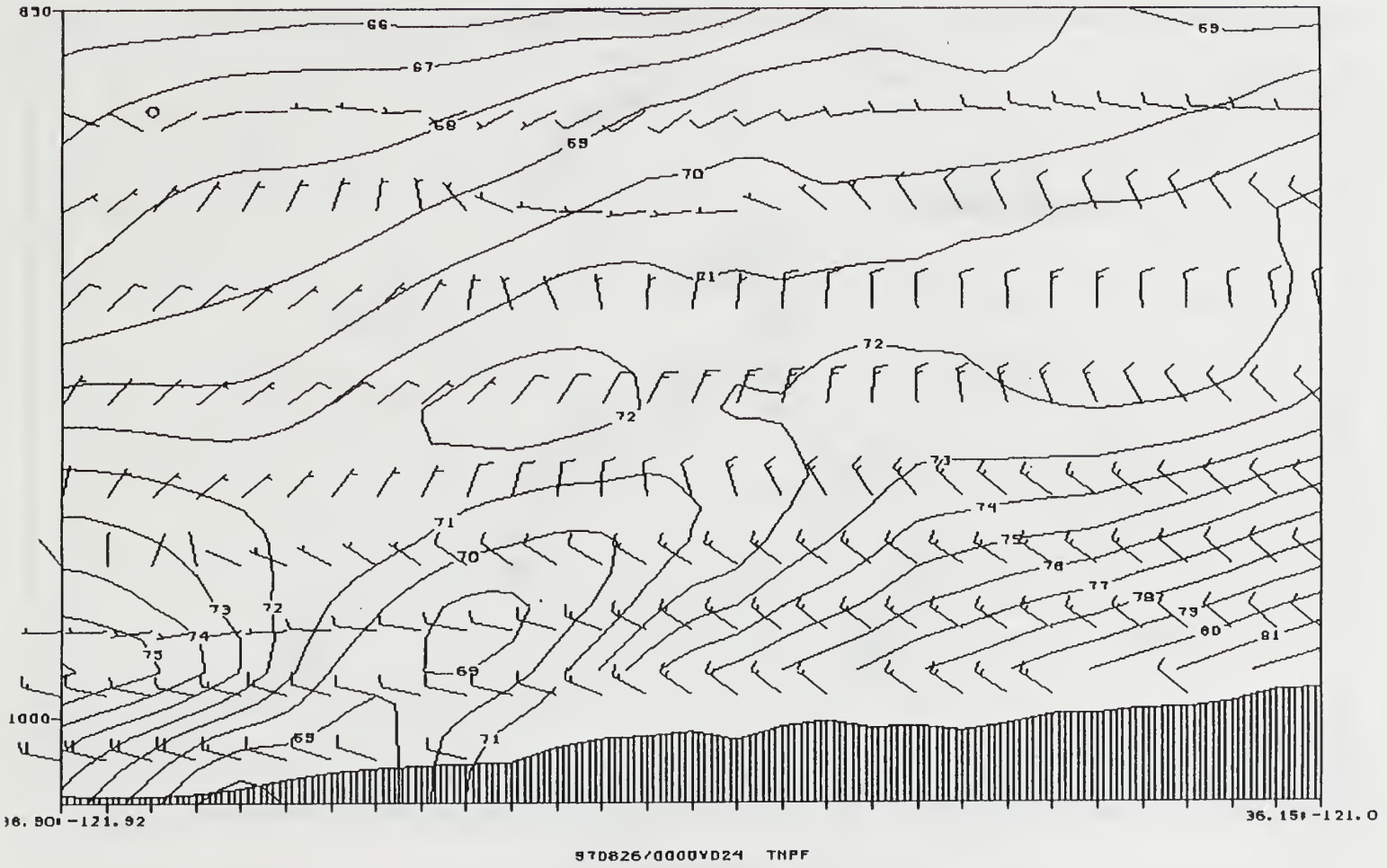

Figure 21. A model cross section of winds and temperature along the Salinas Valley for the 24 hour forecast vaild 0000 UTC 26 August.

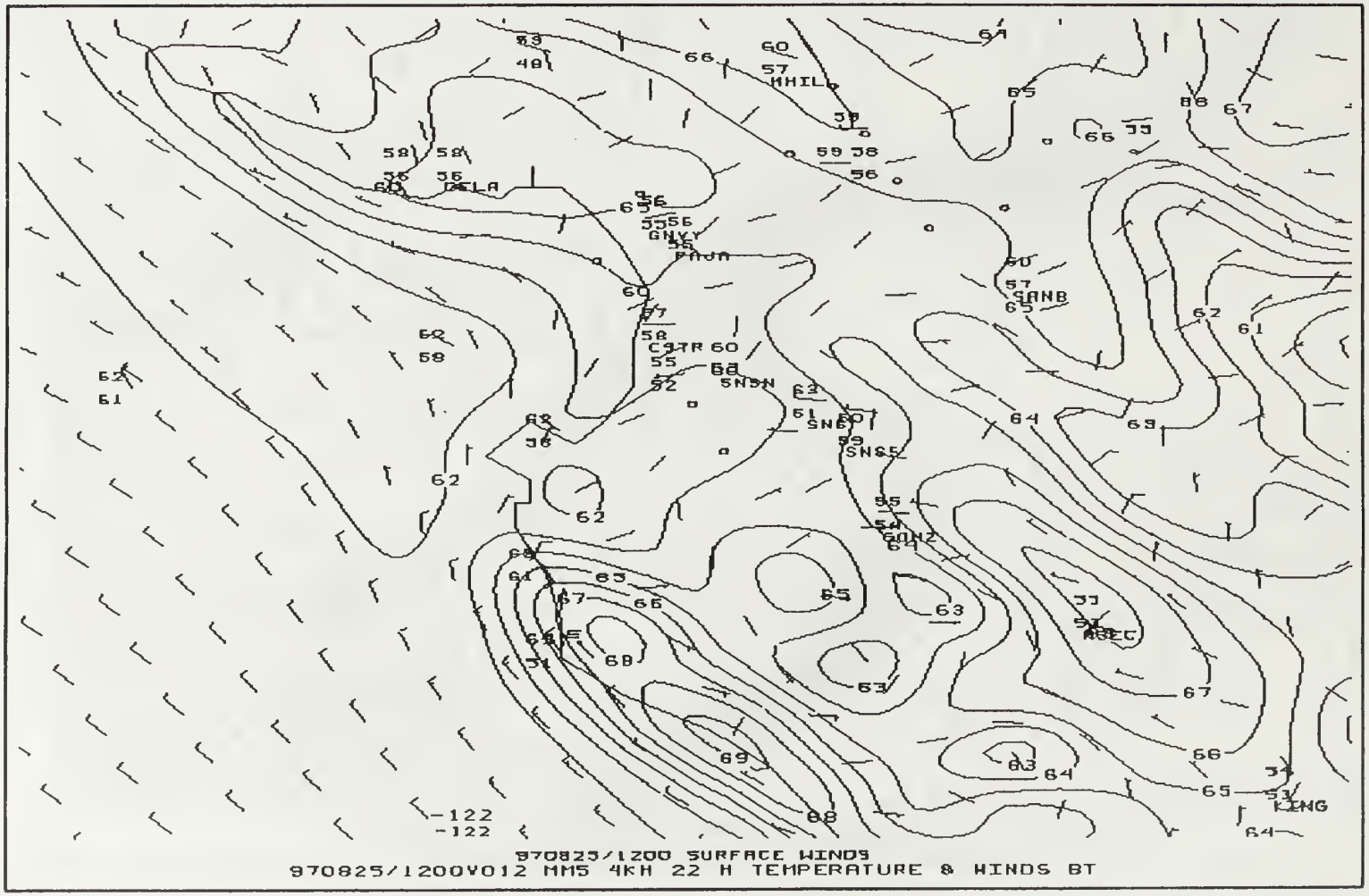

Figure 22. The 12 hour forecast of near surface model winds and temperature and the corresponding surface observations for 1200 UTC 25 August .

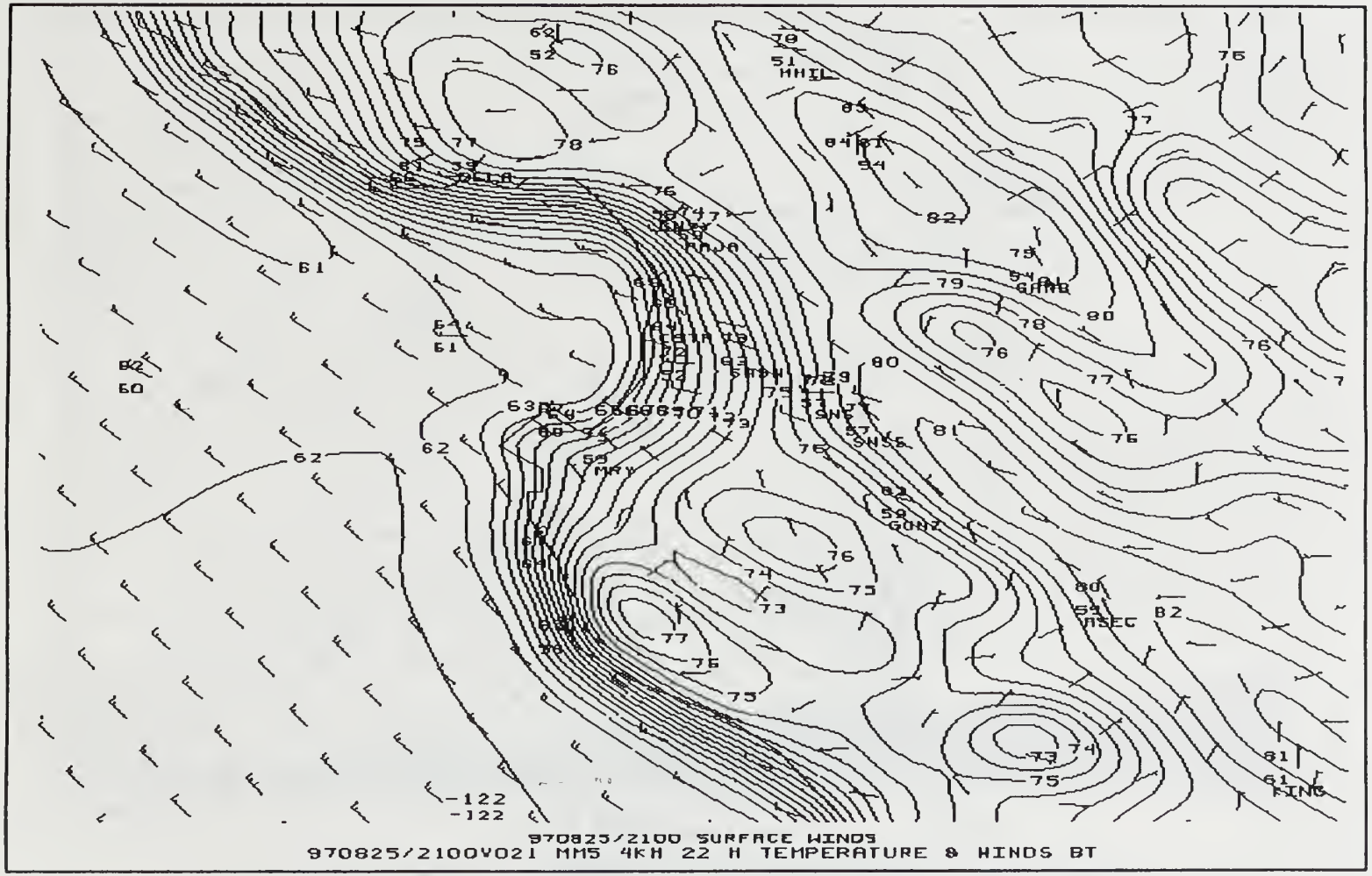

Figure 23. The 21 hour forecast of near surface model winds and temperature and the corresponding surface observations for 2100 UTC 25 August .

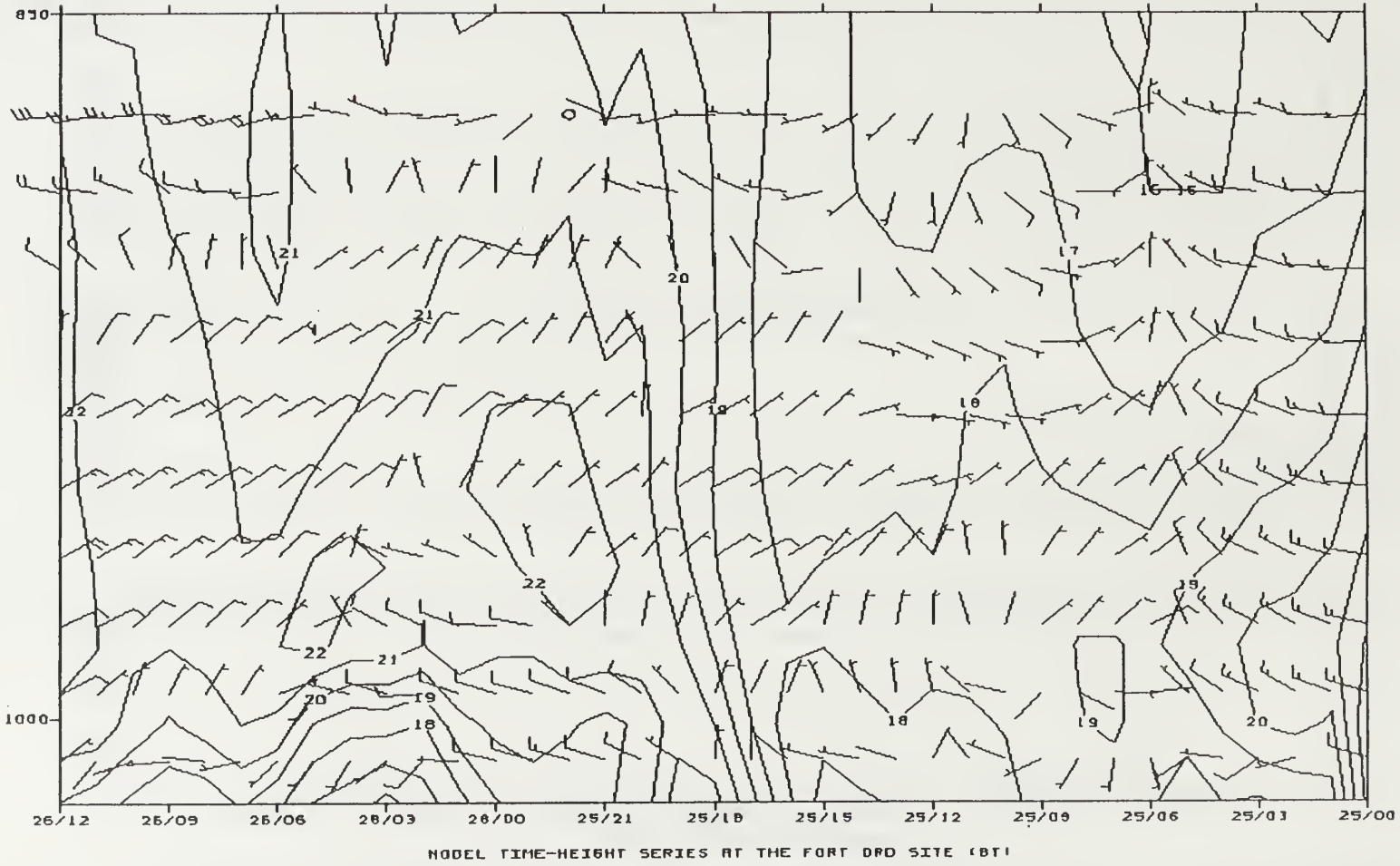

Figure 24. A 36 hour model time height series forecast of winds and temperature up to 850 mb at the latitude and longitude of the Ft. Ord profiler site .

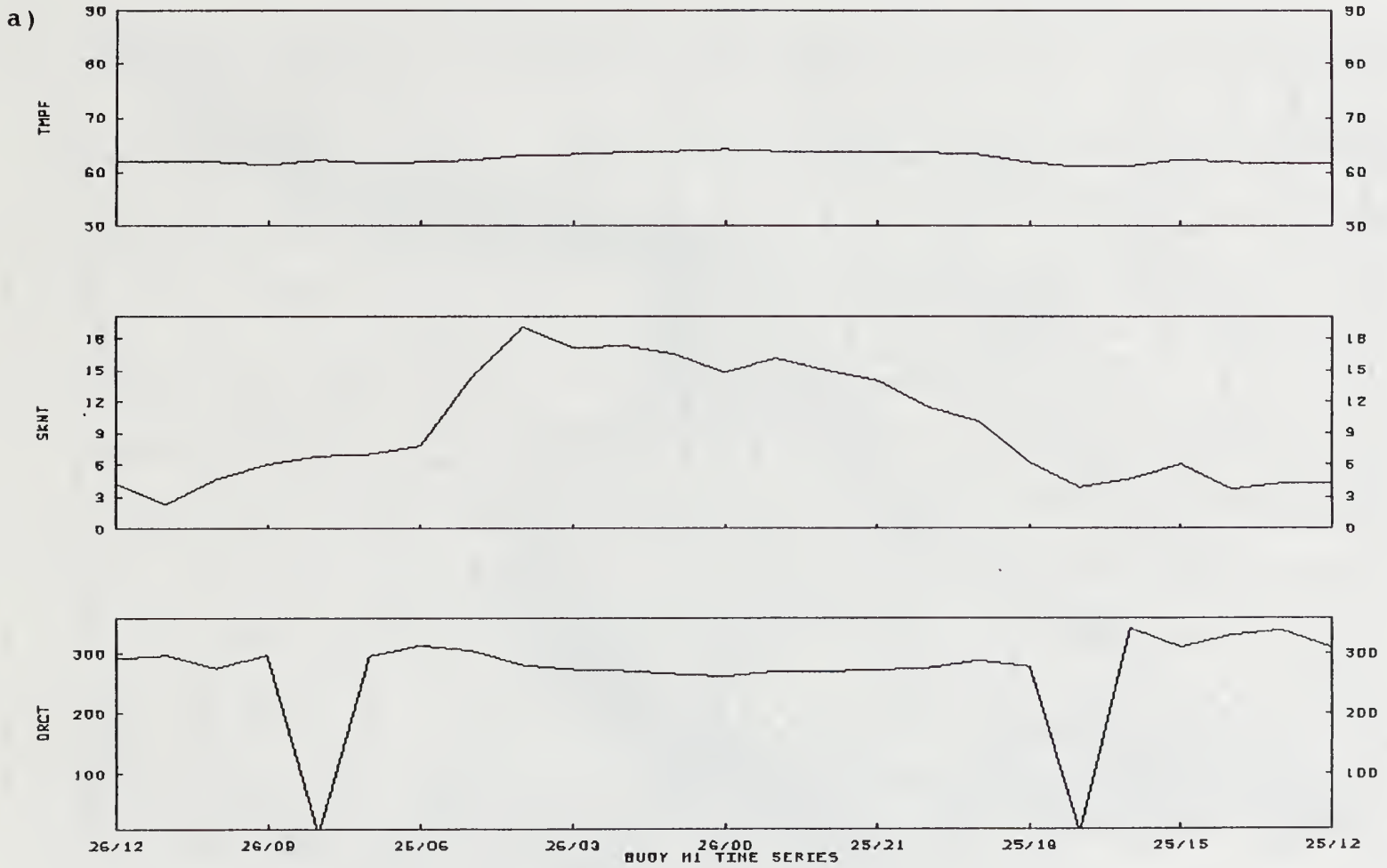

Figure 25a,b,c. A 24 hour time series valid 1200 UTC 25 - 1200 UTC 26 August for buoy M1 of tmeperature, wind speed and wind direction for (a) the observation, (b) the Burk-Thompson model run and (c) the MRF model run.

b)

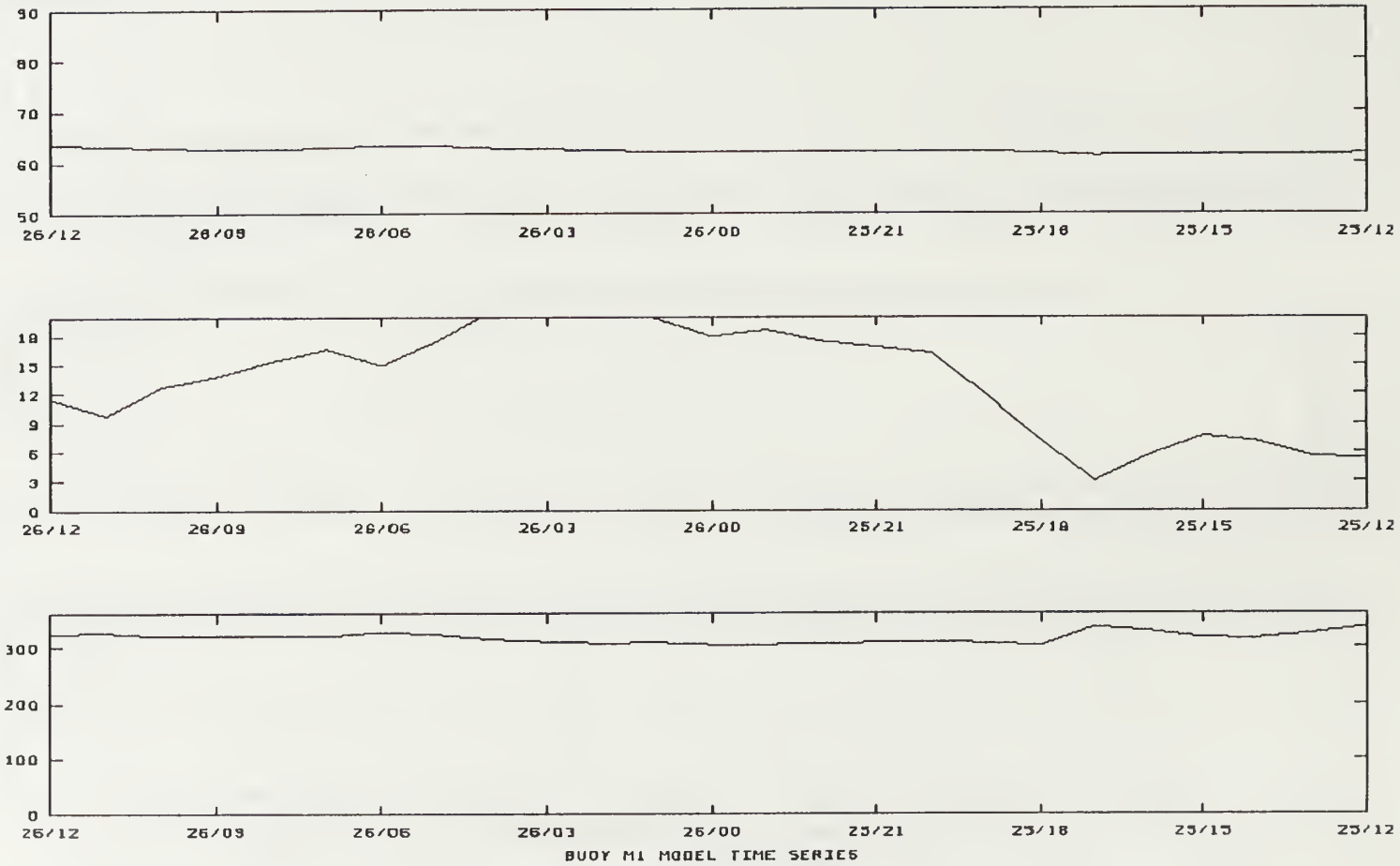
90
80
70
60
50
26/12
26/09
26/06
26/03
26/00
25/21
25/18
25/15
25/12
18
15
12
9
6
3
0
26/12
26/09
26/06
26/03
26/00
25/21
25/18
25/15
25/12
300
200
100
0
26/12
26/09
26/06
26/03
26/00
25/21
25/18
25/15
25/12
BUOY M1 MODEL TIME SERIES

c)

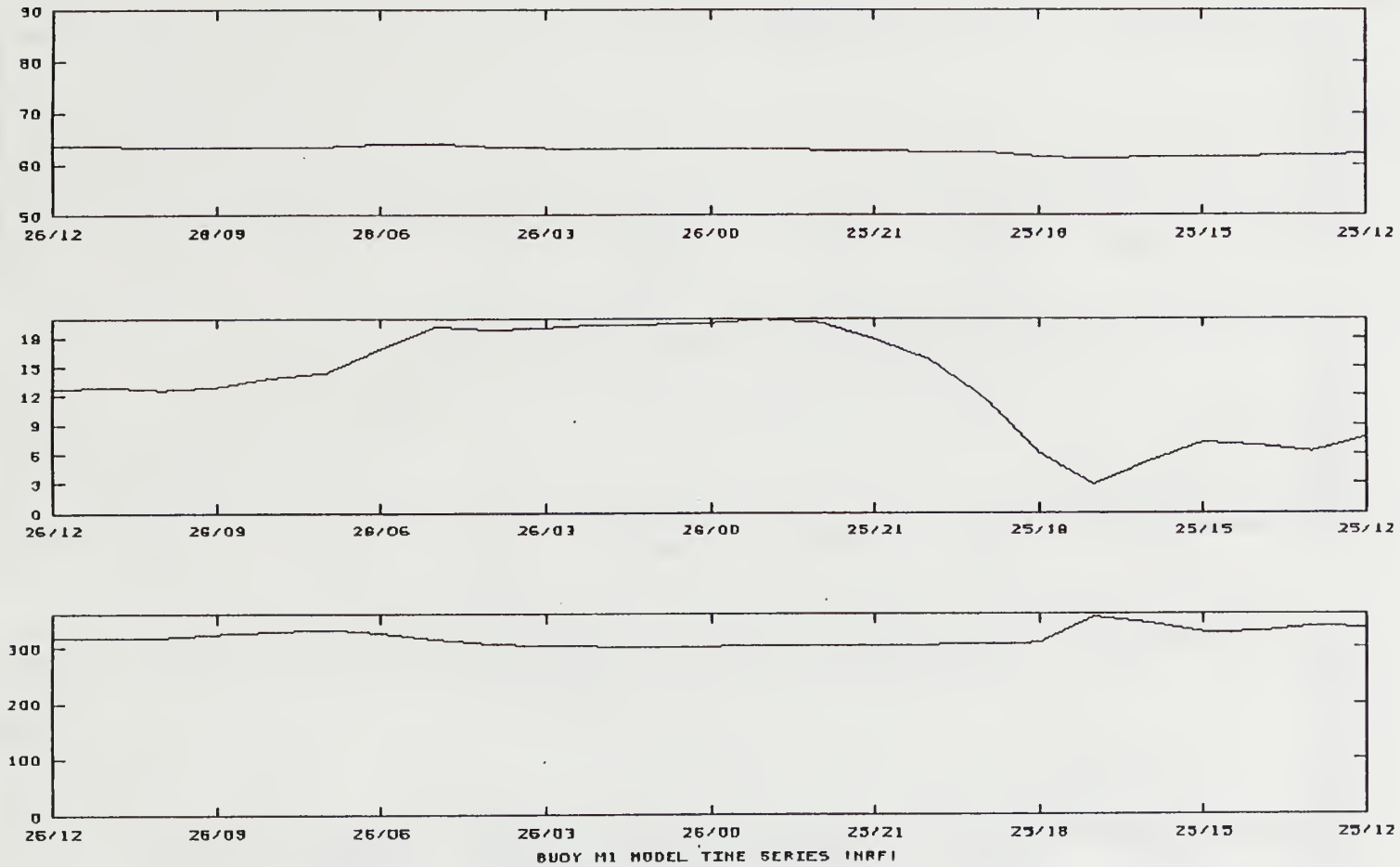
90
80
70
60
50
26/12
26/09
26/06
26/03
26/00
25/21
25/18
25/15
25/12
18
15
12
9
6
3
0
300
200
100
BUOY M1 MODEL TIME SERIES (NRFI)

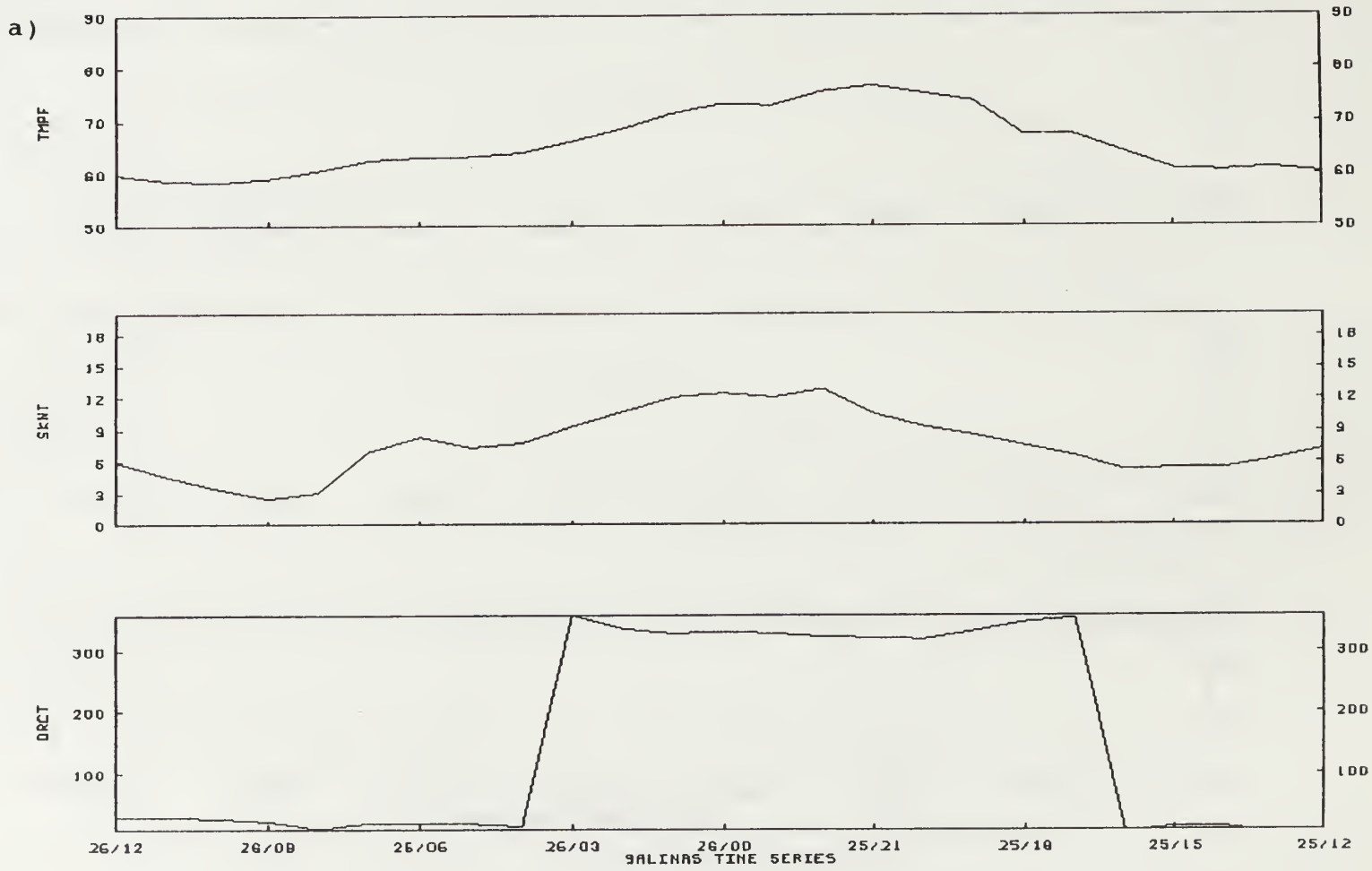

Figure 26a,b. A 24 hour time series valid 1200 UTC 25 - 1200 UTC 26 August for Salina of tmeperature, wind speed and wind direction for (a) the observations, (b) the Burk-Thompson model run and (c) the MRF model run.

b)

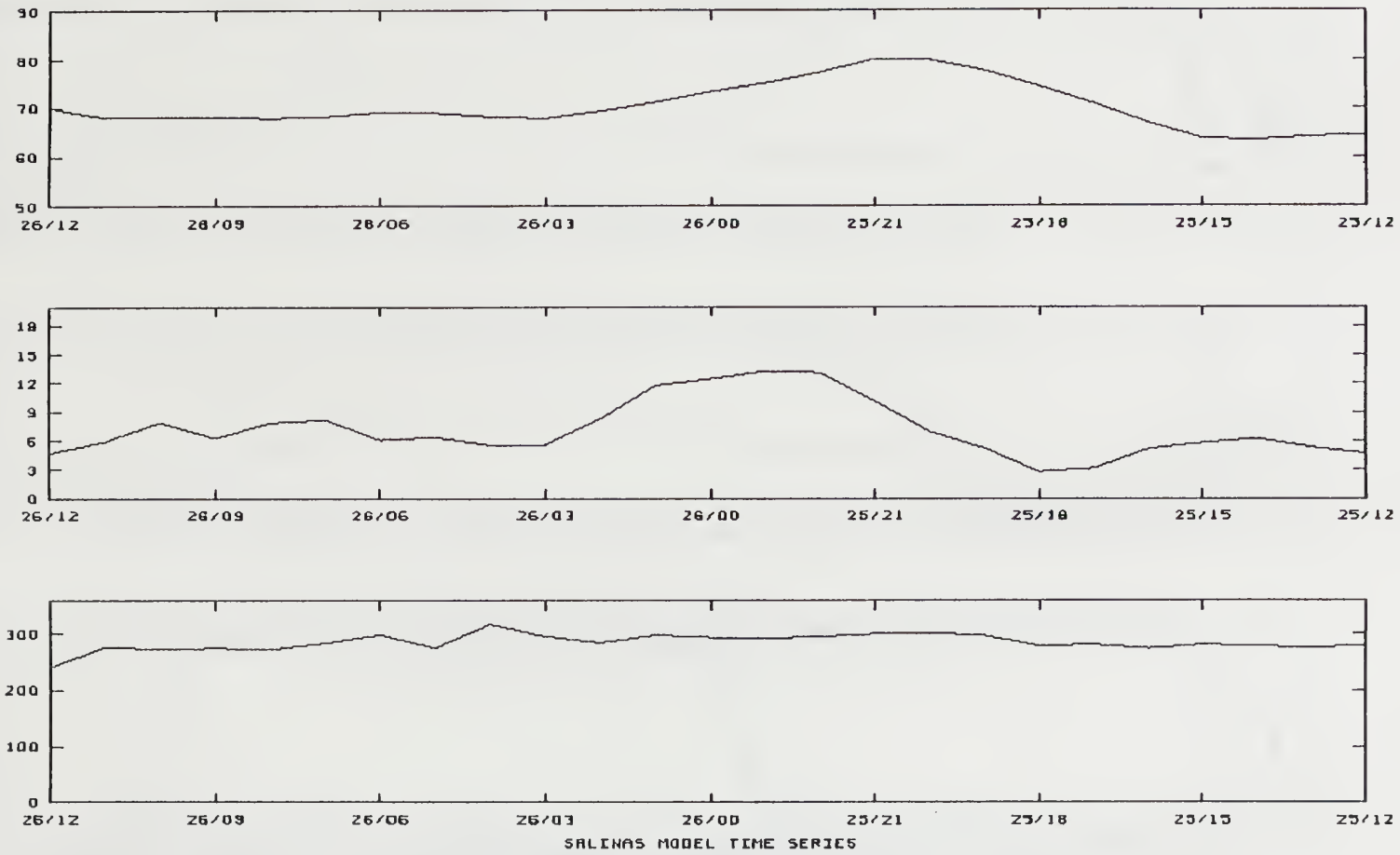
90
80
70
60
50
26/12
26/09
26/06
26/03
26/00
25/21
25/18
25/15
25/12
18
15
12
9
6
3
0
26/12
26/09
26/06
26/03
26/00
25/21
25/18
25/15
25/12
300
200
100
0
26/12
26/09
26/06
26/03
26/00
25/21
25/18
25/15
25/12
SALINAS MODEL TIME SERIES

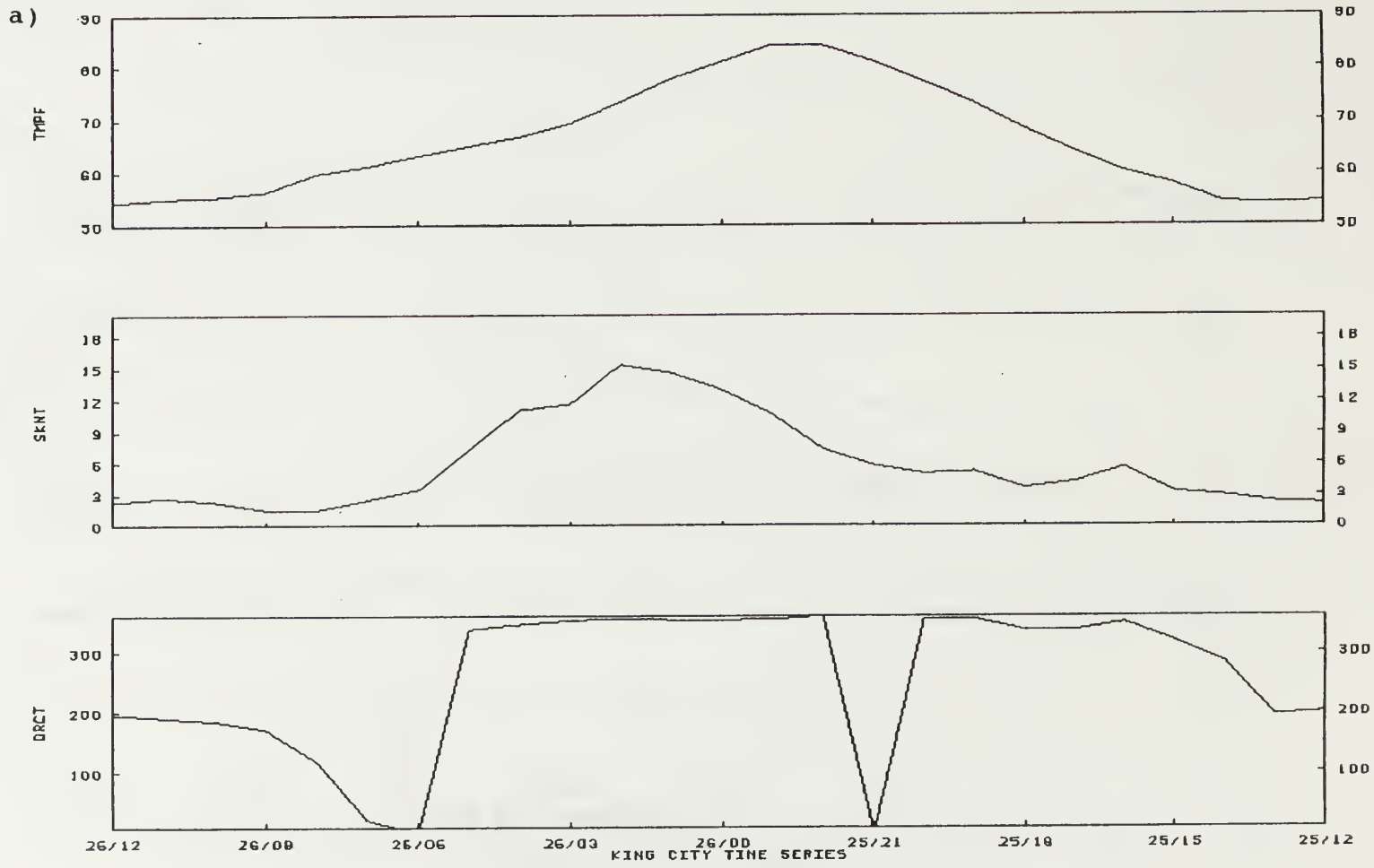

Figure 27a,b. A 24 hour time series valid 1200 UTC 25 - 1200 UTC 26 August for King City of tmeperature, wind speed and wind direction for (a) the observation, (b) the Burk-Thompson model run and (c) the MRF model run.

b)

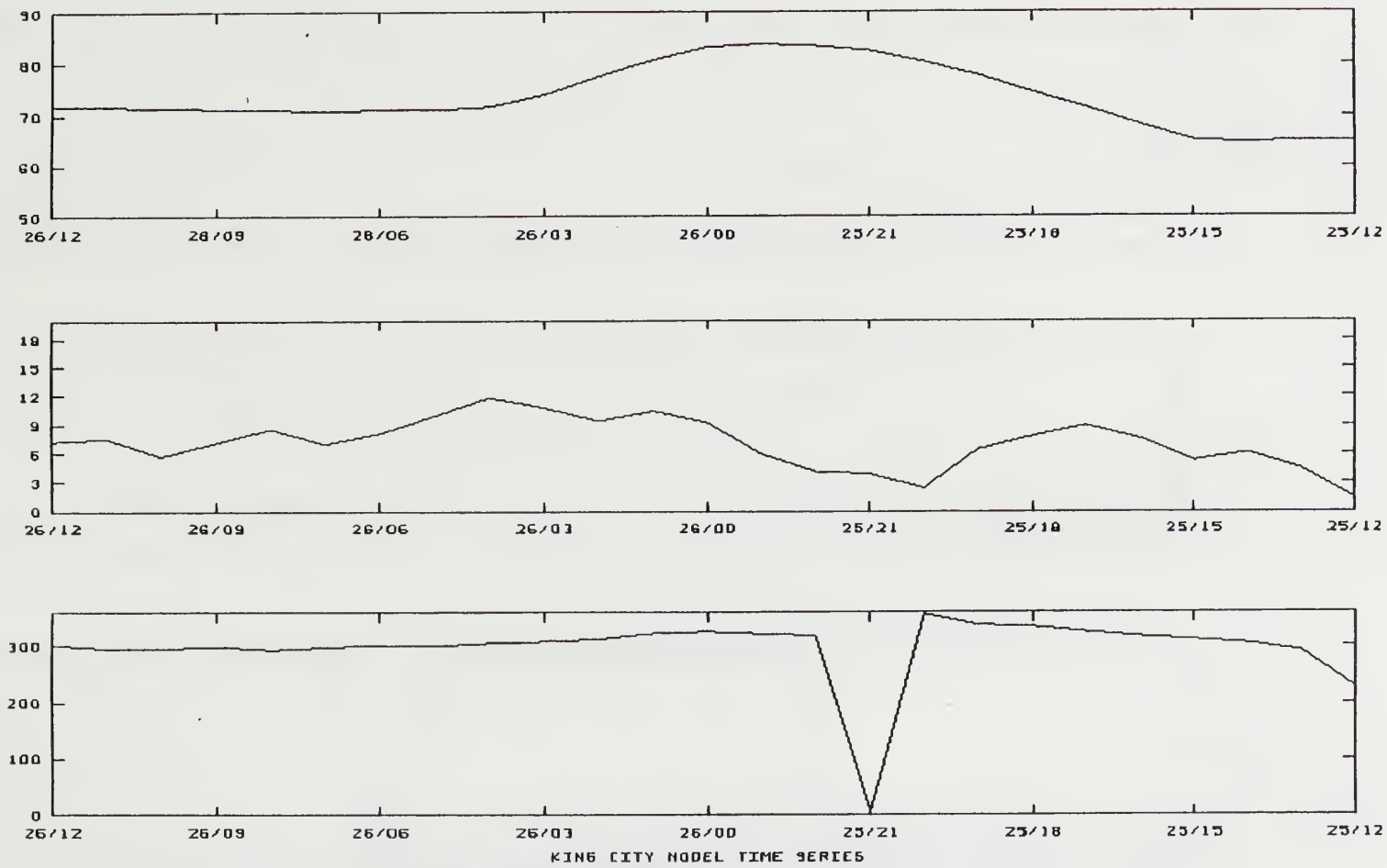
90
80
70
60
50
26/12
26/09
26/06
26/03
26/00
25/21
25/18
25/15
25/12
18
15
12
9
6
3
0
300
200
100
KING CITY MODEL TIME SERIES

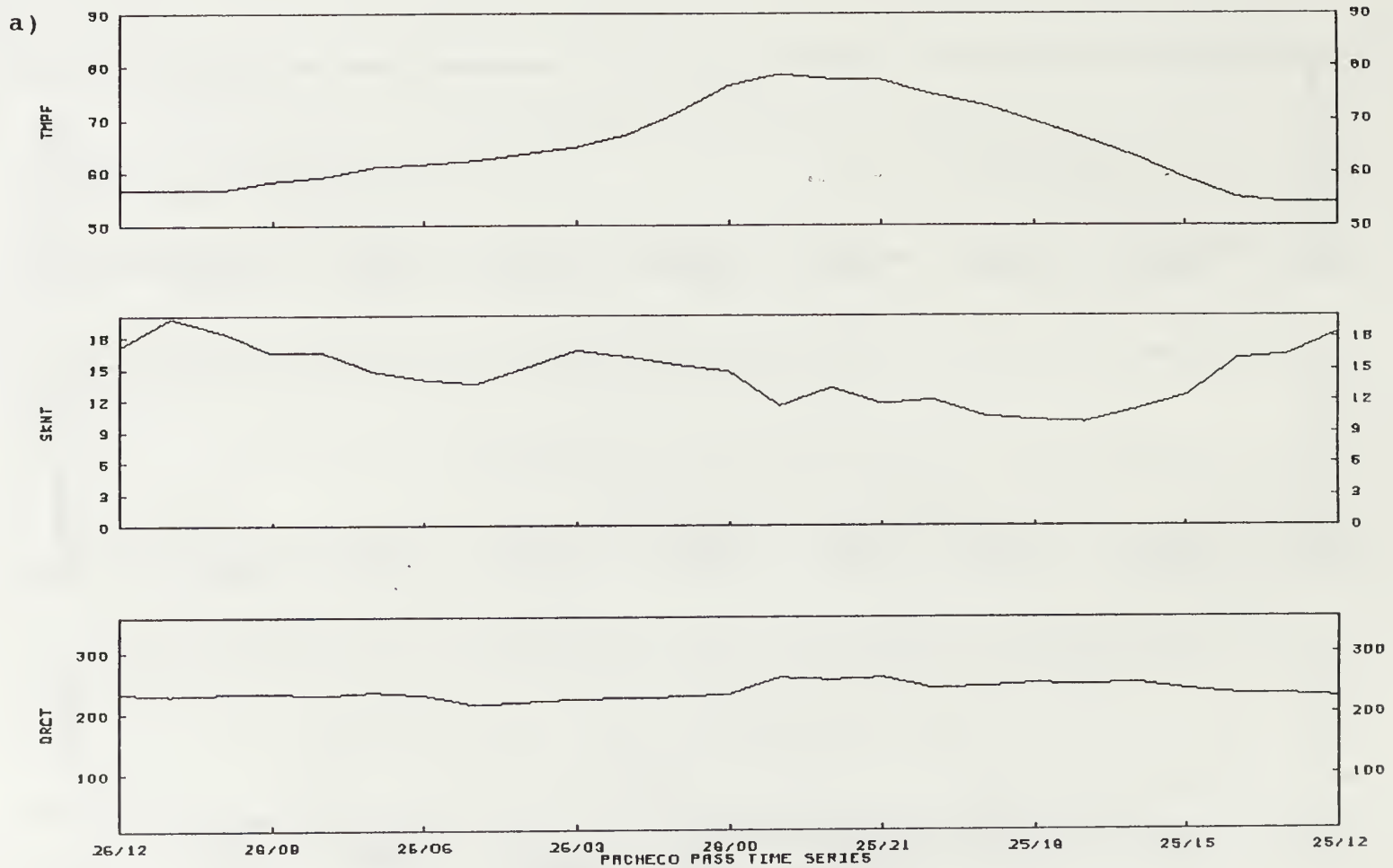

Figure 28a,b,c. A 24 hour time series valid 1200 UTC 25 - 1200 UTC 26 August for Pacheco Pass of tmeperature, wind speed and wind direction for (a) the observation, (b) the Burk-Thompson model run and (c) the MRF model run.

b)

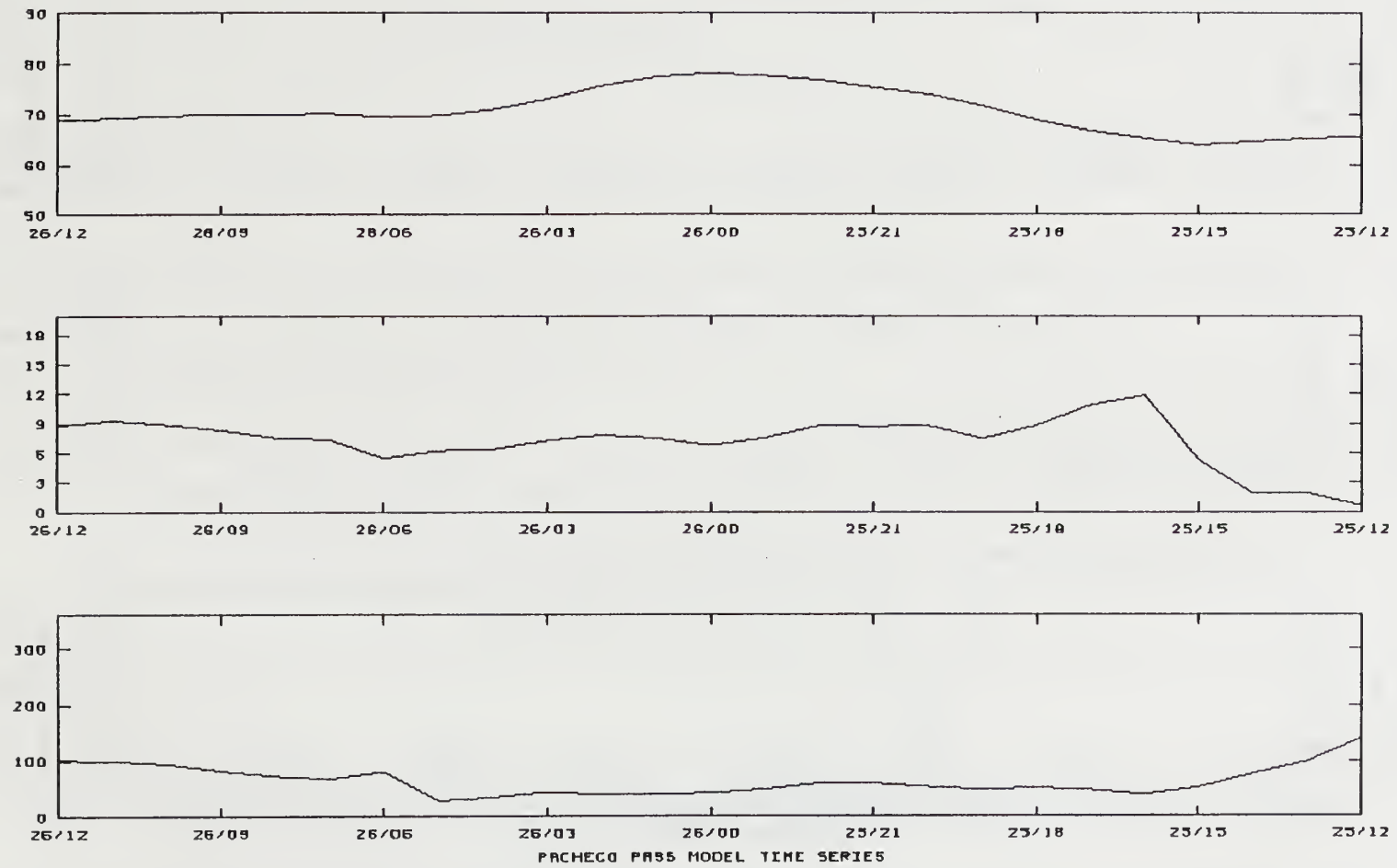

PACHECO PASS MODEL TIME SERIES

c)

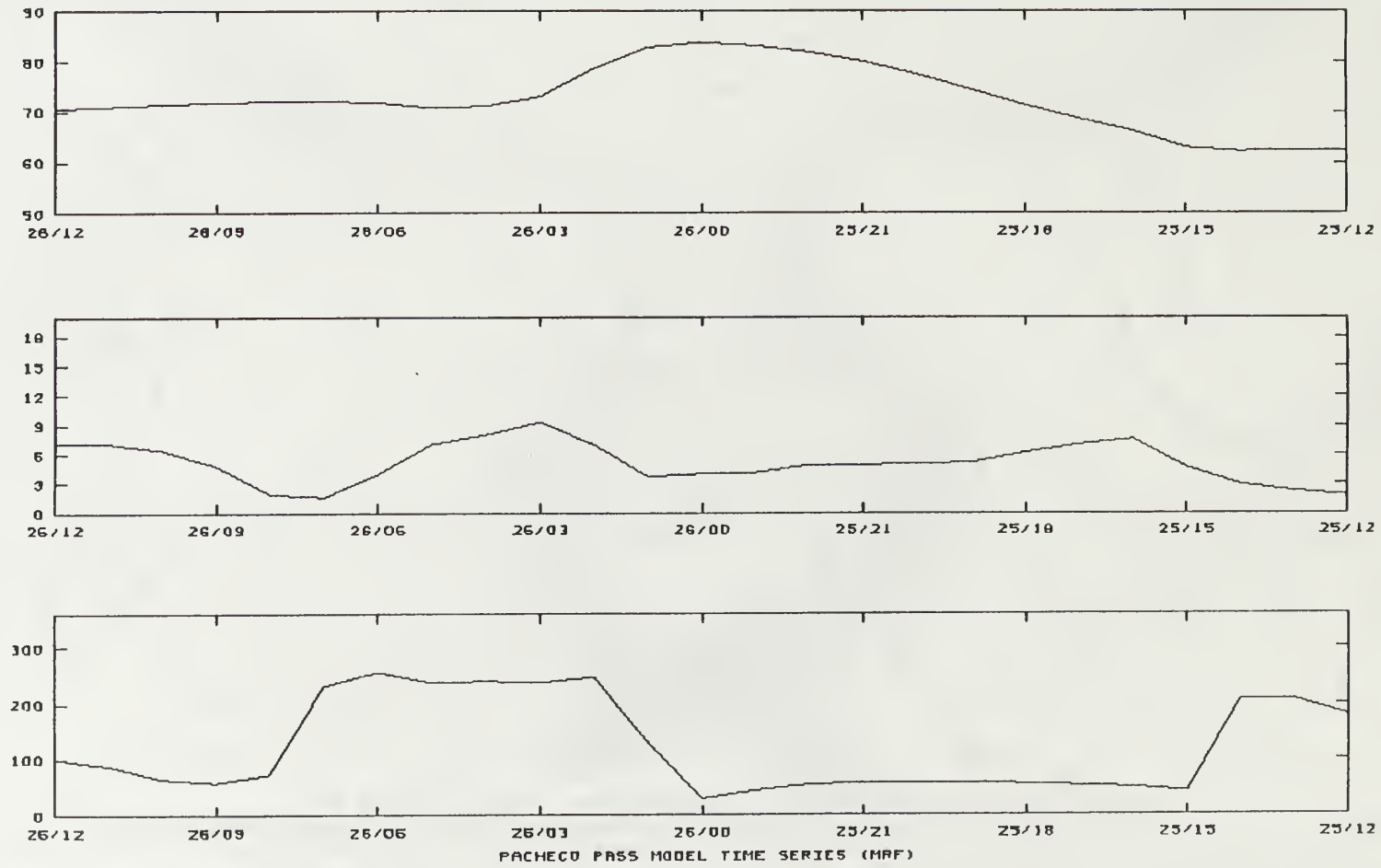
90
80
70
60
50
26/12
26/09
26/06
26/03
26/00
25/21
25/18
25/15
25/12
18
15
12
9
6
3
0
26/12
26/09
26/06
26/03
26/00
25/21
25/18
25/15
25/12
300
200
100
0
26/12
26/09
26/06
26/03
26/00
25/21
25/18
25/15
25/12
PACHECO PASS MODEL TIME SERIES (MAF)

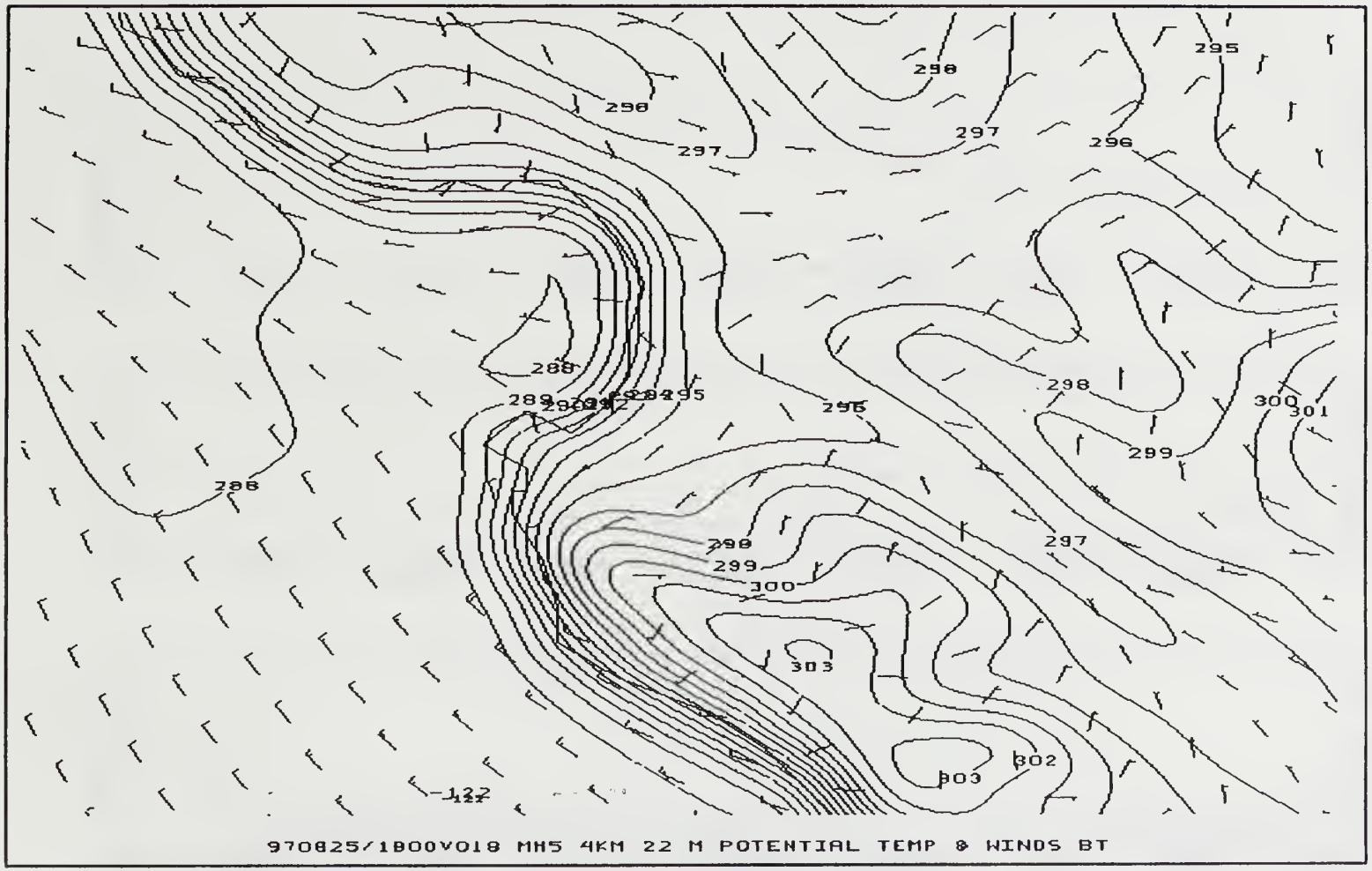

Figure 29. A 18 hour forecast of near surface model winds and potential temperature valid at 1800 UTC 25 August.

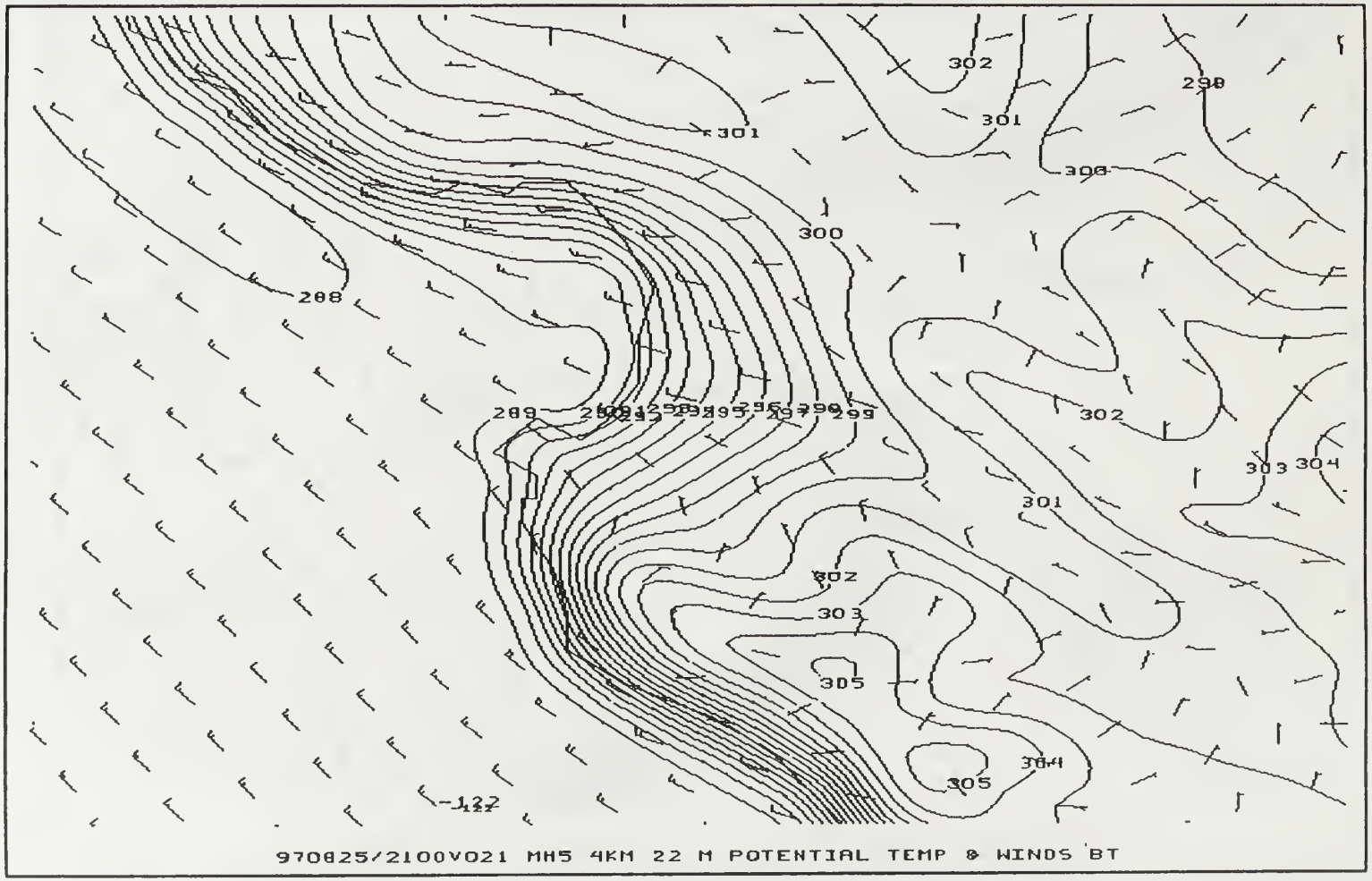

Figure 30. The 21 hour forecast of near surface model winds and potential temperature valid at 2100 UTC 25 August.

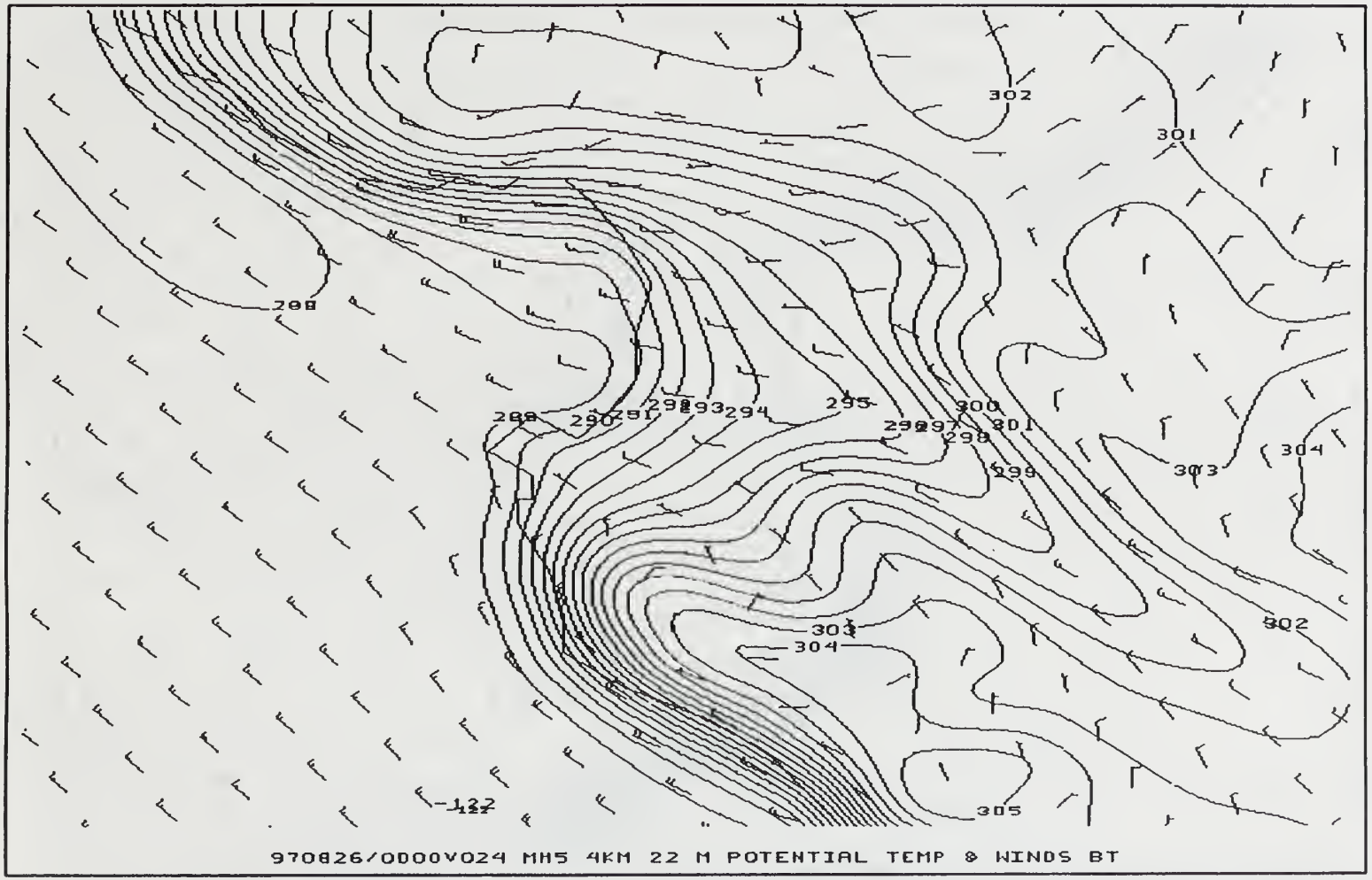

Figure 31. The 24 hour forecast near surface model winds and potential temperature valid at 0000 UTC 26 August.

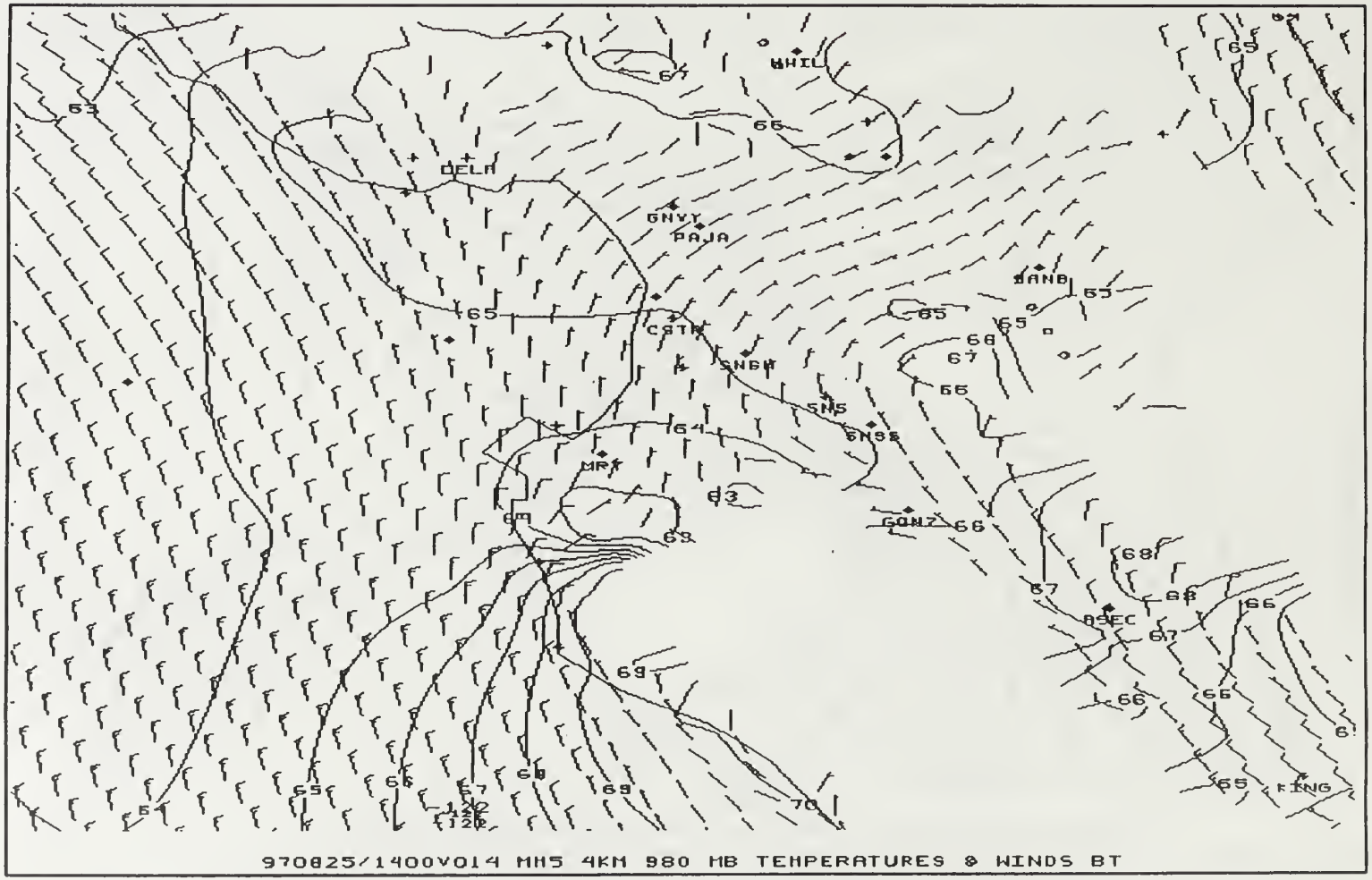

Figure 32. The 14 hour forecast of 980 mb winds and temperatures valid at 1400 UTC 25 August. (Station names are for geographic reference points only)

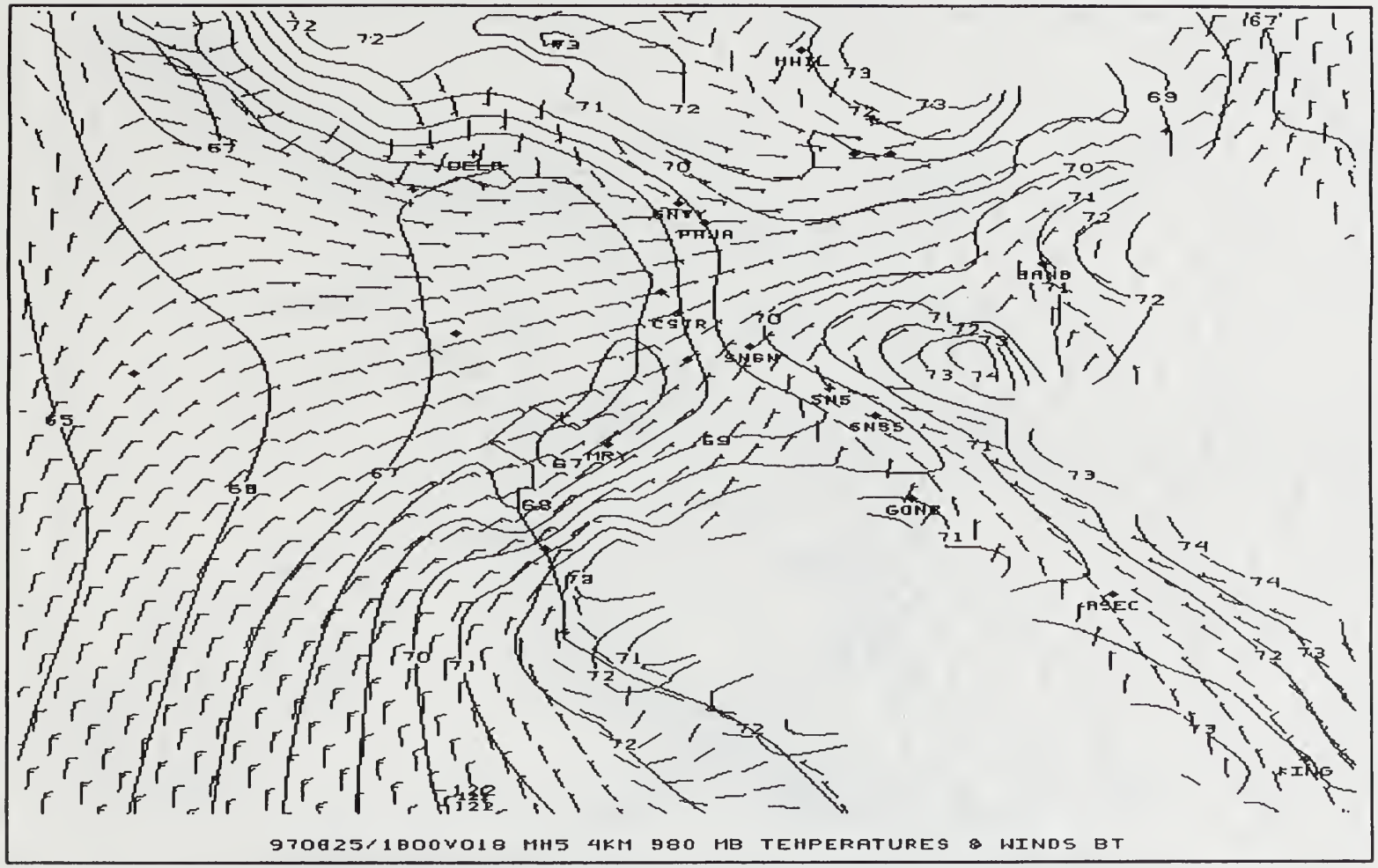

Figure 33. The 18 hour forecast of 980 mb winds and temperatures valid at 1800 UTC 25 August .

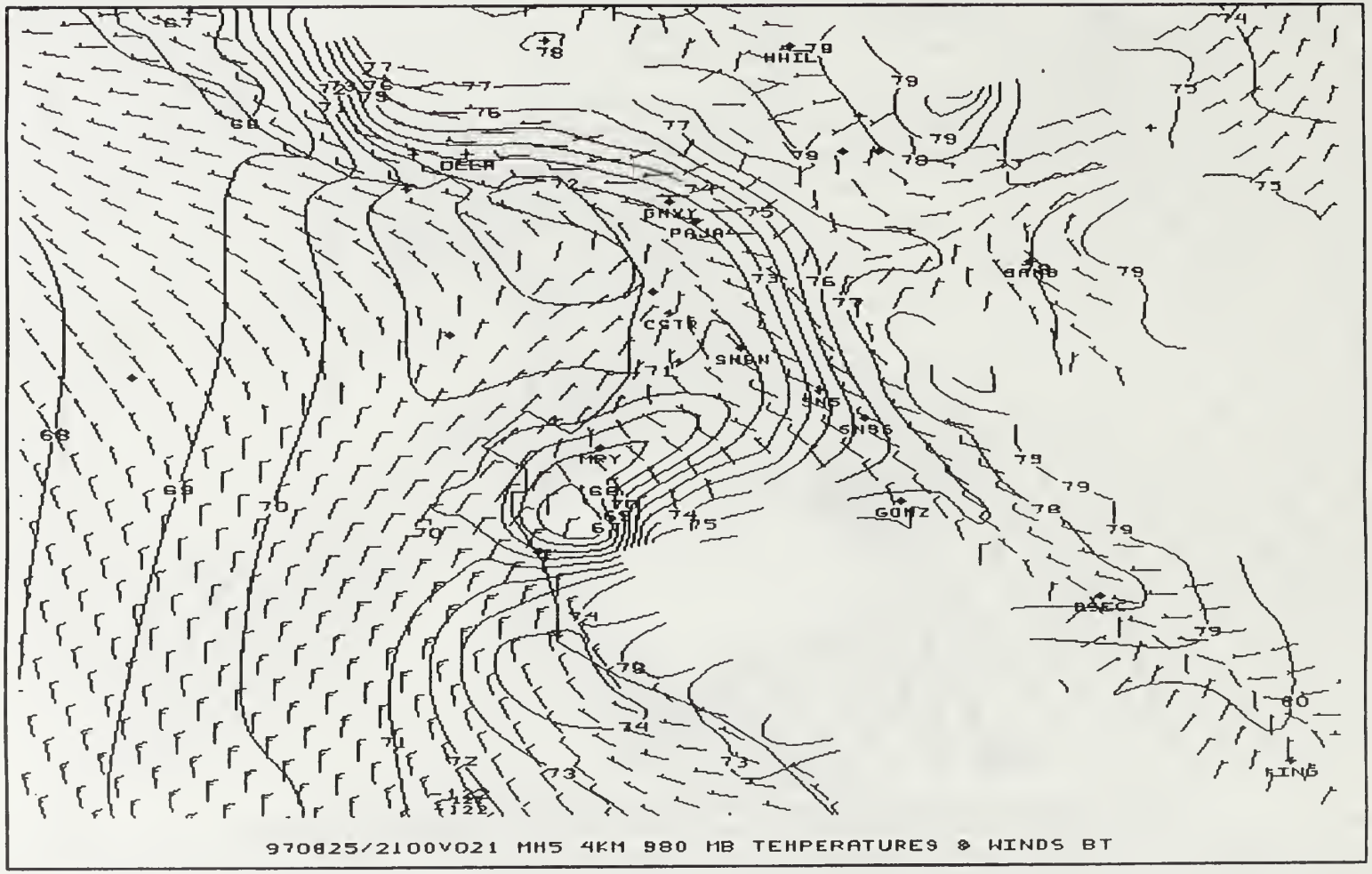

Figure 34. The 21 hour forecast of 980 mb winds and temperatures valid at 2100 UTC 25 August .

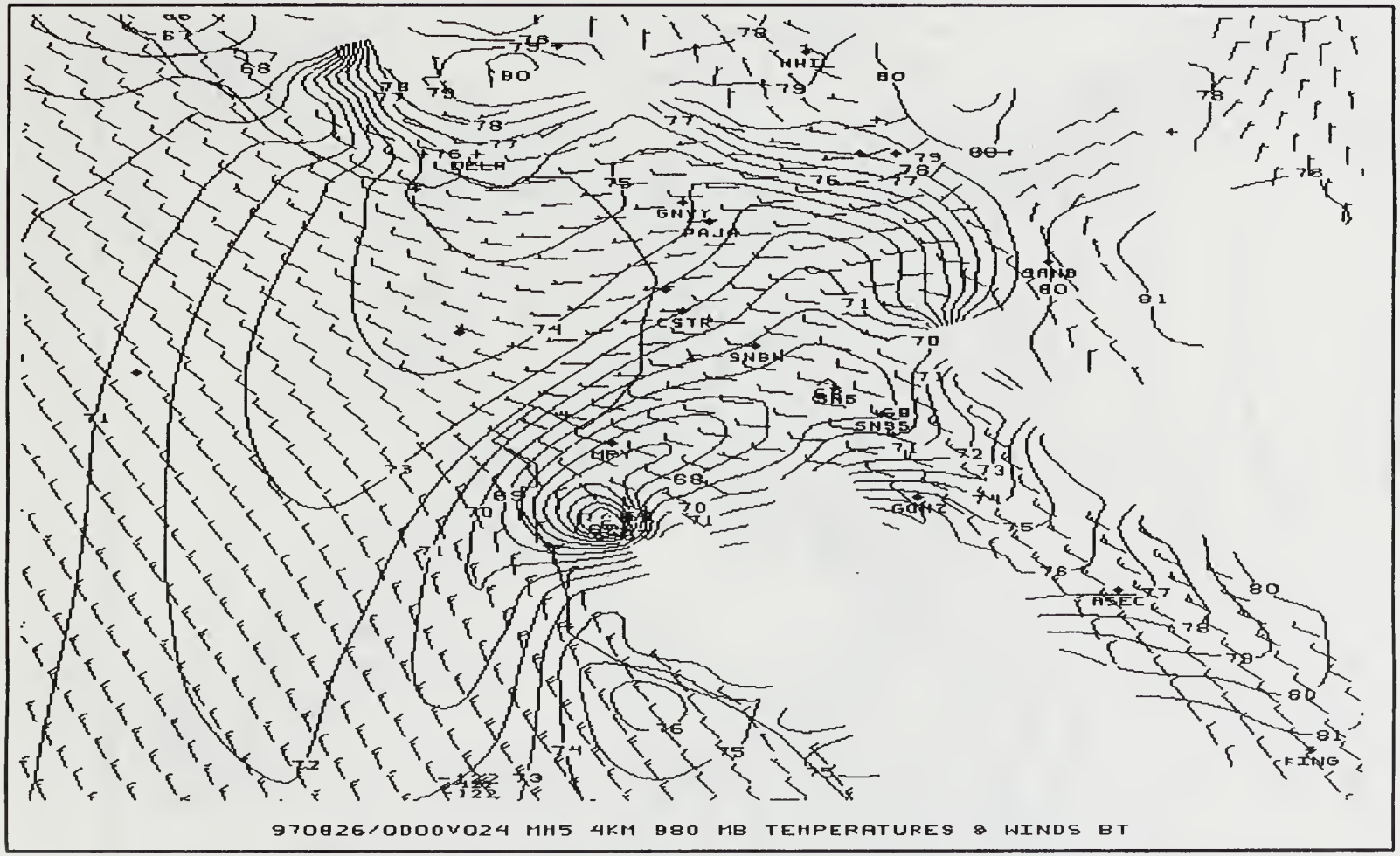

Figure 35. The 24 hour forecast of 980 mb winds and temperatures valid at 0000 UTC 26 August.

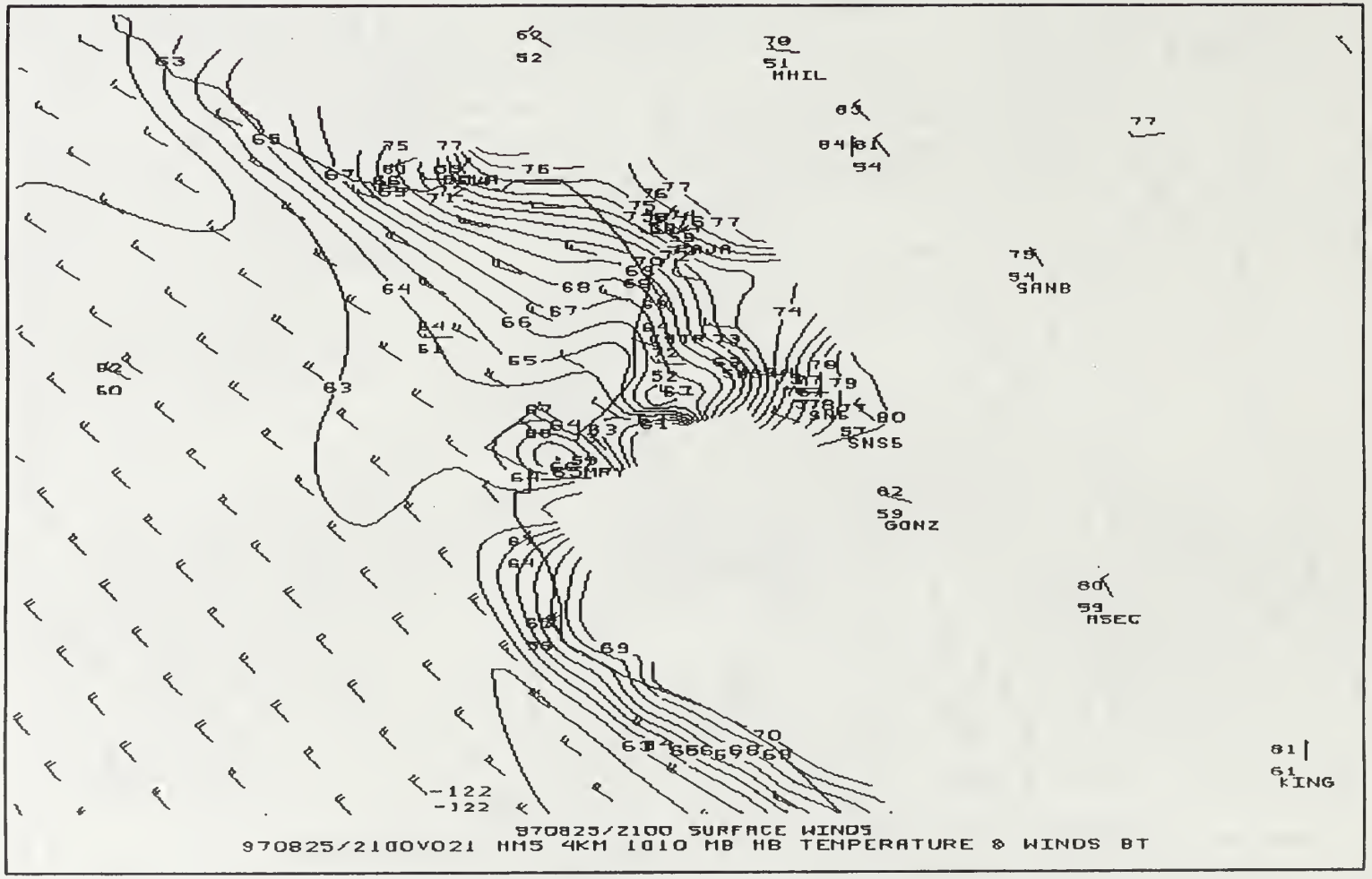

Figure 36. The 21 hour forecast of 1010 mb winds and temperature overlayed on the observed temperatures valid at 2100 UTC 25 August.

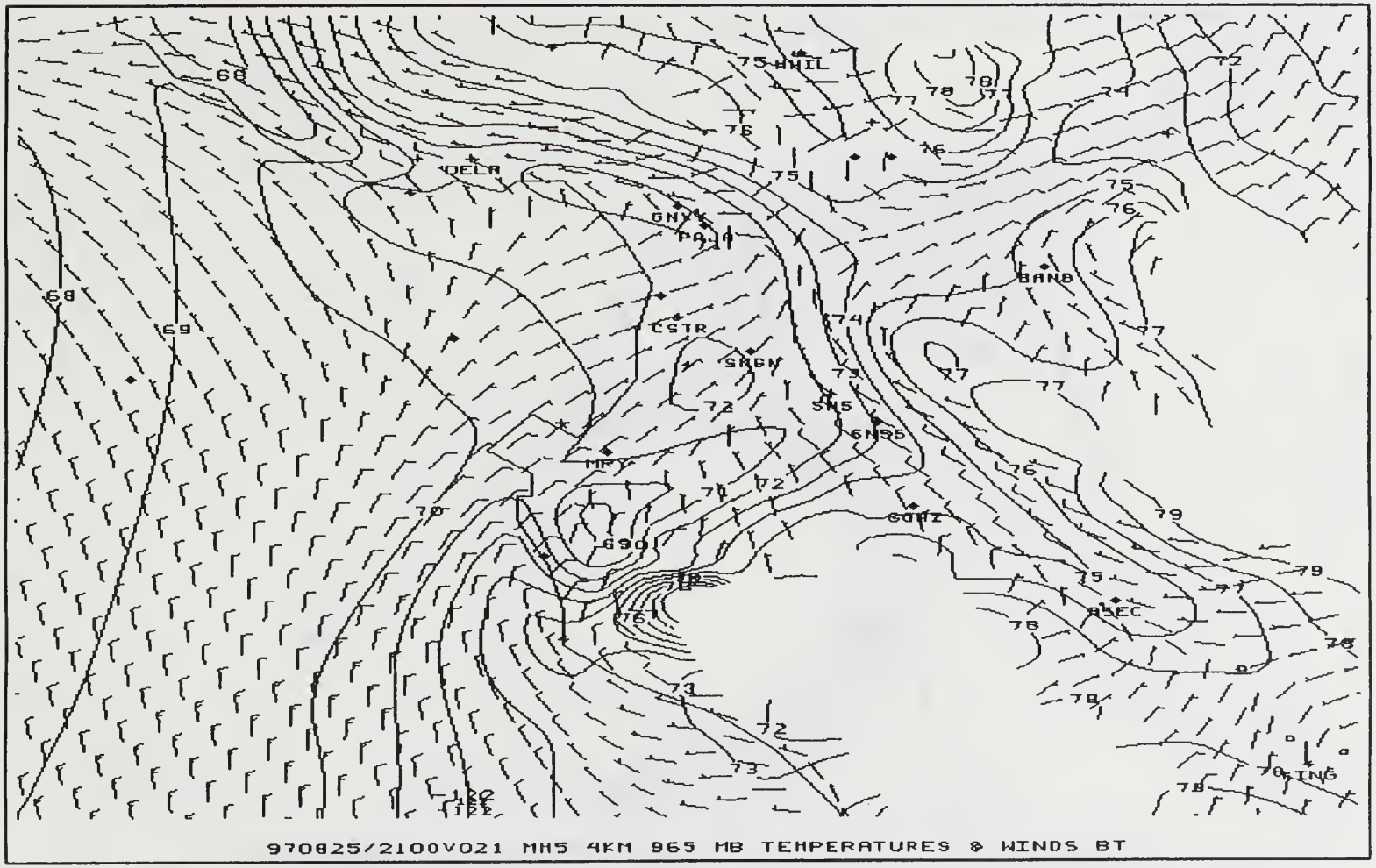

Figure 37. The 21 hour forecast of 965 mb winds and temperatures valid at 2100 UTC 25 August .

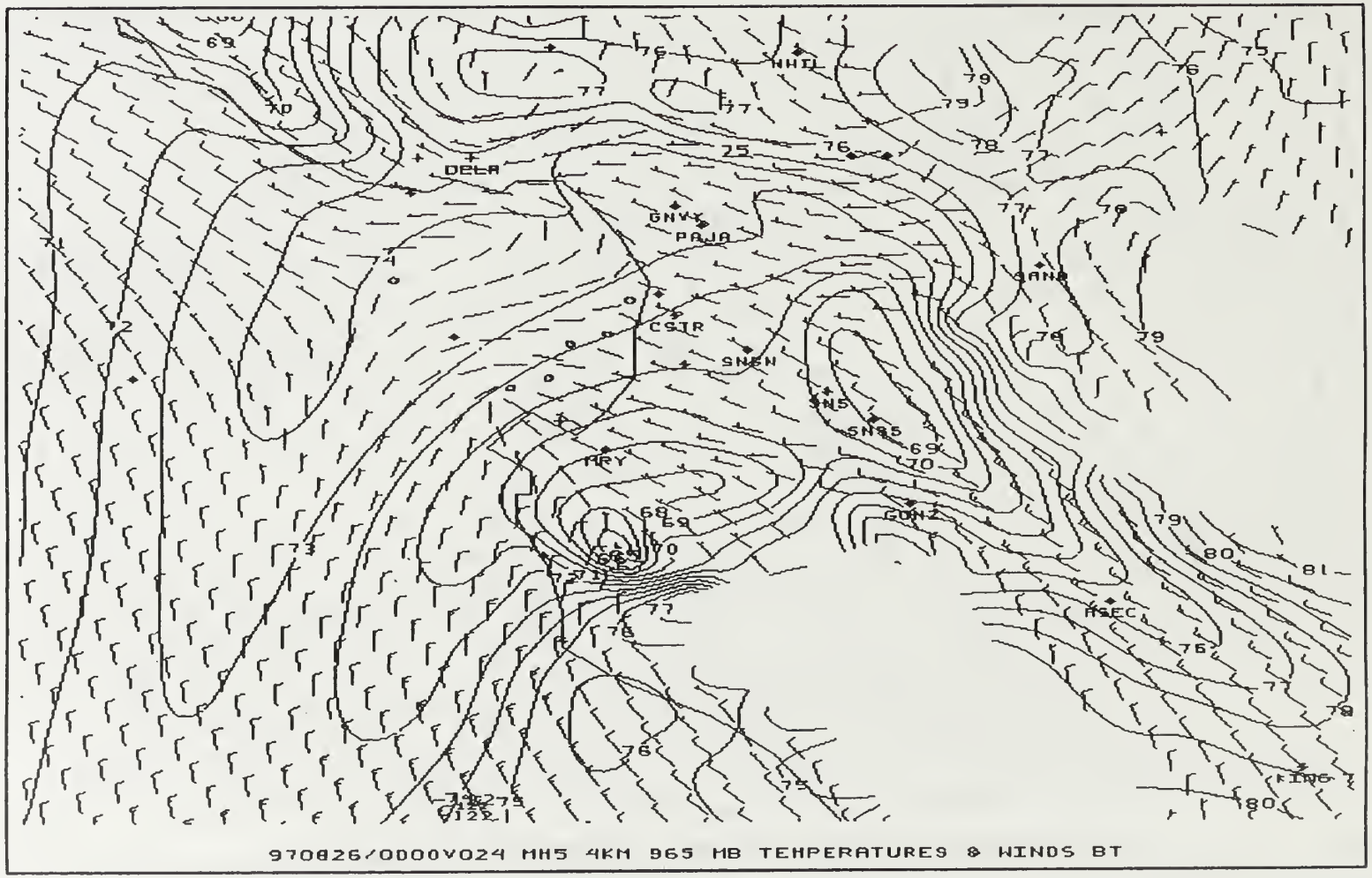

Figure 38. The 24 hour forecast of 965 mb winds and temperatures valid at 0000 UTC 26 August.

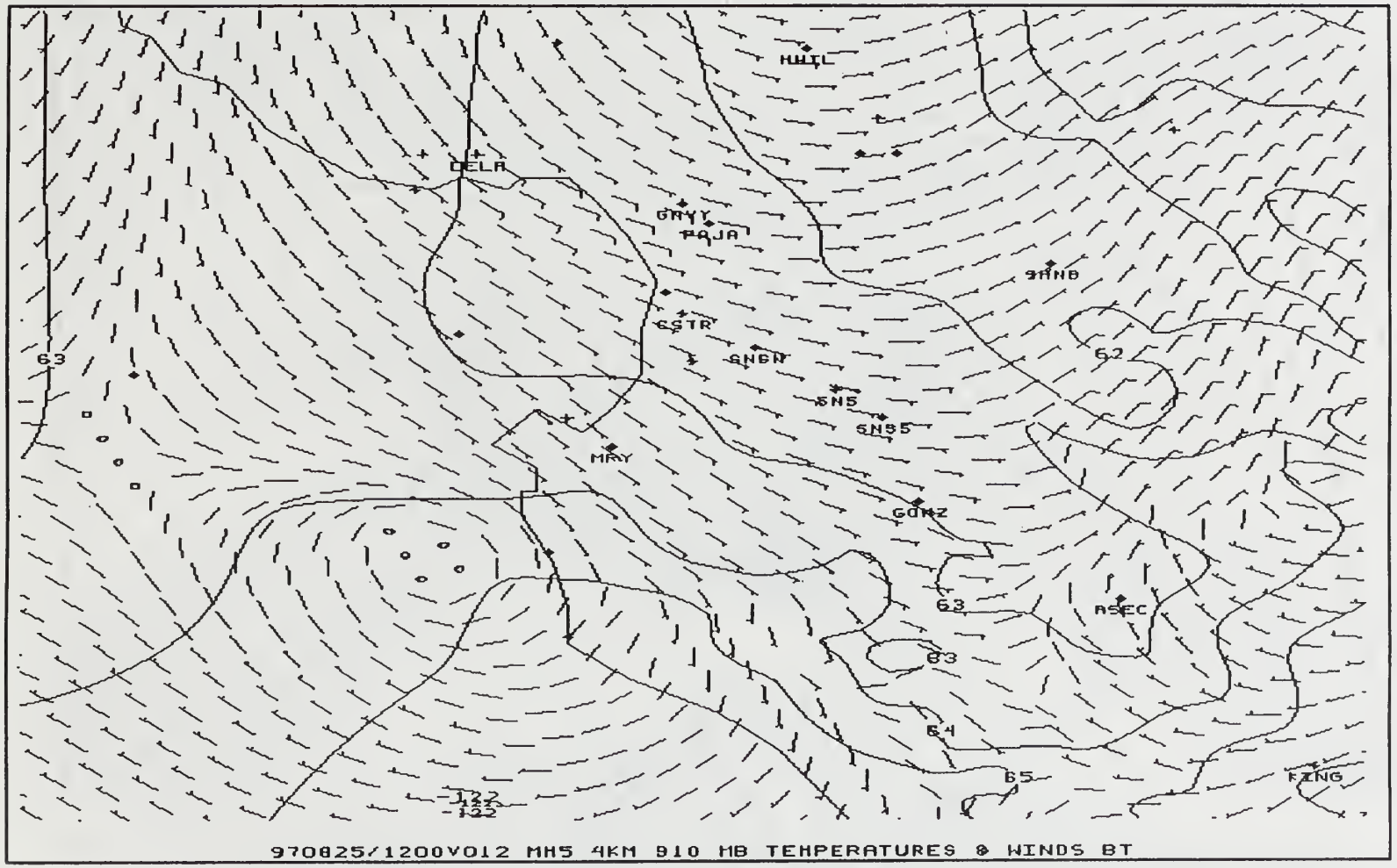

Figure 39. The 12 hour forecast of 910 mb winds and temperatures valid at 1200 UTC 25 August.

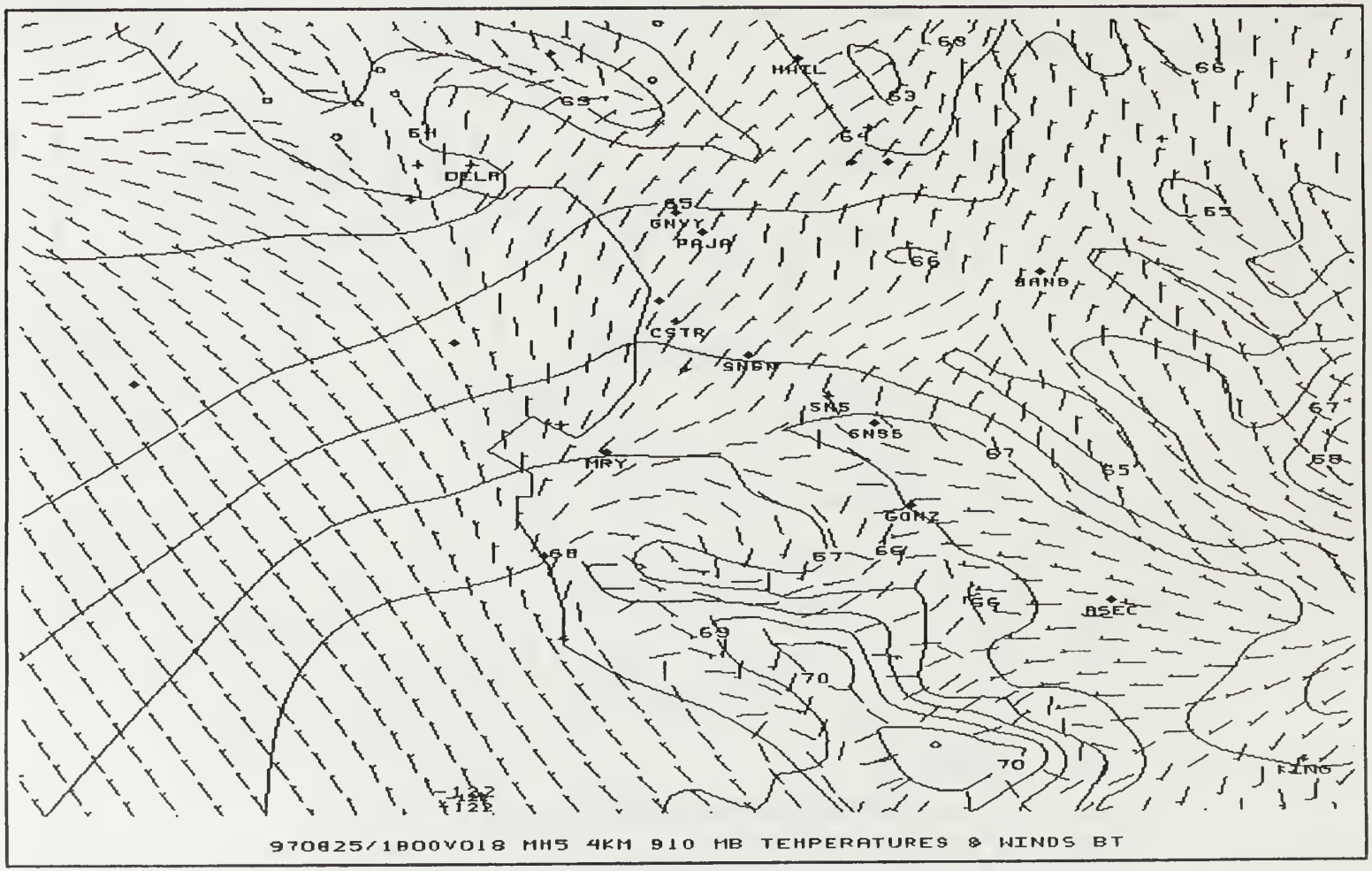

Figure 40. The 18 hour forecast of 910 mb winds and temperatures valid at 1800 UTC 25 August.

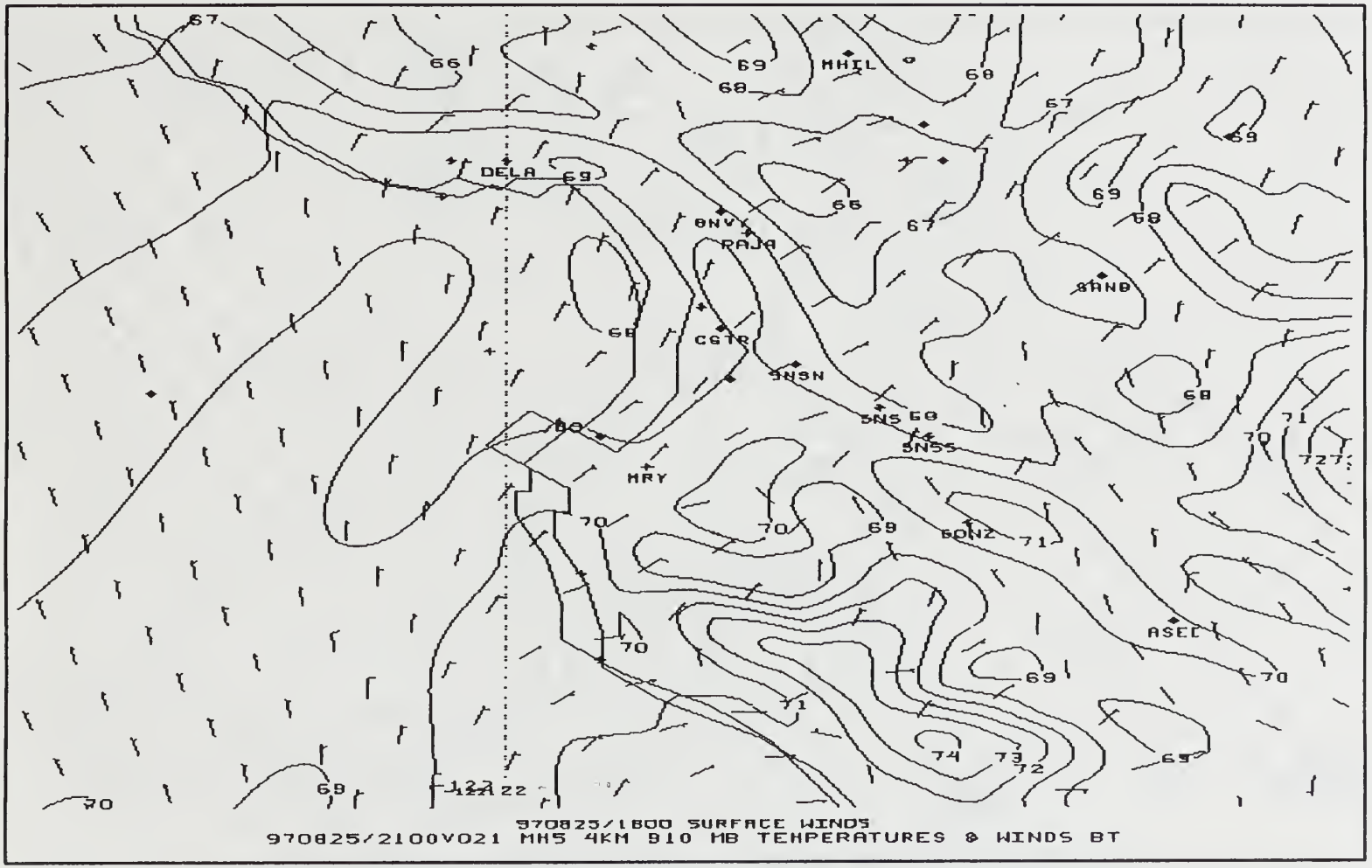

Figure 41. The 21 hour forecast of 910 mb winds and temperatures valid at 2100 UTC 25 August.

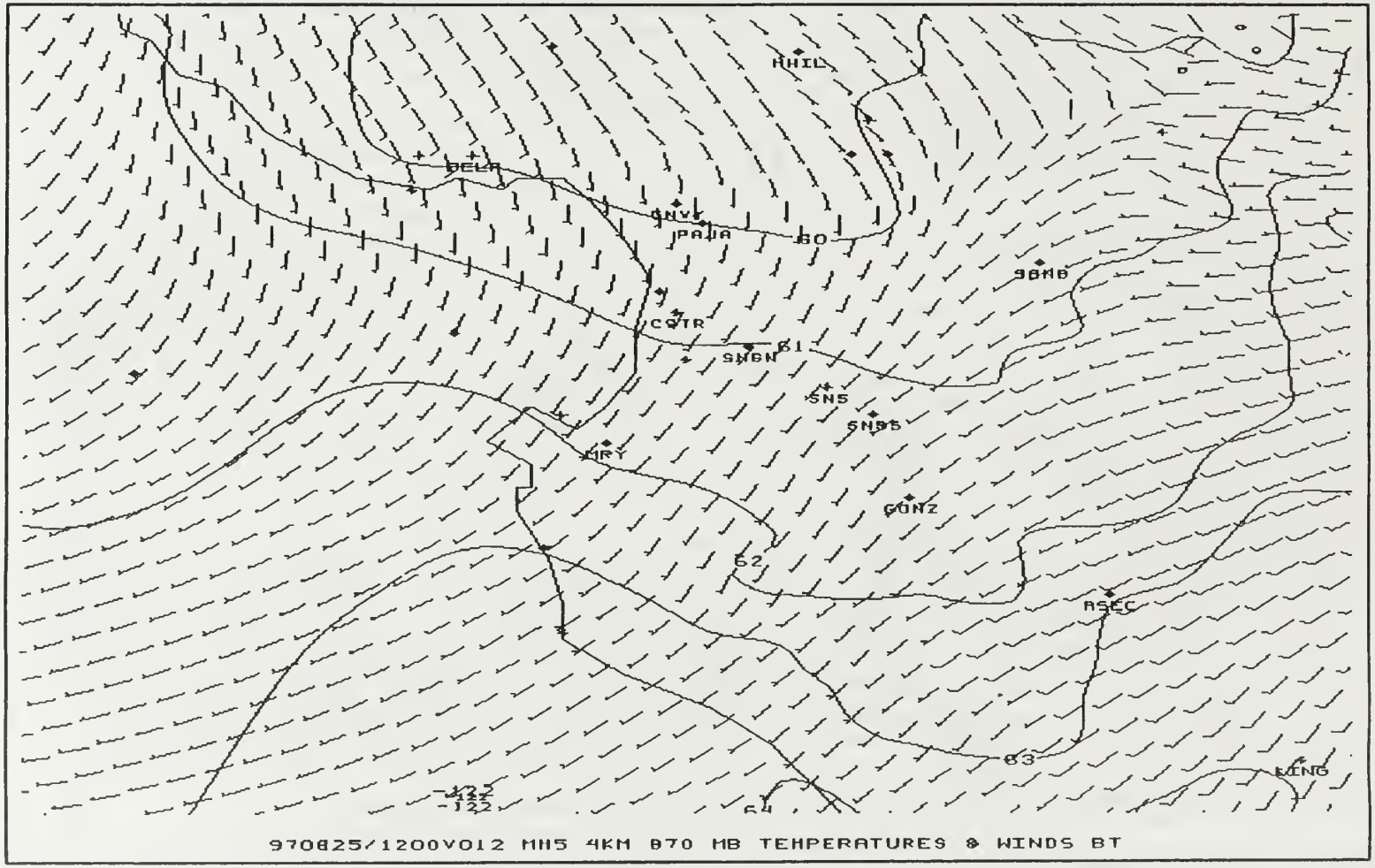

Figure 42. The 12 hour forecast of 870 mb winds and temperatures valid at 1200 UTC 25 August.

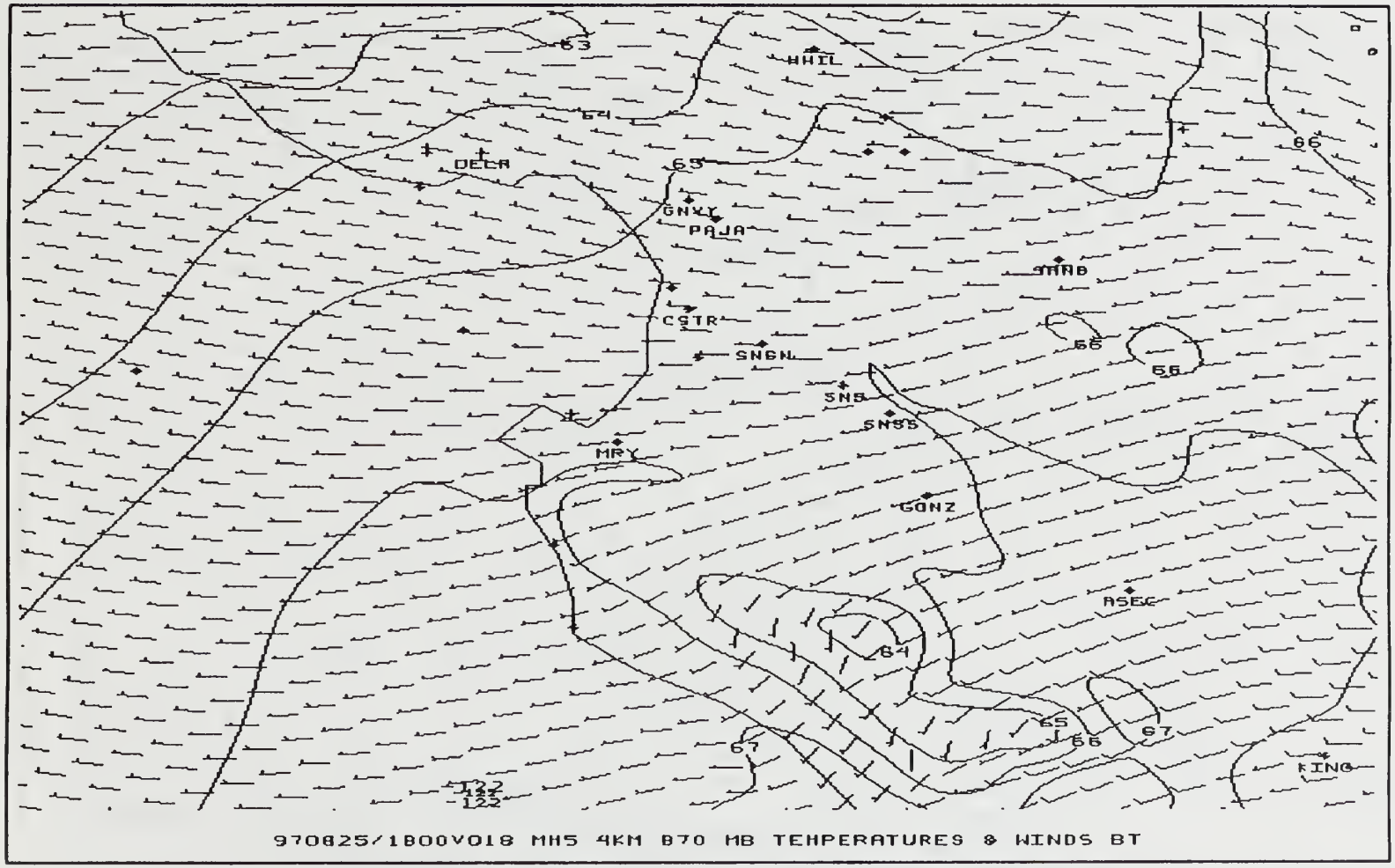

Figure 43. The 18 hour forecst of 870 mb winds and temperatures valid at 1800 UTC 25 August.

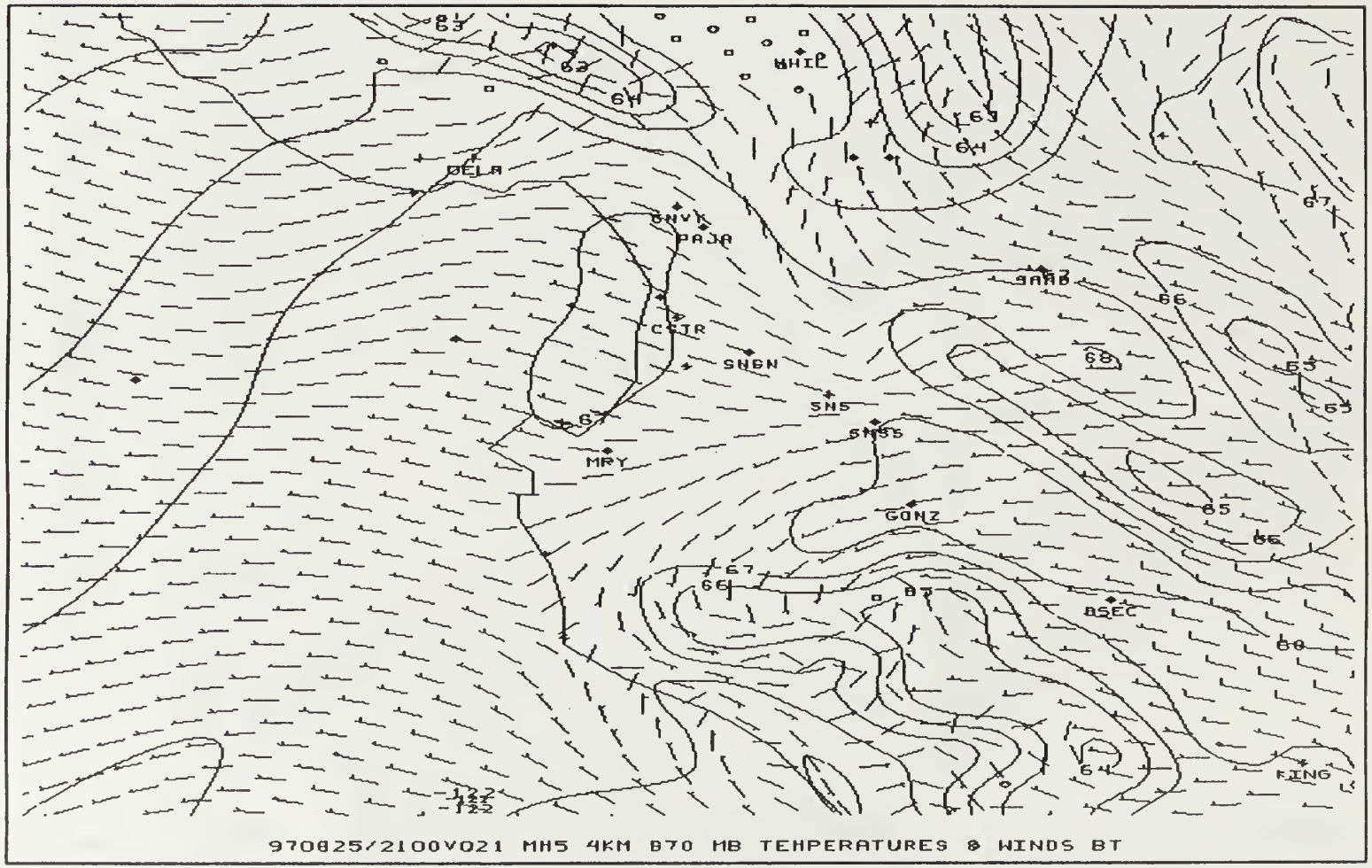

Figure 44. The 21 hour forecast of 870 mb winds and temperatures valid at 2100 UTC 25 August.

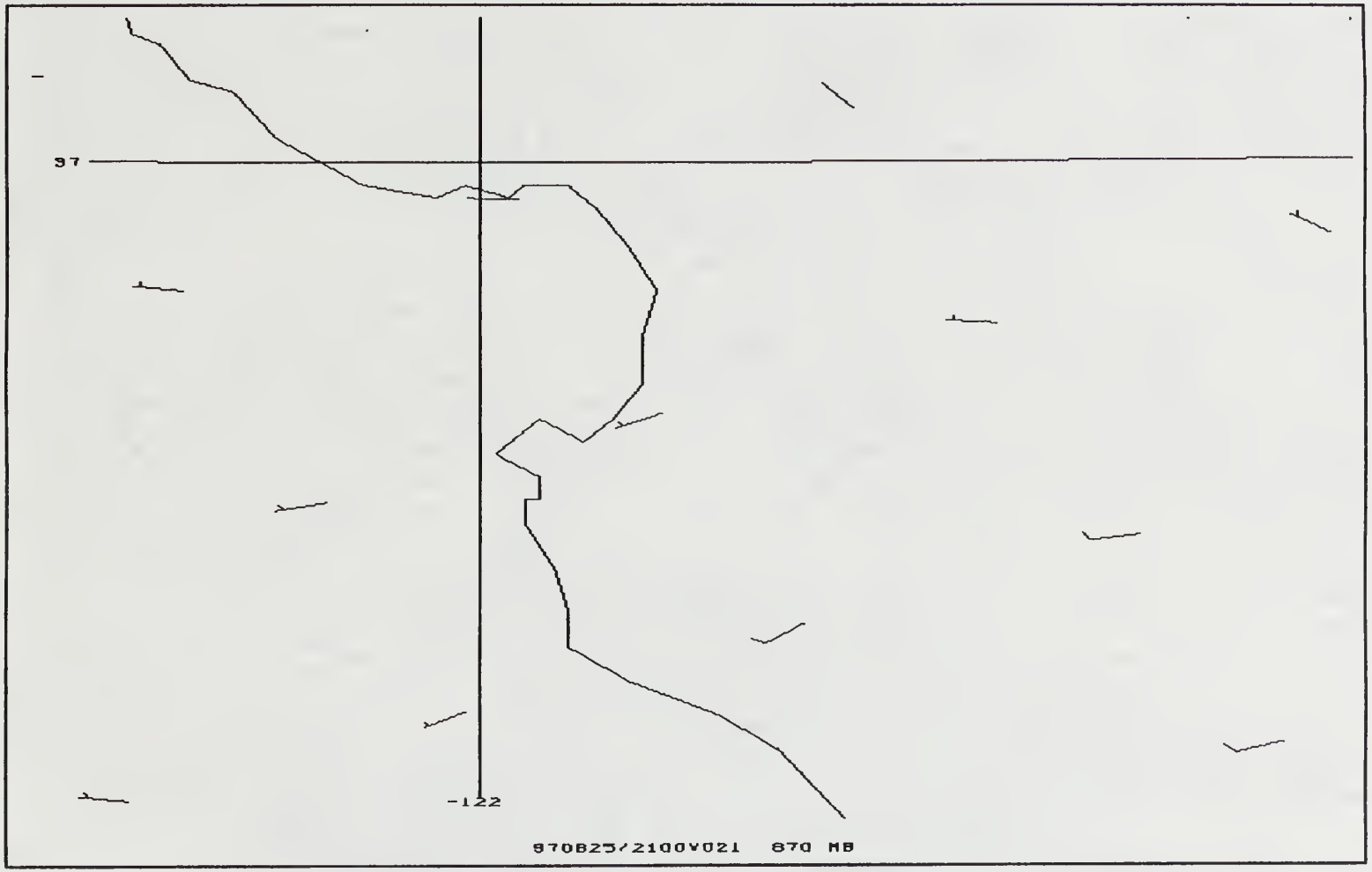

Figure 45. The 21 hour foecast of 870 mb winds in the 36 km MM5 domain, showing the background flow, valid at 2100 UTC 25 August.

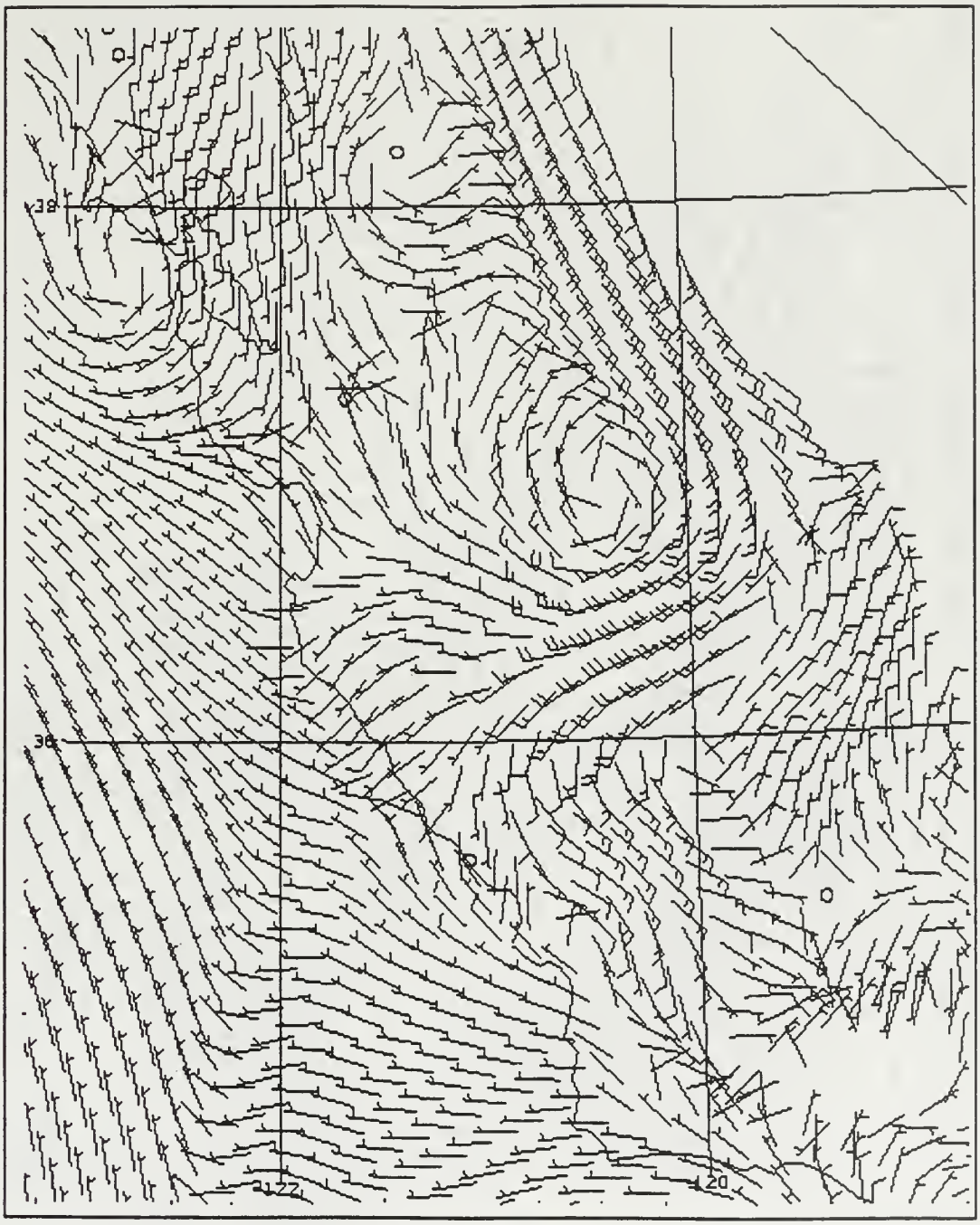

Figure 46. The 18 hour forecast of 12 km MM5 890 mb winds valid at 1800 UTC 25 August.

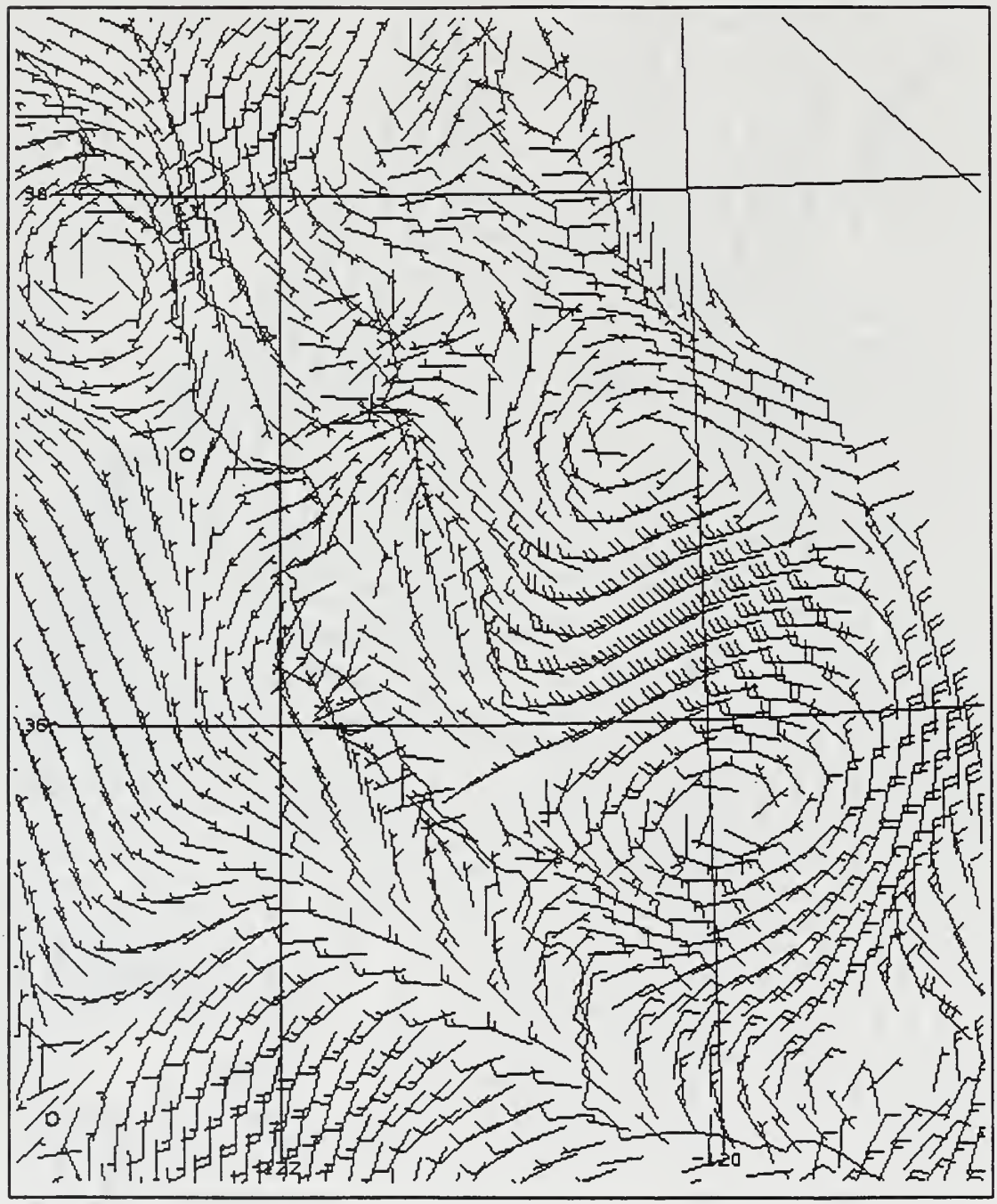

Figure 47. The 24 hour forecast of 12 km MM5 890 mb winds valid at 0000 UTC 26 August.

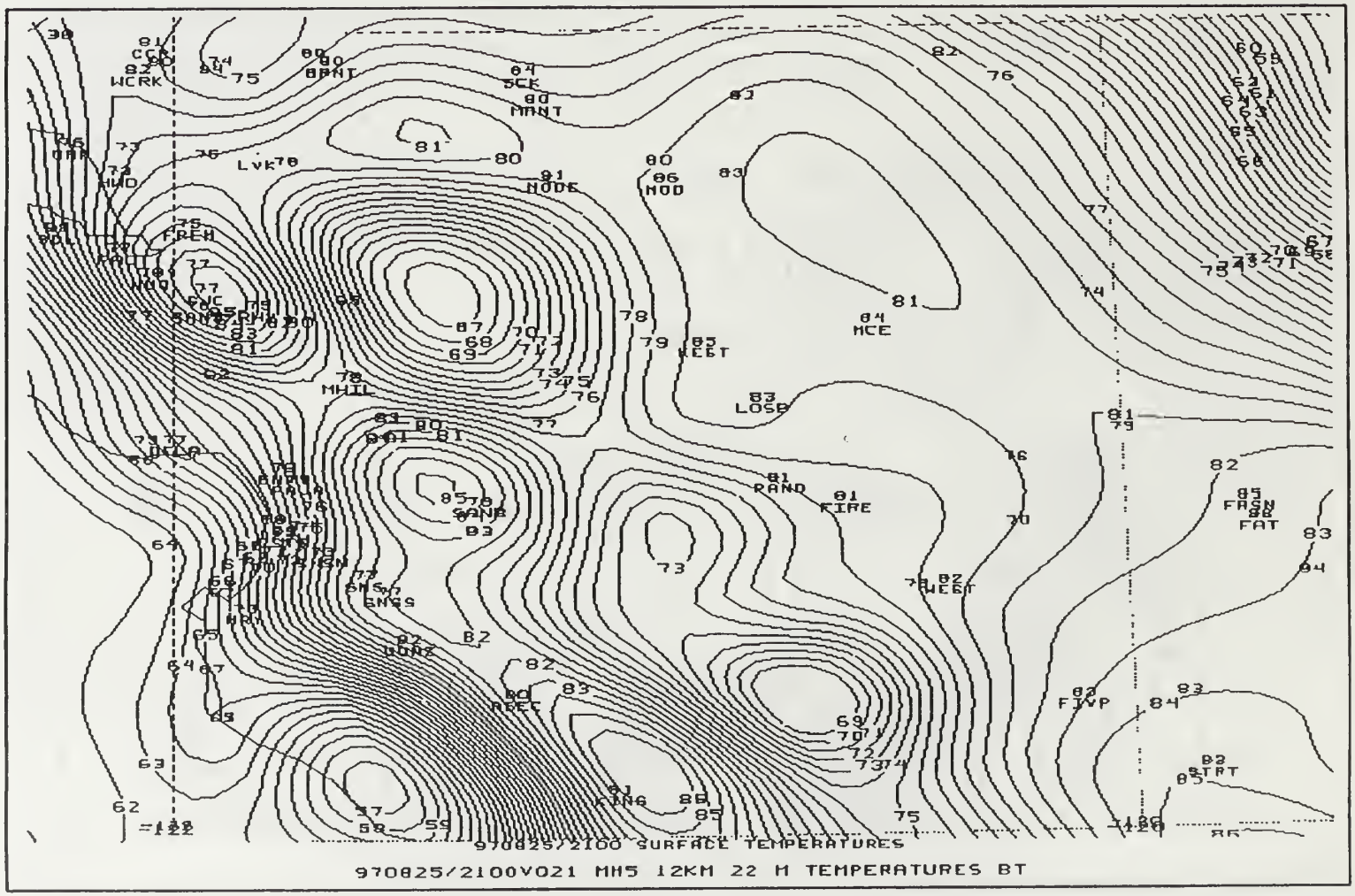

Figure 48. The 21 hour forecast of 12 km MM5 near surface temperatures overlayed on the observed temperatures valid 2100 UTC 25 August. (Burk-Thompson PBL scheme)

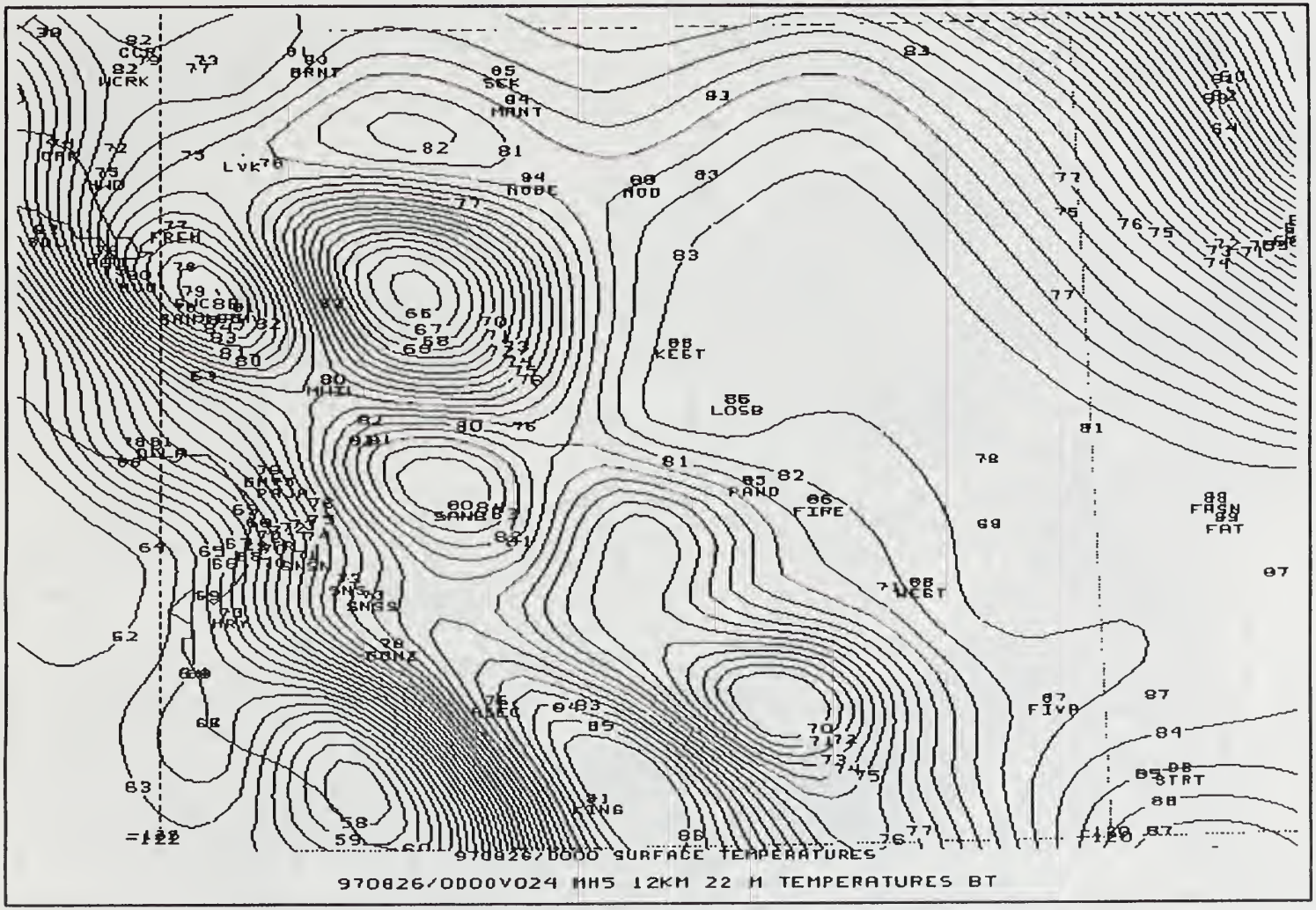

Figure 49. The 24 hour forecst of 12 km MM5 near surface temperatures overlayed on the observed temperatures valid 2100 UTC 25 August. (Burk-Thompson PBL Scheme)

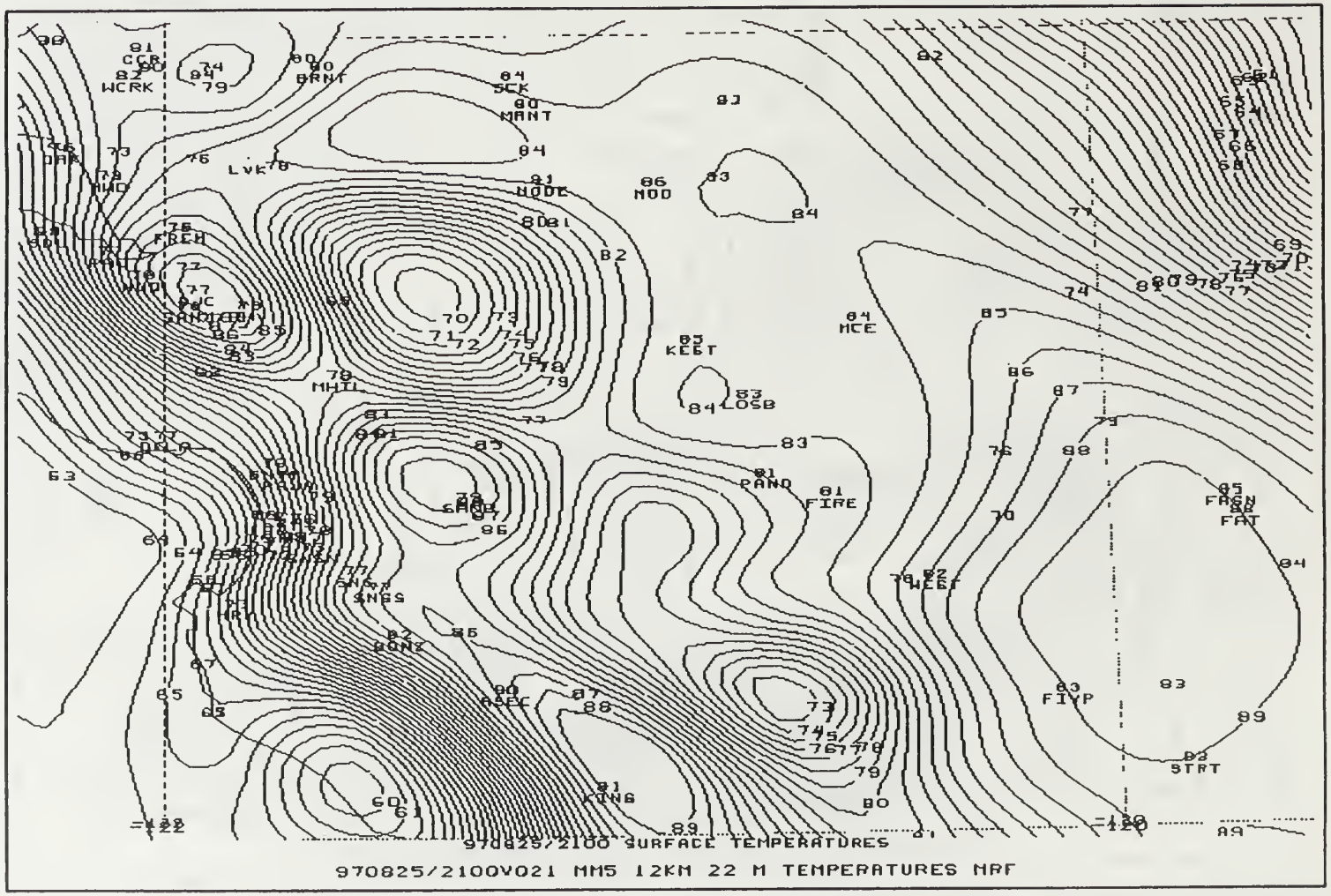

Figure 50. The 21 hour forecast of 12 km MM5 near surface temperatures overlayed on the observed temperatures valid at 2100 UTC 25 August. (MRF PBL scheme)

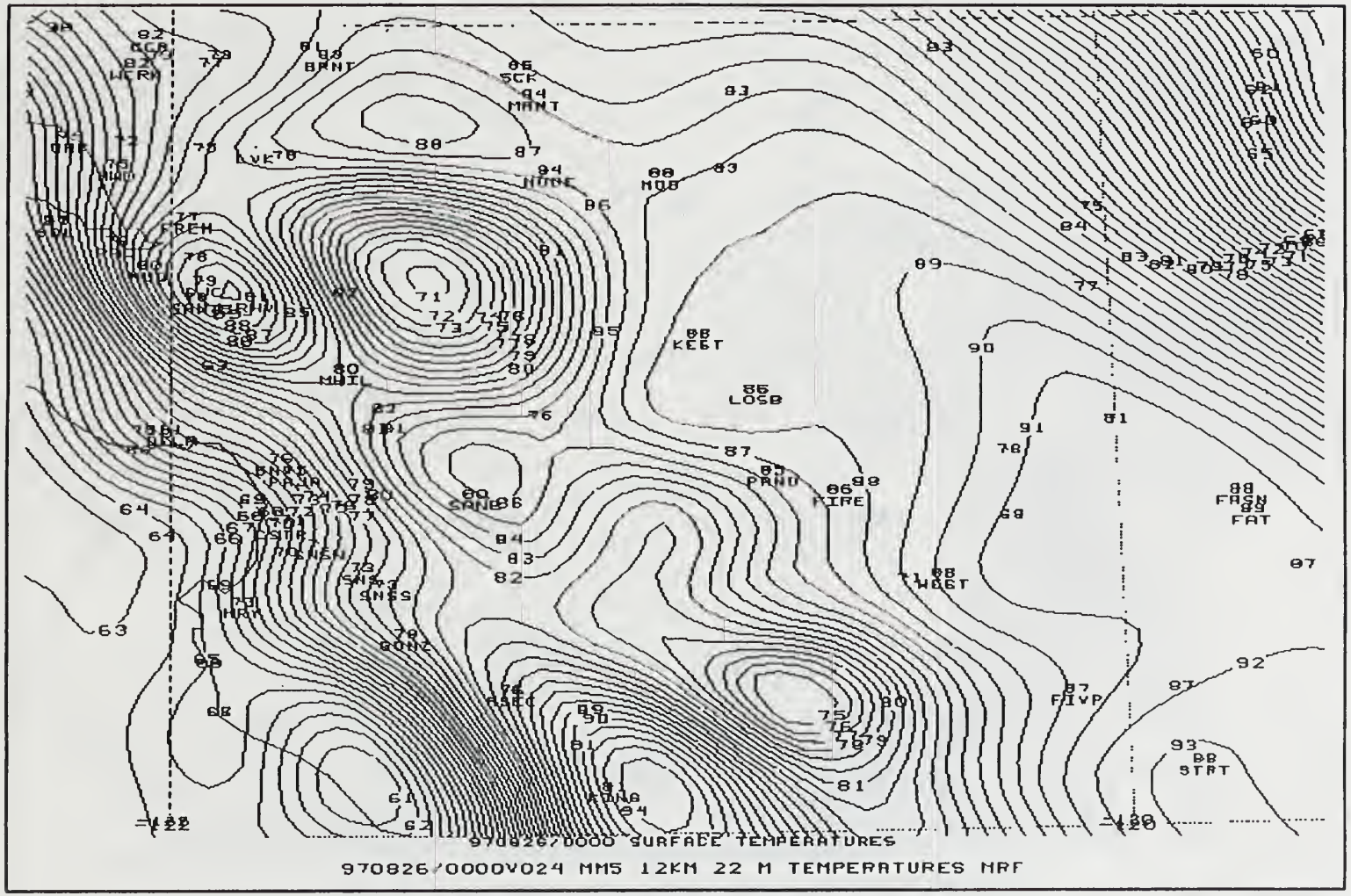

Figure 51. The 24 hour forecast of 12 km MM5 near surface temperatures overlayed on the observed temperatures valid at 2100 UTC 25 August. (MRF PBL scheme)

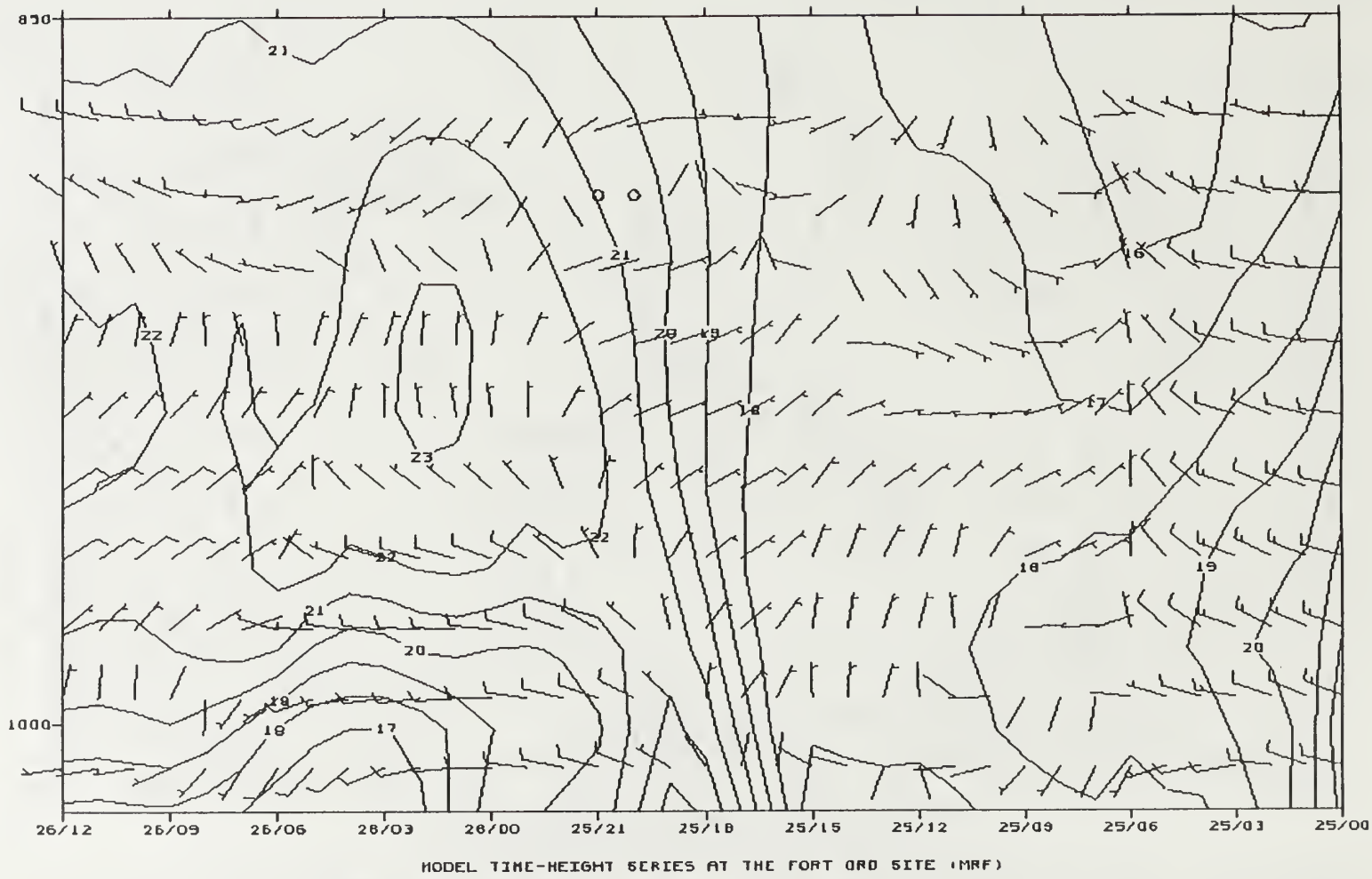

Figure 52. A 36 hour model time height series of winds and temperature up to 850 mb at the latitude and longitude of the Ft. Ord profiler site. (MRF PBL scheme)

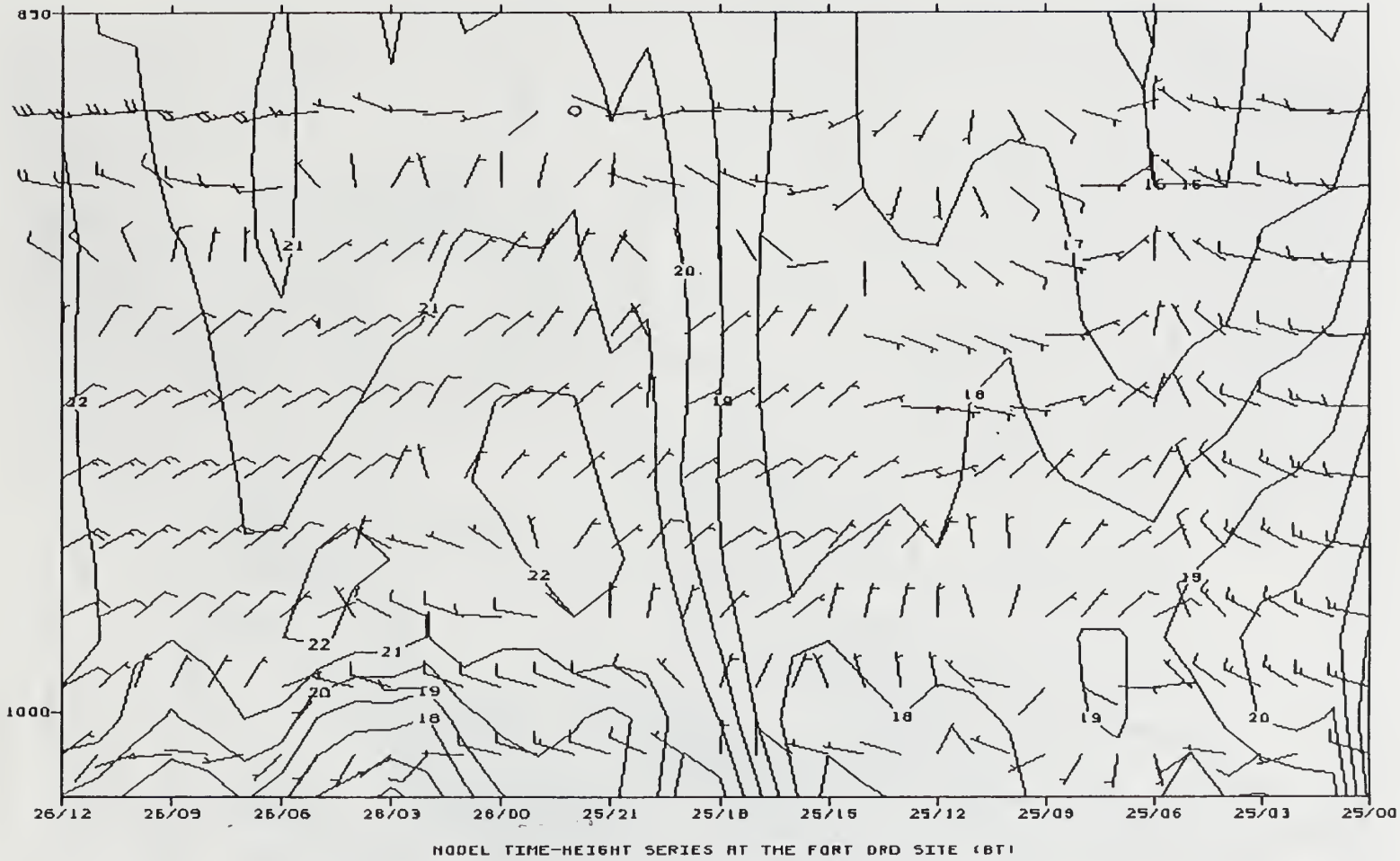

Figure 53. A 36 hour model time height series of winds and temperature up to 850 mb at the latitude and longitude of the Ft. Ord profiler site. (Burk-Thompson PBL scheme).

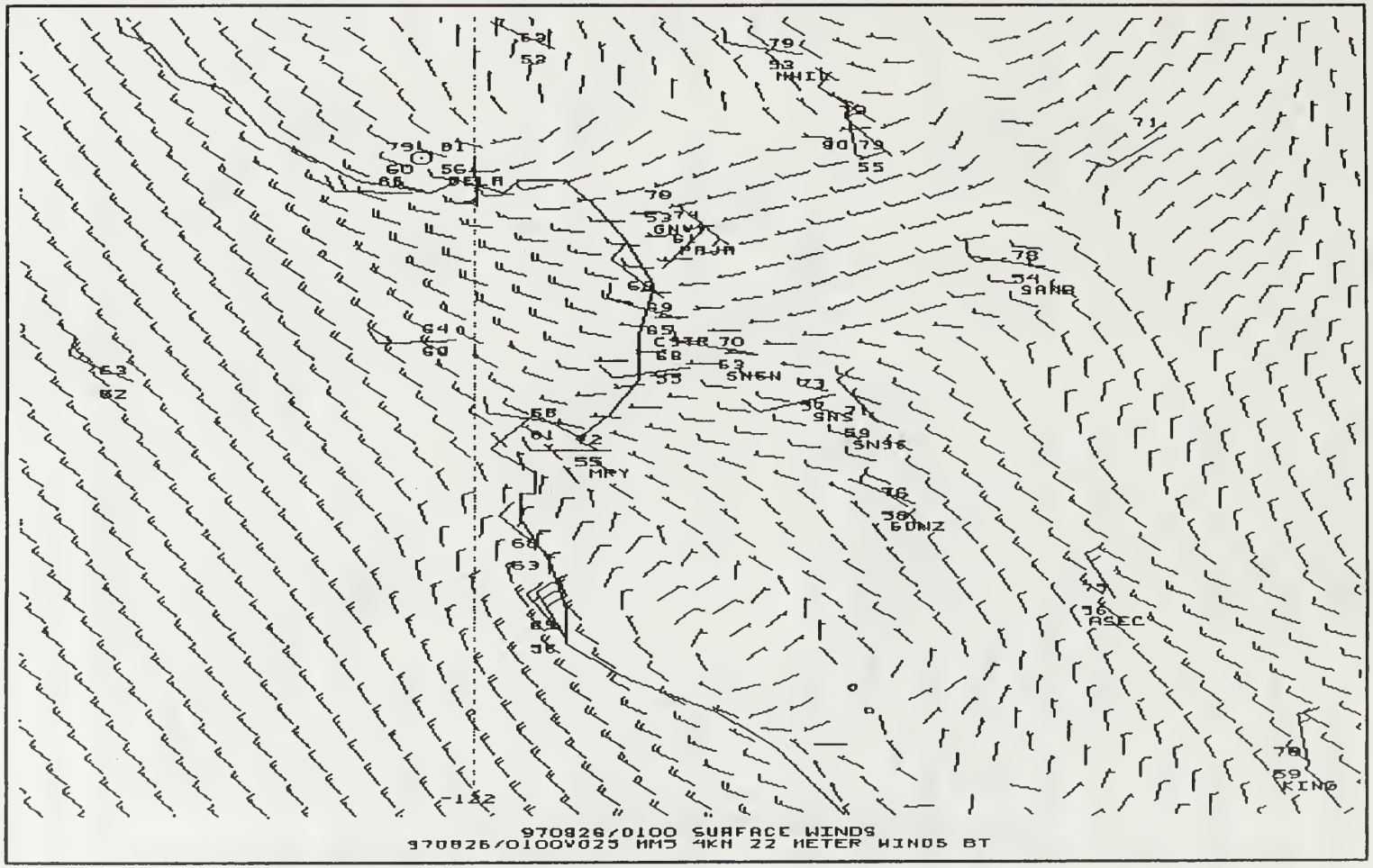

Figure 54. The 25 hour forecast of 4 km MM5 near surface winds overlayed on surface observations valid at 0100 UTC 26 August. (Burk-Thompson PBL scheme)

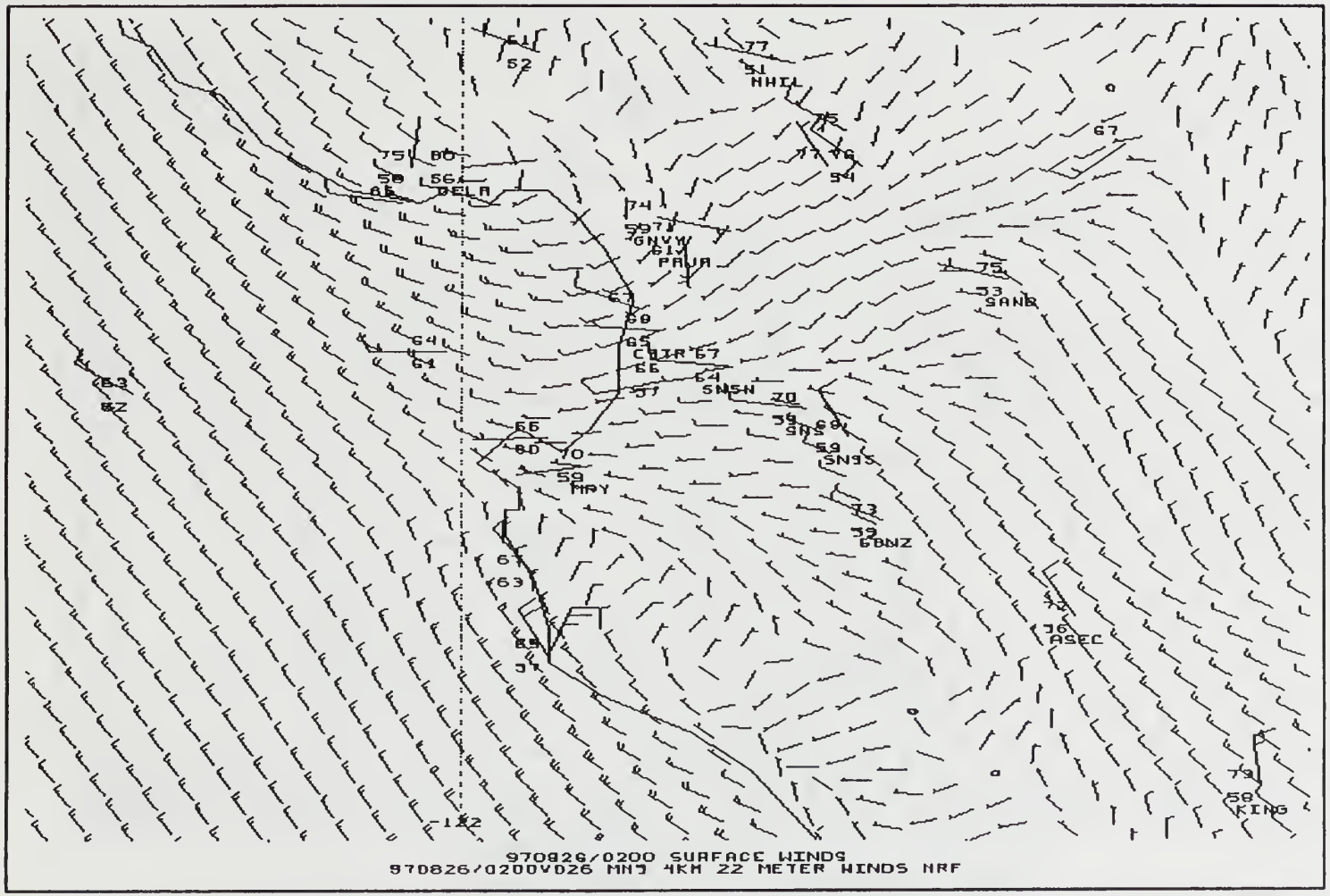

Figure 55. The 26 hour forecast of 4 km MM5 near surface winds overlayed on surface observations valid at 0200 UTC 26 August.(MRF PBL scheme)

VI. SUMMARY AND CONCLUSIONS

The day of the controlled burn on the former property of Fort Ord was neither a typical summer day nor an average August day with a strong marine inversion and significant heating aloft. The day of the fire had no substantial inversion, with maximum heating occurring at the surface. The only identifiable inversion occurred after the sea breeze propagated inland, lasting through the night and reinforced by nocturnal cooling. This weakly stratified day is consistent with the analyzed synoptic evolution and matches the surface pattern of the ridge regime (Knapp 1994).

The sea breeze evolution over Monterey Bay and the Salinas Valley region was not a classic sea breeze mainly due to the mountain-valley thermal forcing. There were two distinct wind surges at the Fort Ord site, one at 1800 UTC and then at 2000 UTC 25 August. The first wind surge was due to local mountain-valley forcing, and the second wind surge was due to large-scale forcing from California's Central Valley, the large-scale sea breeze. This case best fits the classification of a double surge sea breeze found by Round (1993).

When compared to the observations, both MM5 runs with the Burk-Thompson and MRF PBL scheme, show some promise in simulating both the horizontal and vertical aspects of the

sea breeze evolution. The model showed distinct responses to local and large-scale forcing, thus supporting the hypothesis that local forcing is responsible for the initial wind speed increase during the early morning hours. The model heating of the east and southern aspects in the morning hours changes the wind direction, turning the wind towards the heated slopes as warmer air rises up the slopes creating relative low pressure at the base with higher pressure at the coast. This was the driving force for the initial wind speed increase, the local sea breeze along Monterey Bay. This also implies that local mountain-valley forcing can play a major role in the sea breeze evolution in the Monterey Bay area.

The model showed a reasonable response in the Salinas Valley, though there were some discrepancies in the sea breeze evolution. The propagation of the sea breeze front was within 2 hours of the observed propagation with a similar magnitude in the wind speed. The first major discrepancy was in the Pacheco Pass, where the incorrect thermal forcing resulted in the simulated winds the reverse of observations. The second discrepancy occurred later in the forecast. The winds are stronger than normal after the first cycle of the sea breeze. This was the case with offshore flow in the Burk-Thompson PBL run, while in the MRF PBL scheme, the Salinas Valley sea breeze lasted too long into the night.

It is believed that the MRF PBL has a better surface scheme than the Burk-Thompson scheme, since the MRF discrepancies were not as large as those in the Burk-Thompson. This was best shown in the comparison of the model winds through the Pacheco Pass (Figure 28a,b,c) and the temperatures of the coastal and Central valleys (Figures 49,51).

The model also forecast some larger scale circulation's in the Central Valley that seemed to be generated or at least fed by the diurnal cycle of the sea breeze. Further investigation is needed to find the cause of and proof of the existence of these circulations.

VII. RECOMMENDATIONS FOR FURTHER RESEARCH

Based on the MM5 simulation, there are several recommendations for further research. More sea breeze simulations are needed for other Round (1993) sea breeze types; the onset, gradual onset, double surge and frontal. These sea breezes should be simulated with clear skies and stratus over the region to see the changes in the sea breeze structure and forcing, and investigate the effects of changes in the boundary layer stability. Since there were some discrepancies after the first sea breeze cycle, it might be beneficial to run the model out to 24-hour rather than to 36 hours, but still capturing one cycle of the sea breeze. Increasing the 4 km domain might be beneficial by including more of the Central Valley and move the boundary conditions still further form Monterey Bay. Capturing more of the Central Valley might result in improving the large scale thermal forcing in the 4 km domain. Initializing the model closer to the event, such as 0600 UTC or 1200 UTC, might improve the forecast.

Based on the results of this 4-km grid simulation in the Pacheco Pass, it might be beneficial to increase the grid resolution over the Monterey Bay to 1.3 km along with increasing the terrain resolution. The key to increasing the resolution is to improve the terrain features in the area. This alone will not make the necessary changes to

improve the simulation, but would only be needed to compliment the improvements made on the surface forcing. Further investigation is needed to improve the PBL schemes and increase the capabilities of the model simulation of the sea breeze evolution, mainly the surface heating. The current schemes show biases and further investigation is required to determine what must be changed, the land use table or other factors in the parameterization.

Given the model results, there are many geographical areas which could prove valuable to investigate with observational equipment such as portable wind profilers and surface observations. These areas include Pacheco Pass, the Monterey Bay area near Moss Landing or Castroville, Paso Robos, the pass to the east of Paso Robos, and several spots in the Central Valley in order to investigate how far into the valley the sea breeze can be detected. These same instruments used in the Central Valley could also be used to investigate the existence of the simulated circulations that were most prominent at 890 mb in both MM5 runs.

LIST OF REFERENCES

Arritt, R. W., 1993: Effects of the large-scale flow on characteristic features of the sea breeze. *J. Appl. Meteor.*, **32**, 116-125.

Atkinson, B. W., 1981: *Mesoscale Atmospheric Circulations*. Academic Press, New York, 495 pp. (see pp. 125-209)

Banta, R. M., 1995: Sea breezes shallow and deep on the California coast. *Monthly Weather Review*, **123**, 3614-3622.

Bayler, G., and H. Lewit, 1992: The Navy Operational Global and Regional Atmospheric Prediction System at Fleet Numerical Center, *Weather and Forecasting*, **7**, 273-279.

Bossert, J. E., F. H. Harlow, R. R. Linn, J. M. Reisner, A. B. White, and J. L. Winterkamp, 1998: Coupled weather and wildfire behavior modeling at Los Alamos: An overview. Preprints, Second Conf. on Fire and Forest Meteorology. Phoenix, AZ, Amer. Meteor. Soc., 1-5.

Buckley, R. L., and R. J. Kurzeja, 1996: Mesoscale modeling of the inland nocturnal sea breeze. Preprints, Conference on Coastal Oceanic and Atmospheric Prediction, Atlanta, GA, 376-381.

Burk, S. D. and W. T. Thompson, 1989: A vertically nested regional numerical prediction model with second-order closure physics. *Mon. Wea. Rev.*, **117**, 2305-1733.

Dudhia, J., 1989: Numerical study of convection observed during the Winter Monsoon Experiment using a mesoscale two-dimensional model. *J. Atmos. Sci.*, **46**, 3077-3107.

Estogue, M. A., 1961: A theoretical investigation of the sea breeze. *Quart. J. Roy. Met. Soc.*, **97**, 136-146.

Fagan, M., 1988: The sea breeze circulation during the Land Sea Breeze Experiment (LASBEX) in Central California. Master's Thesis, Meteorology Department, Naval Postgraduate School, Monterey California.

Ferguson, S. A., 1998, Real-time mesoscale model forecasts for fire and smoke management. Preprints, Second Conf. on

Fire and Forest Meteorology. Phoenix, AZ, Amer. Meteor. Soc., 161-164.

Fosberg, M. A., and Schroeder, 1966: Marine air penetration in Central California, *J. Appl. Meteor.*, **5**, 573-589.

Foster, M. D., 1996: California Sea Breeze Structure and Its Relation to the to the Synoptic Scale, Ph D Dissertation, Meteorology Department, Naval postgraduate School, Monterey California.

Grell, G. A., J. Dudhia, and D. R. Stauffer, 1995: A description of the fifth generation Penn State/NCAR Mesoscale Model (MM5), NCAR Technical Note, NCAR, Boulder, Colorado.

Gould, K. J., C. G. Herbster, J. D. Korotky, and P. H. Ruscher, 1996: WRS-88D, GOES-8, and MM5 mesoscale model observations of the Florida panhandle sea breeze circulation under different synoptic flow regimes. Conference on Coastal Oceanic and Atmospheric Prediction, Atlanta, GA, 364-369.

Herbster, C. G., J. Brenner, R. M. Suddaby, R. J. Carr, B. S. Lee, L. G. Arvanitis, and D. P. Brackett, 1998: Real time mesoscale modeling in support of fire weather forecasting. Preprints, Second Conf. on Fire and Forest Meteorology. Phoenix, AZ, Amer. Meteor. Soc., 149-152.

Herbster, C. G., and P. H. Ruscher, 1996, The Tallahassee Area Sea Breeze Experiment (TASBEX) - Observations and modeling study. Conference on Coastal Oceanic and Atmospheric Prediction, Atlanta, GA, 382-387.

Hong, S. Y. and H. L. Pan, 1996: Nonlocal boundary layer vertical diffusion in a medium-range forecast model. *Monthly Weather Review*, **124**, 2322-2339.

Intrieri, J. M., C. G. Little, W. J. Shaw, P. A. Durkee, and R. M. Hardesty, 1990: The Land/Sea Breeze Experiment (LASBEX). *Bull. Amer. Meteor. Soc.*, **72**, 656-664.

Johnson, A. Jr. and J. J. O'Brien, 1973: A study of an Oregon sea breeze event. *J. Appl. Meteor.*, **12**, 1267-1283.

Kain, J. S., and J. M. Fritsch, 1990: A one-dimensional entraining/ detraining plume model and its implication in convective parameterization. *J. Atmos. Sci.*, **47**, 2784-2802.

Knapp, M. C., 1994: Synoptic-Scale Influence on the Monterey Bay Sea Breeze, Master's Thesis, Meteorology Department, Naval Postgraduate School, Monterey California.

Kondo, H., and K. Gambo, 1979: The effect of the mixing layer on the sea breeze circulation and the diffusion of pollutants associated with land-sea breezes. *Journal of the Meteorological Society of Japan*, **57**, 560-575.

Nuss, W. A: and D. W. Titley, 1994: Use of multiquadric interpolation for meteorological objective analysis. *Monthly Weather Review*, **122**, 1611-1631.

Pielke, R. A., 1984: *Mesoscale Meteorological Modeling*, Academic Press, New York, 612 pp.

Round, R. D., 1993: Climatology and Analysis of the Monterey Bay Sea Breeze. Master's Thesis, Meteorology Department, Naval Postgraduate School, Monterey, California.

Schroeder, M. J., M. A. Fosberg, O. P. Cramer, C. A. O'Dell, 1967: Marine air invasion of the Pacific coast: a problem analysis. *Bull. Amer. Meteor. Soc.*, **48**, 802-808.

Stec, J. D., 1996: Wind Profiler Study of the Central Coast Sea/Land Breeze. Master's Thesis, Meteorology Department, Naval Postgraduate School, Monterey, California.

Wexler, R., 1946: Theory and observations of land sea breezes. *Bull. Amer. Meteor. Soc.*, **27**, 272-286.

Yetter, J. Jr., 1990: The Nature of the Propagation of the Sea Breeze Fronts in Central California. Master's Thesis, Meteorology Department, Naval Postgraduate School, Monterey, California.

Zhong, S., and E. S. Takle, 1993: The effects of large scale winds on the sea-land breeze circulations in an area of complex coastal heating. *J. Appl. Meteor.*, **32**, 1181-1195.

INITIAL DISTRIBUTION LIST

No. Copies

1. Defense Technical Information Center 2
   8725 John J. Kingman Rd., STE 90944
   Ft. Belvoir, Virginia 22060-6218

2. Dudley Knox Library.....2
   Naval Postgraduate School
   411 Dyer Rd.
   Monterey, California 93943-5101

3. Meteorology Department.....1
   Chairman, Code MR/Wx
   Naval Postgraduate School
   589 Dyer Rd Rm 254
   Monterey CA 93943-5114

4. Prof. Wendell A. Nuss.....1
   Code MR/NU
   Naval Postgraduate School
   589 Dyer Rd Rm 254
   Monterey CA 93943-5114

5. Prof. Douglas K Miller.....1
   Code MR/DM
   Naval Postgraduate School
   589 Dyer Rd Rm 254
   Monterey CA 93943-5114

6. Mr. Steven M. Taylor 2
   c/o Mr. and Mrs. Michael Taylor
   6 Wiegand Lane
   Delmar, NY 12054